AN INVESTIGATION OF TRANSFORMER-COUPLED PUSH-PULL AUDIO AMPLIFIERS

A THESIS

Presented to

the Faculty of the Division of Graduate Studies

Georgia Institute of Technology

In Partial Fulfillment

of the Requirements for the Degree

Master of Science in Electrical Engineering

by

Harry Wilkerson Ragsdale

December 1948

102461

AN INVESTIGATION OF TRANSFORMER-COUPLED PUSH-PULL AUDIO AMPLIFIERS

Approved:

Date Approved by Chairman Dec. 10, 1948

ACKNOWLEDGMENTS

I wish to express my sincere appreciation to Professor M. A. Honnell of the Department of Electrical Engineering for his invaluable aid and guidance during the course of this investigation.

TABLE OF CONTENTS

AN INVESTIGATION OF TRANSFORMER-COUPLED PUSH-PULL AUDIO AMPLIFIERS

INTRODUCTION

It is the purpose of this thesis to investigate various phases of a transformer-coupled push-pull audio amplifier.

A study of the influence of the following capacitances on the amplifier characteristics was conducted:

(a) The normal input capacitance of the vacuum tubes, which includes the dynamic component of this input capacitance;

(b) The normal input capacitance of the vacuum tubes with the effect of the dynamic component canceled out by symmetrical neutralization;

(c) The distributed capacitance of the input transformer;

(d) The capacitances between various windings and between windings and the case of the input transformer.

Further, a more complete equivalent circuit for the input or interstage transformer than is generally described in the available American literature was synthesized.

The techniques and importance of neutralization for radio-frequency amplifiers have long been known and extensively utilized. However, it was felt that neutralization of the effect of the grid-to-plate capacitance in a push-pull audio amplifier might be of some value in extending the range of the frequency response of the amplifier. Consequently, one phase of this investigation was devoted to the study

of the effect of symmetrical, or balanced, neutralization upon the frequency response of the amplifier.

As a corollary to the foregoing study, the effect of a resistive load across the secondary of the input transformer upon the overall amplifier characteristics was also studied.

An additional phase of this investigation was a detailed inquiry into the effects of the capacitances associated with the input transformer upon the overall characteristics of the amplifier.

Two of the more common methods of driving a push-pull audio amplifier are through the use of (a) a resistance-coupled stage, and (b) a transformer-coupled stage. However, the work of this thesis does not delve into the many possibilities of other methods of coupling, but, rather, the scope is limited to the more detailed study of a transformer-coupled audio amplifier.

Prior to the actual construction of the amplifier used in the various tests, a series of 6B4G tubes were aged for fifteen hours, at reduced voltage, in order to stabilize the tube characteristics before the tubes were placed in the actual circuit.

After the aging process was completed, the average plate characteristics for each tube was determined, and the actual curves for each tube were plotted. These characteristics were carefully compared, and, finally, two tubes with almost identical characteristics were chosen to be used in the amplifier circuit. The average plate characteristics for the tubes actually used are shown plotted on Figure 1.

During the actual construction, care was taken to maintain physical symmetry throughout by giving attention to the positioning of

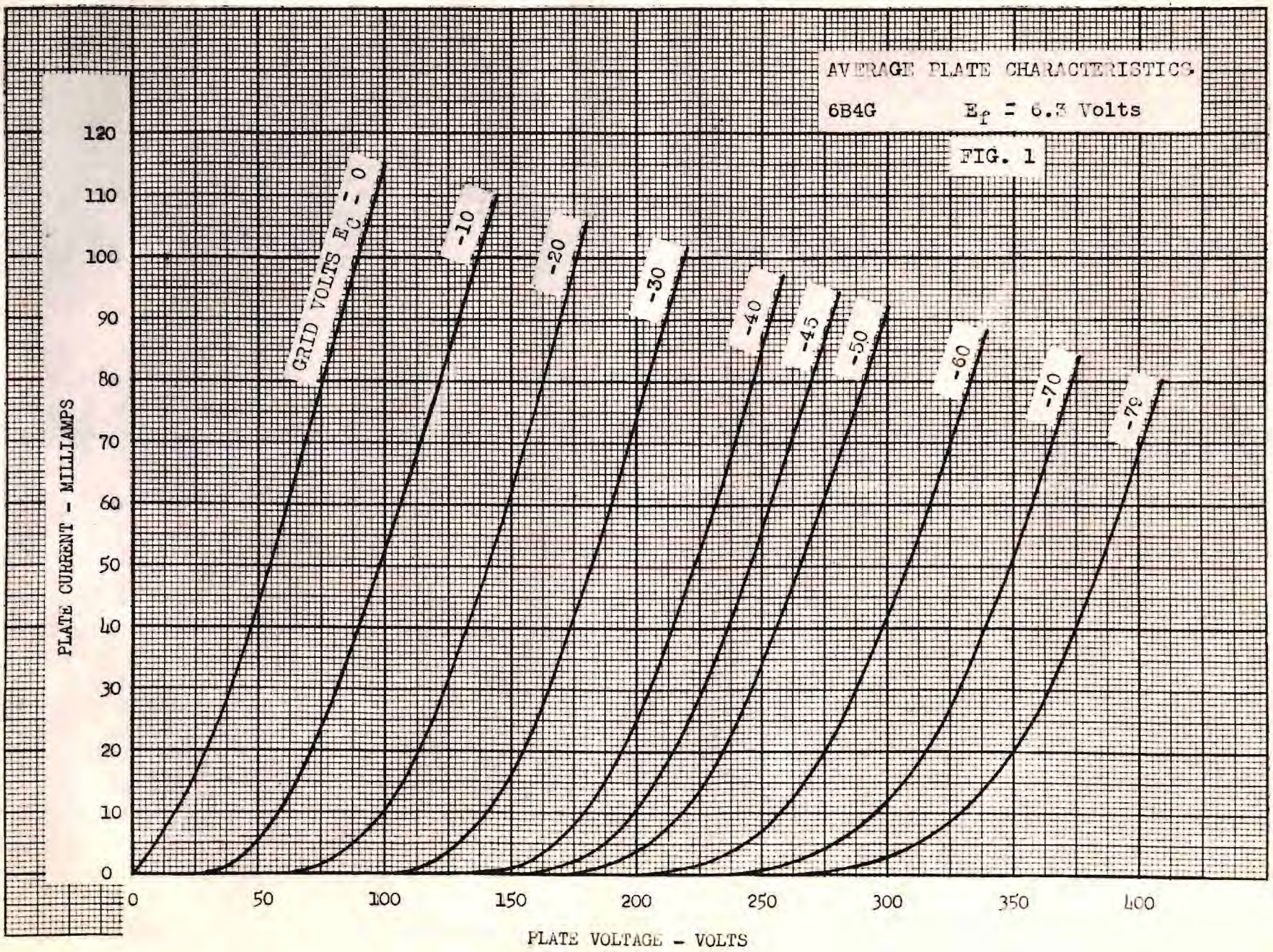
AVERAGE PLATE CHARACTERISTICS
6B4G E_f = 6.3 Volts
FIG. 1
GRID VOLTS E_c = 0
-10
-20
-30
-40
-45
-50
-60
-70
-75
PLATE CURRENT - MILLIAMPS
120
110
100
90
80
70
60
50
40
30
20
10
0
0
50
100
150
200
250
300
350
400
PLATE VOLTAGE - VOLTS

the component parts, and the placing of the leads used in the hook-up.

At audio frequencies and the region just above the audio range, the positioning of parts and the length of leads do not normally play a major role in affecting the frequency response of the amplifier. However, to avoid any possible sources of errors resulting from the above causes, all possible care was exercised during the construction of the amplifier.

The input, or interstage, transformer and the output transformer were both high quality "Linear Standard" transformers manufactured by the United Transformer Corporation. The manufacturer guarantees both transformers to have a uniform frequency response from 30 c.p.s. to 20,000 c.p.s. within $\pm$ 1 db. The features of these transformers are listed in Table 1.

DISCUSSION

The Transformer-Coupled Push-Pull Audio Amplifier Circuit

The circuit diagram for the transformer-coupled push-pull audio amplifier is shown on Figure 2.

In most respects, this is a conventional type of push-pull audio amplifier. However, to insure that the amplifier would be as free as possible from any voltage supply transients, additional filtering was employed in the plate, grid, and filament circuits as shown on the diagram. These capacitors are C-1, C-2, C-5, C-6, and C-7. All values of circuit components are listed separately in Table 2.

P-1, P-2, and R-1 compose the bias voltage adjusting system. It was found that after the two potentiometers were originally set to give the desired value of bias voltage, no further adjustments were necessary.

The grid, plate, and filament circuits were each provided with individual meters, and were frequently monitored to insure that they remained at the desired values.

C-3 and C-4 are the variable air-trimmer type neutralizing condensers.

T-1 is the input transformer, UTC, type LS-10, and T-2 is the output transformer, UTC, type LS-55.

R-2 is the input transformer secondary-load resistance.

The audio oscillator used as a signal source was connected to the input terminals, which were General Radio type plugs employed to aid in making measurements. While at the output terminals, a 500 ohm,

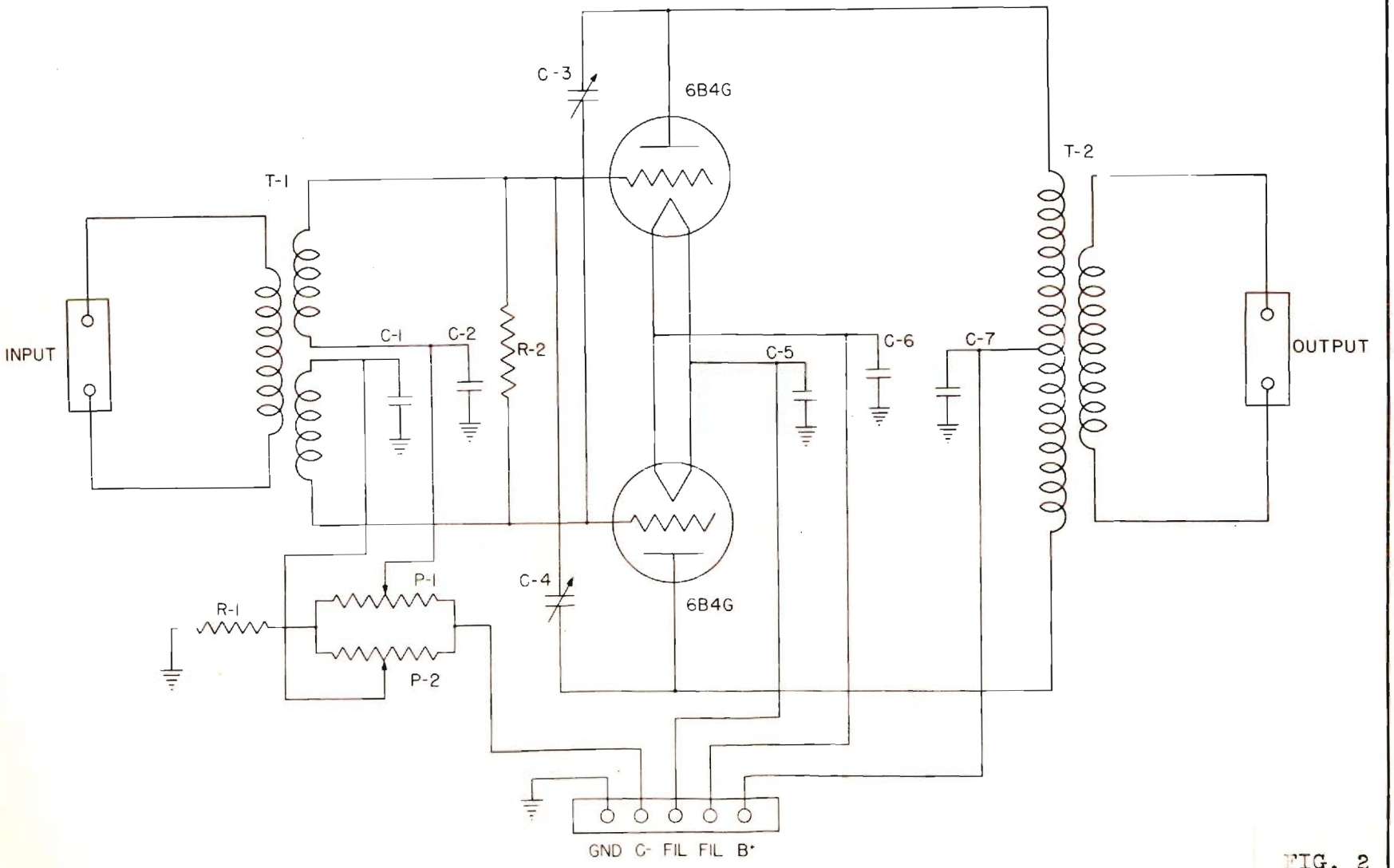

FIG. 2

NEUTRALIZED PUSH-PULL
AUDIO AMPLIFIER

32 watt, non-inductive resistance was connected.

A photograph of the complete amplifier is shown on Figure 3. In addition, a photograph of the amplifier together with the associated equipment used in making the amplification and phase measurements is shown on Figure 4.

The basic amplifier circuit as constructed does not contain its own power supply, but rather was provided with an external terminal strip in order that separate and variable power supplies might be used for the plate voltage source, the bias voltage source, and the filament voltage source.

The primary power source to each of the separate power supplies was a voltage-regulated, 60-cycle, 117-volt source as provided in the Electronics Laboratory of the School of Electrical Engineering.

The driving signal source for the amplifier was a Hewlett-Packard Audio Oscillator, Type 200-C, variable in frequency from 20 c.p.s. to 200 KC, and variable in output voltage from 0 volts to approximately 20 volts, R.M.S.

A General Radio Vacuum-Tube Voltmeter, Type 726-A, was provided to measure the input and output voltages of the amplifier, and a Dumont Oscilloscope, Type 208, was used to measure the phase characteristics of the amplifier.

To insure that the two tubes actually used were as nearly balanced as possible, the plate voltage and bias voltage were checked at each tube socket pin and found to be respectively equal. Furthermore, the plate currents were measured for each tube and were found to remain equal over the entire frequency range used in all of the tests described in succeeding sections of this report.

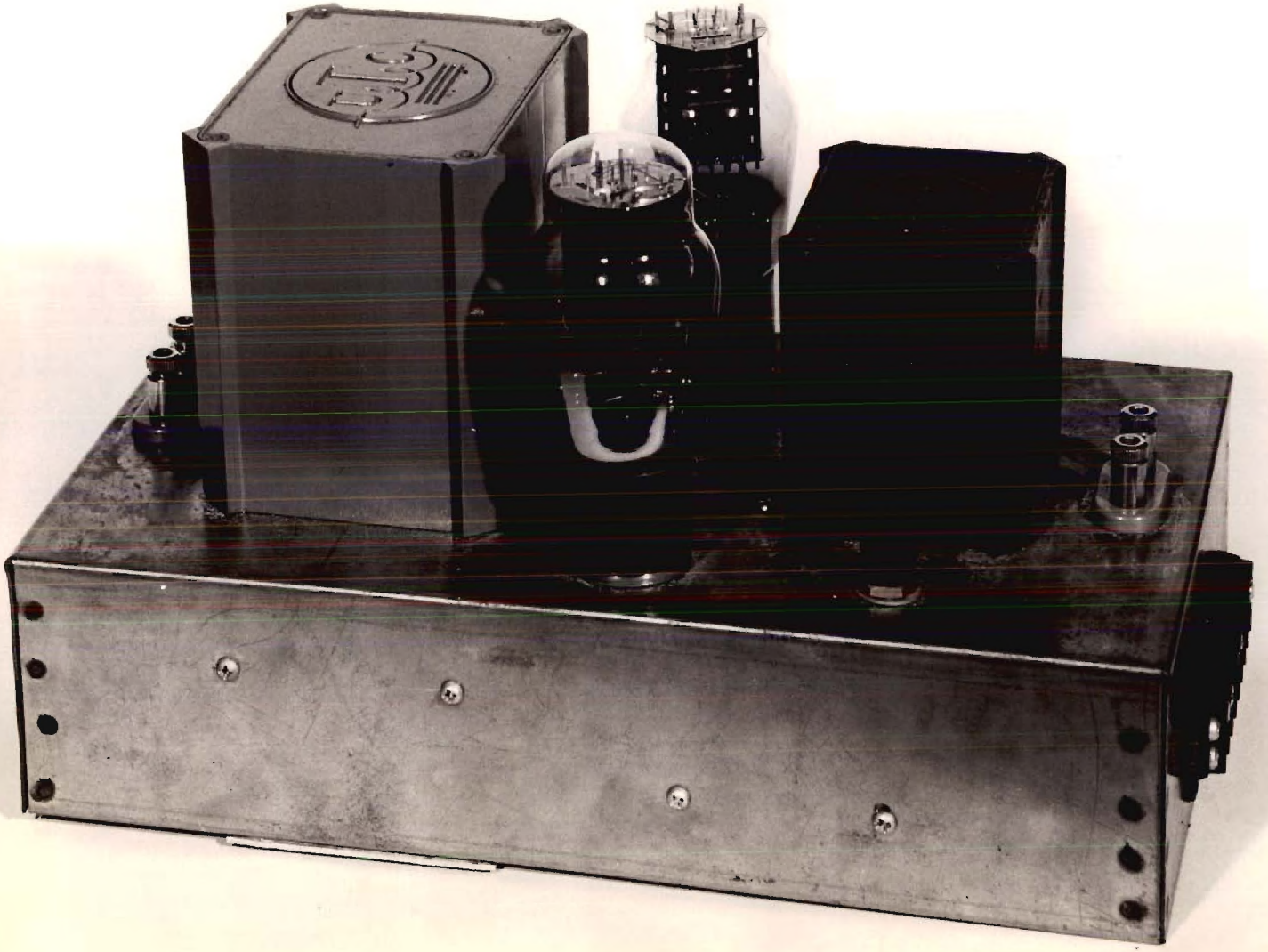

NEUTRALIZED PUSH-PULL AUDIO AMPLIFIER

FIG. 3

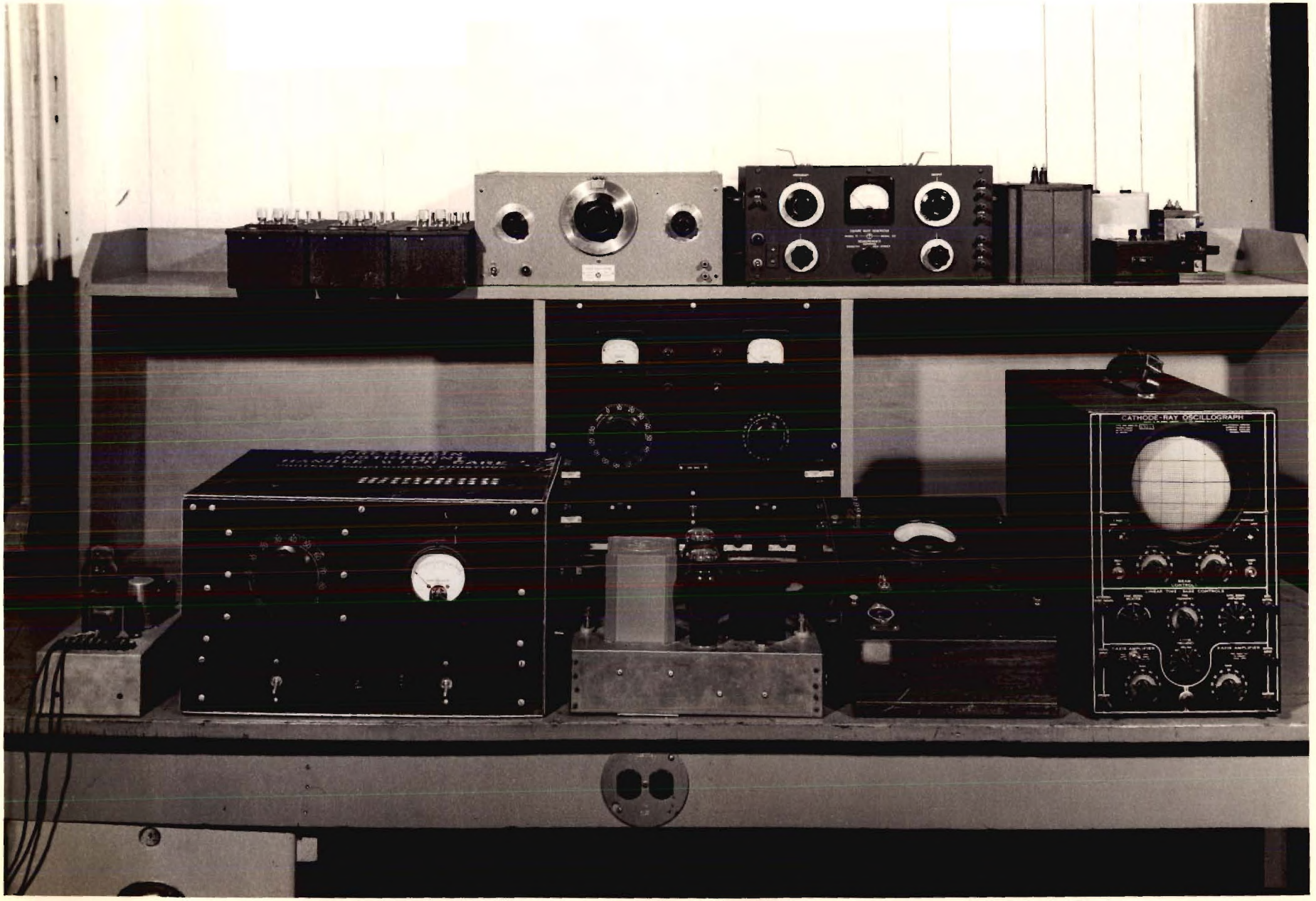

EQUIPMENT USED WITH AMPLIFIER TO MEASURE AMPLIFICATION AND PHASE CHARACTERISTICS

FIG. 4

The Frequency-Response and Phase Characteristics of the Amplifier

With the equipment arranged as described in the preceding section, the initial test was made on the amplifier.

The first test was to determine the overall frequency-response and phase characteristics with the amplifier operation as follows:

Operation - - - - - - - -	Class A
Plate Voltage - - - - - -	250 volts d.c.
Bias Voltage - - - - - -	-45 volts d.c.
Filament Voltage - - - -	6.3 volts a.c.

The signal voltage was maintained constant at 2 volts as the frequency was varied. This in effect gives a zero-impedance signal source.

The results of this test were plotted on Figure 5 and Figure 6. It will be noted that the overall amplification and phase characteristics are of a somewhat unusual shape, when compared with the characteristics of transformer-coupled audio amplifiers generally found in standard literature.

This variation consists of two peaks in the frequency-response curve at the high end of the frequency spectrum, instead of the single peak usually found. The phase characteristics are likewise of an unusual shape over this same frequency region. An explanation for these unusual shapes will be attempted in a later section of this thesis.

It will be noted in Figure 5 that the two peaks in the frequency-response curve are quite pronounced. The frequency response is essen-

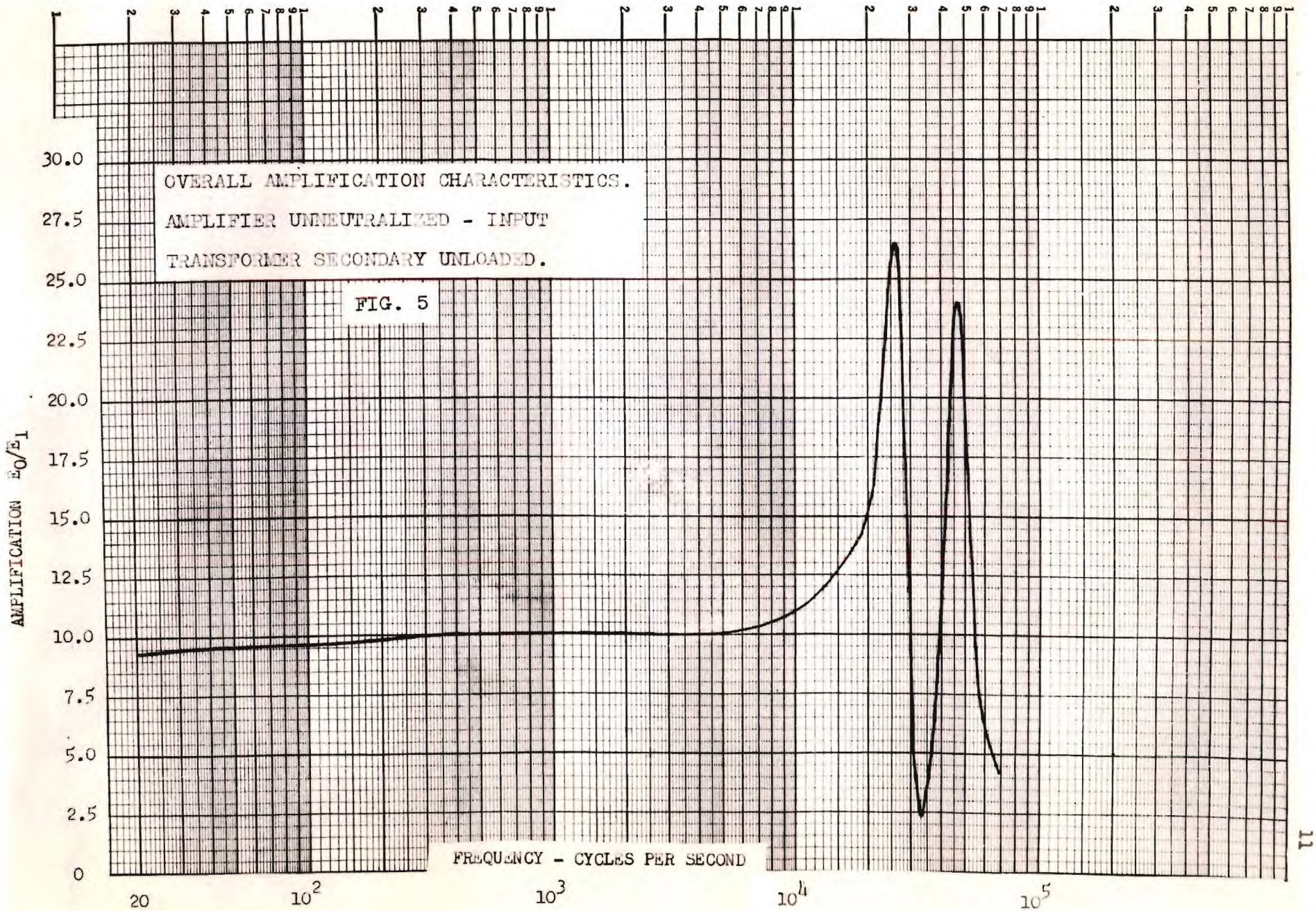
OVERALL AMPLIFICATION CHARACTERISTICS.
AMPLIFIER UNNEUTRALIZED - INPUT
TRANSFORMER SECONDARY UNLOADED.
FIG. 5
AMPLIFICATION E_0/E_1
30.0
27.5
25.0
22.5
20.0
17.5
15.0
12.5
10.0
7.5
5.0
2.5
0
20
10^2
10^3
10^4
10^5
FREQUENCY - CYCLES PER SECOND

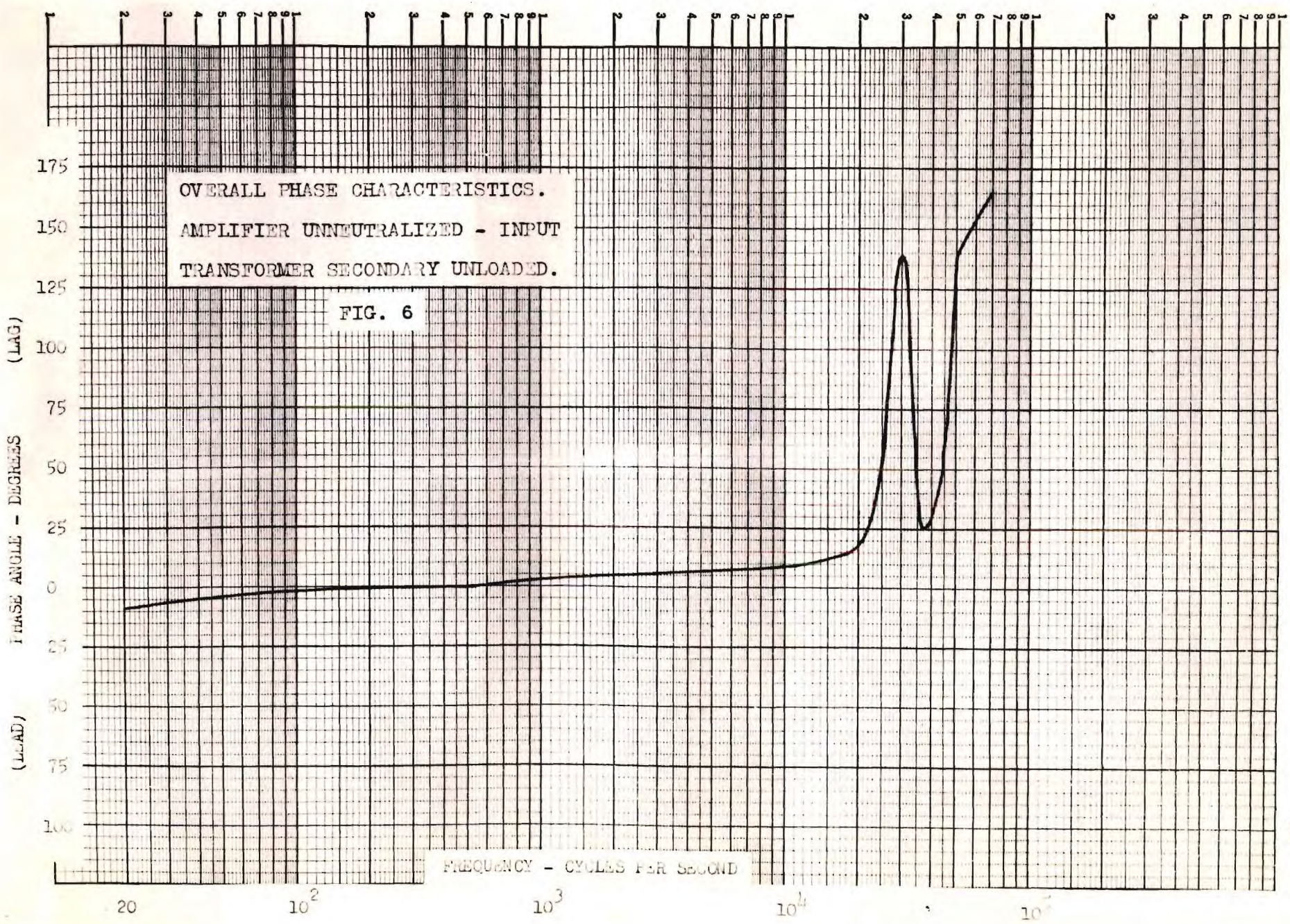
OVERALL PHASE CHARACTERISTICS.
AMPLIFIER UNNEUTRALIZED - INPUT
TRANSFORMER SECONDARY UNLOADED.
FIG. 6
PHASE ANGLE - DEGREES
(LAG)
(LEAD)
175
150
125
100
75
50
25
0
25
50
75
100
FREQUENCY - CYCLES PER SECOND
20
10^2
10^3
10^4
10^5

tially constant from 20 c.p.s. to 10 KC, but above the latter frequency rises very rapidly to a maximum value at 26 KC, falls sharply to a minimum at 33 KC, and then climbs to a second maximum at 47 KC. After which point it again drops off rather rapidly.

To reduce the magnitude of the sharp peaks, the next test was to determine the proper value of shunting resistance to be connected across the secondary terminals of the input transformer. The proper value of shunting resistance was determined by connecting a calibrated decade resistance box across the full transformer secondary, and by trial-and-error method, a value of resistance was selected that reduced the sharp peaks appreciably, but, yet, did not reduce the overall amplification more than 20% over the remaining portion of the audio-frequency spectrum. The value of resistance selected was 100,000 ohms.

With the same operating conditions of Test No. 1, and the shunting resistance connected, the amplification and phase characteristics of the amplifier were again measured and plotted on Figure 7 and Figure 8, respectively. It will now be noted that the frequency-response curve is quite flat from 20 c.p.s. to 29 KC. In a like manner, there is a similar improvement in the phase characteristics in the upper frequency region.

The variations in the phase response follow rather closely the variations observed in the frequency-response curve.

The resistance connected across the secondary of the transformer greatly reduced the circuit Q at the resonance points, and reduced slightly the amplification over the remaining portion of the frequency range. This value of secondary resistance needed can also be determined by another method. This is done by choosing a proper ratio of R_1 and R_2,

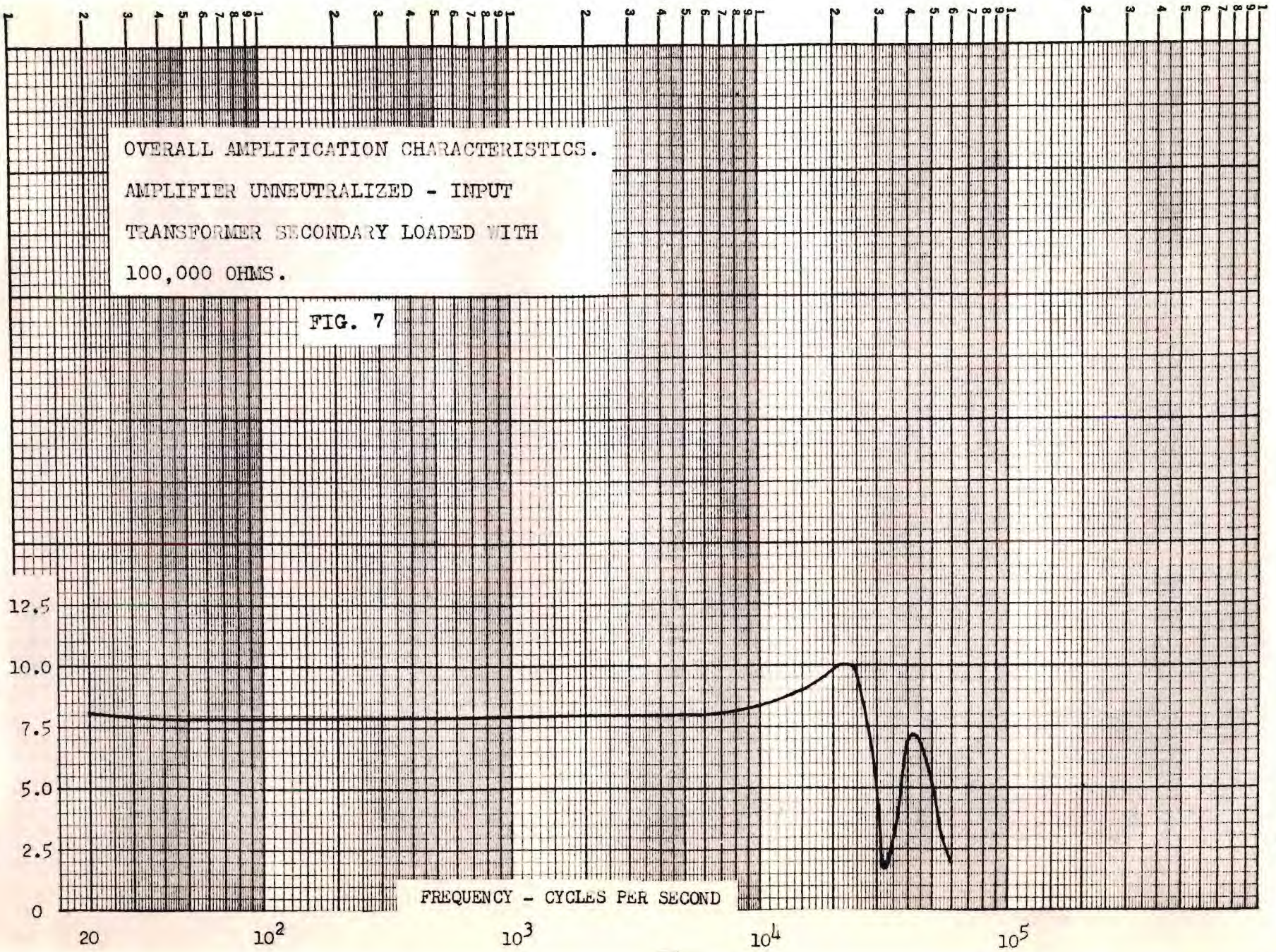
OVERALL AMPLIFICATION CHARACTERISTICS.
AMPLIFIER UNNEUTRALIZED - INPUT
TRANSFORMER SECONDARY LOADED WITH
100,000 OHMS.
FIG. 7
AMPLIFICATION E_O / E_I
12.5
10.0
7.5
5.0
2.5
0
20
10^2
10^3
10^4
10^5
FREQUENCY - CYCLES PER SECOND

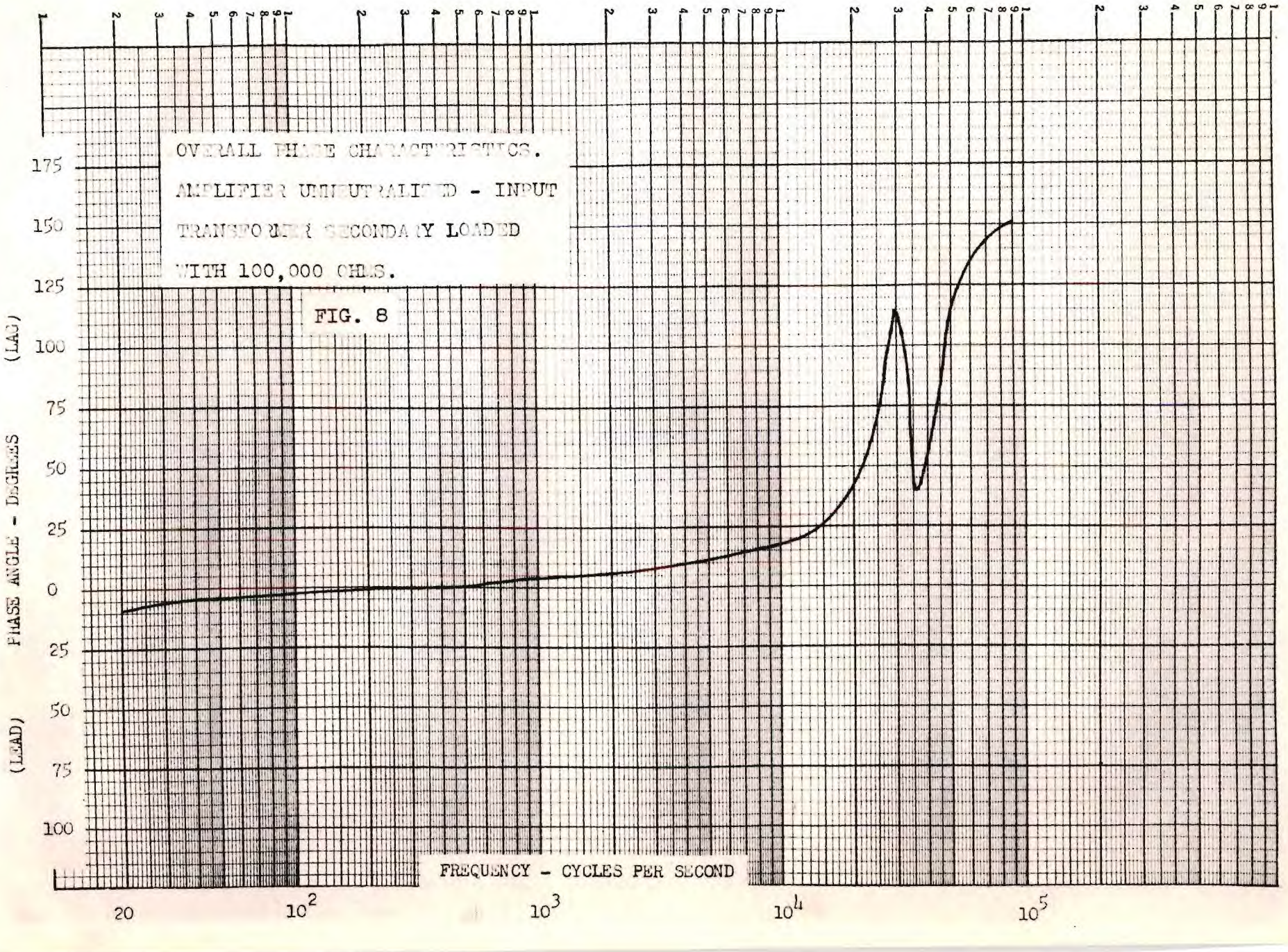
OVERALL PHASE CHARACTERISTICS.
AMPLIFIER UNNEUTRALIZED - INPUT
TRANSFORMER SECONDARY LOADED
WITH 100,000 OHMS.
FIG. 8
PHASE ANGLE - DEGREES
(LAG)
(LEAD)
175
150
125
100
75
50
25
0
25
50
75
100
FREQUENCY - CYCLES PER SECOND
20
10^2
10^3
10^4
10^5

where R_2 is the resistance connected across the transformer secondary, and R_1 is the sum of the equivalent generator resistance and the total transformer resistance in series. This latter method is clearly explained by the article in the footnote.[1]

In general, the value of resistance necessary to give a flat response, is also the value which will give a response to transients which is substantially nonoscillatory.

Next, a series of three tests was made to determine the effect of different values of symmetrical neutralization upon the overall amplification and phase characteristics of the amplifier.

This type of neutralization was accomplished by connecting one variable air-trimmer type condenser from the plate of tube No. 1 to the grid of tube No. 2 and by connecting an identical type condenser from the plate of tube No. 2 to the grid of tube No. 1. These air trimmers were variable in value from a minimum of 7.5 uuf to a maximum of 55 uuf.

To determine the value of capacitance required for complete neutralization, the amplifier was operated under normal conditions, and an oscilloscope was connected across the output load terminals. The plate supply voltage of the amplifier was then cut off, and the magnitude of the signal voltage remaining on the oscilloscope was the amount due to the effect of the grid-to-plate capacitance of the tubes. Each air-trimmer was alternately adjusted until the output voltage shown on the oscilloscope was reduced to zero magnitude.

---

[1]Paul W. Klipsch, "Design of Audio-Frequency Amplifier Circuits Using Transformers," Proc. I.R.E., Vol. 24, p. 219, February, 1936.

The neutralization process was checked at a number of different frequencies from 1.0 KC to 50 KC and was found to be independent of frequency, since the same setting for the neutralizing condensers was arrived at in each case.

Each air trimmer was measured on a General Radio Impedance Bridge, Type 650A, and each was found to be set at 20 uuf. The static grid-to-plate capacitance for each tube was determined to be 17 uuf by the use of standard measuring techniques.

With the amplifier now neutralized, the amplification and phase characteristics were again measured, and the results plotted on Figure 9 and Figure 10, respectively.

By comparison of the frequency-response curves for the neutralized and unneutralized conditions (both with a 100,000 ohm resistance across the secondary of the input transformer), the effect of neutralization can be determined.

A clearer comparison can be made by observing the curves on Figure 11 and Figure 12, which are normalized curves for the two conditions described above.

It can be seen that the neutralization process produces no outstanding changes in the frequency-response characteristic of the amplifier. However, the changes noted are as follows: the first peak was moved from 22 KC up to 25 KC, the minimum dip between peaks was reduced somewhat, but remained at the same position, and the second peak was moved from 42 KC to 45 KC.

By comparison of the two phase characteristics, it can be seen that neutralization causes little change.

The second test of this series was made with each neutralizing

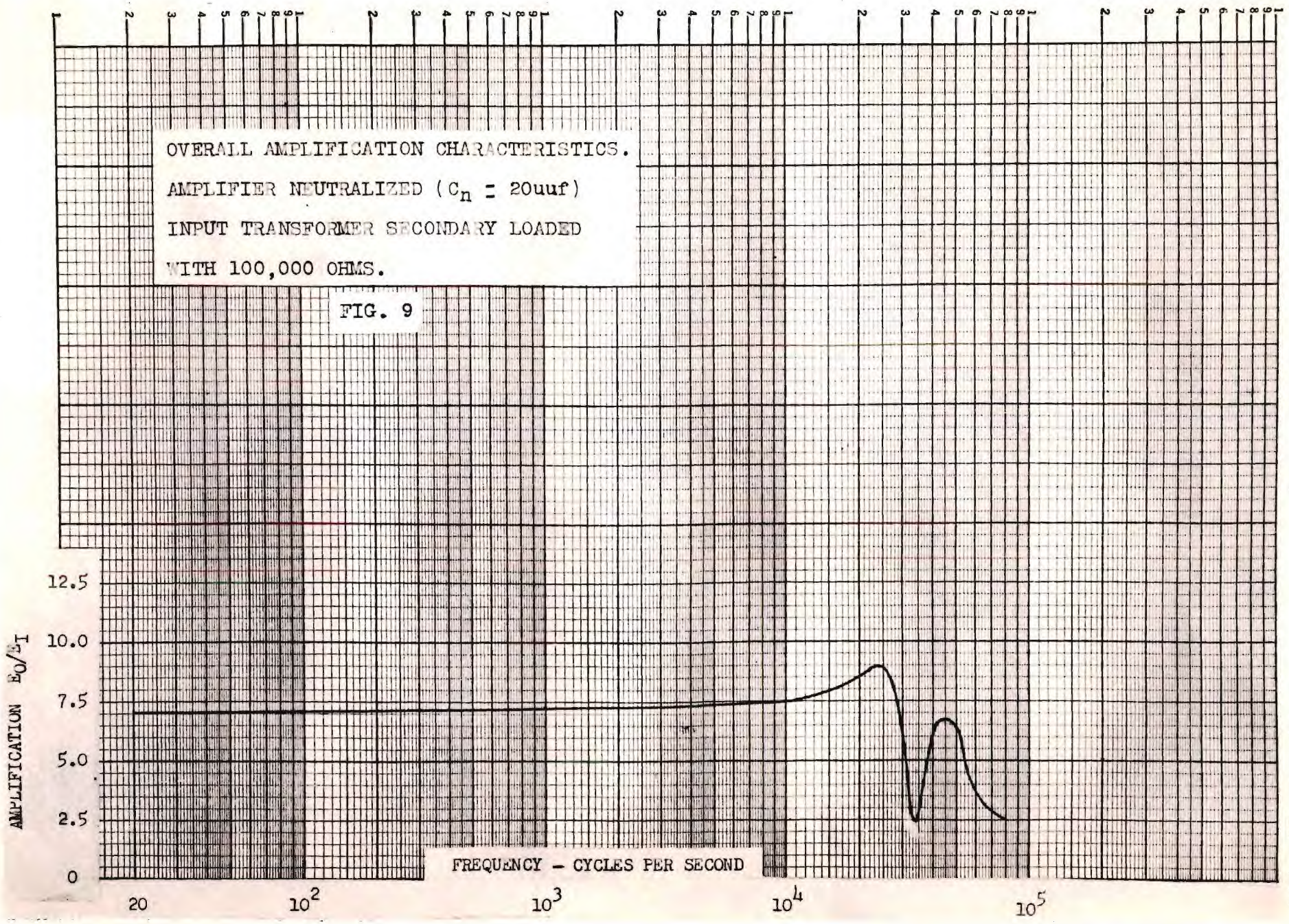
OVERALL AMPLIFICATION CHARACTERISTICS.
AMPLIFIER NEUTRALIZED (C_n = 20uuf)
INPUT TRANSFORMER SECONDARY LOADED
WITH 100,000 OHMS.
FIG. 9
AMPLIFICATION E_O/E_I
12.5
10.0
7.5
5.0
2.5
0
FREQUENCY - CYCLES PER SECOND
20
10^2
10^3
10^4
10^5

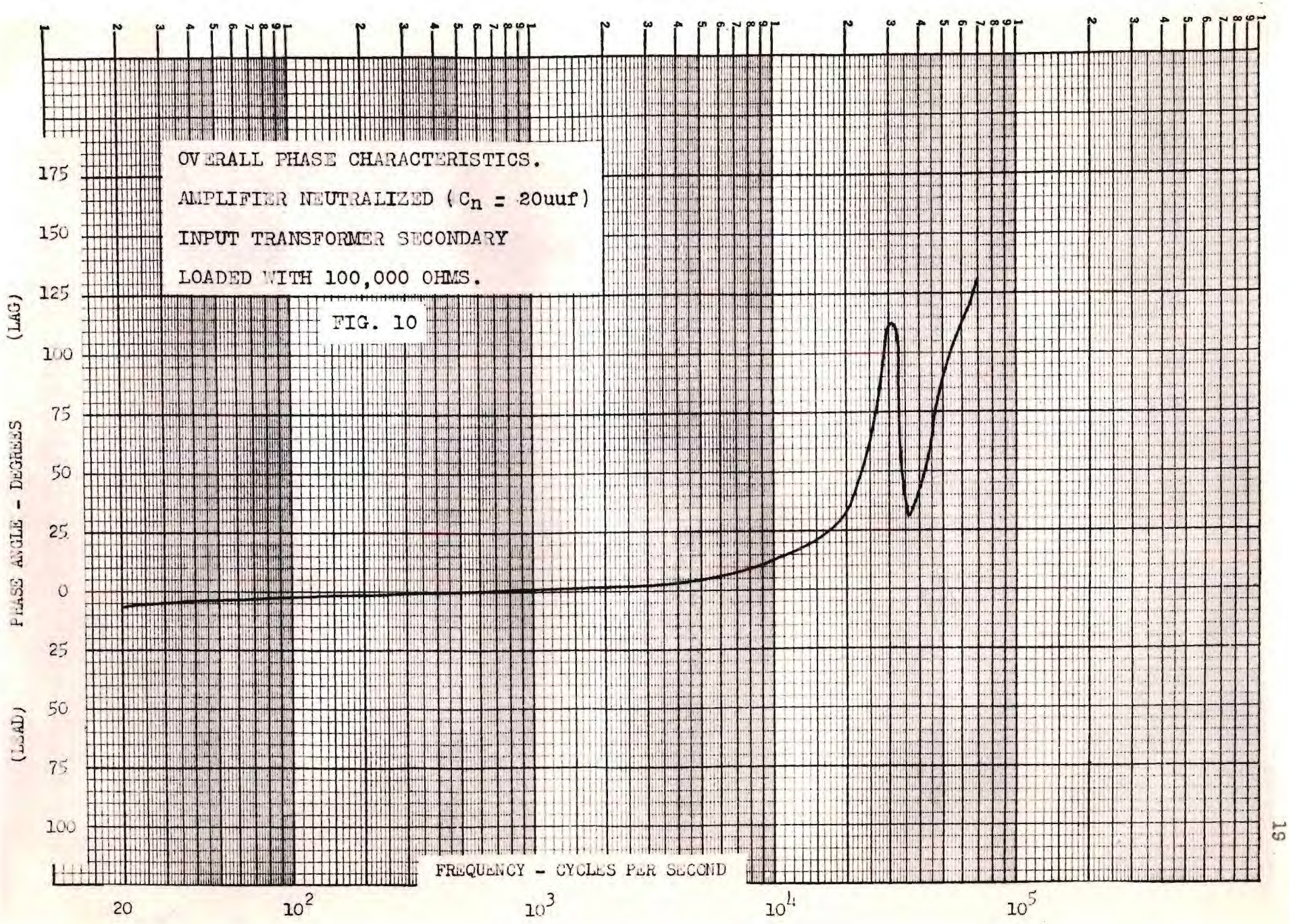
OVERALL PHASE CHARACTERISTICS.
AMPLIFIER NEUTRALIZED (C_n = 20uuf)
INPUT TRANSFORMER SECONDARY
LOADED WITH 100,000 OHMS.
FIG. 10
PHASE ANGLE - DEGREES
(LAG)
(LEAD)
175
150
125
100
75
50
25
0
25
50
75
100
FREQUENCY - CYCLES PER SECOND
20
10^2
10^3
10^4
10^5

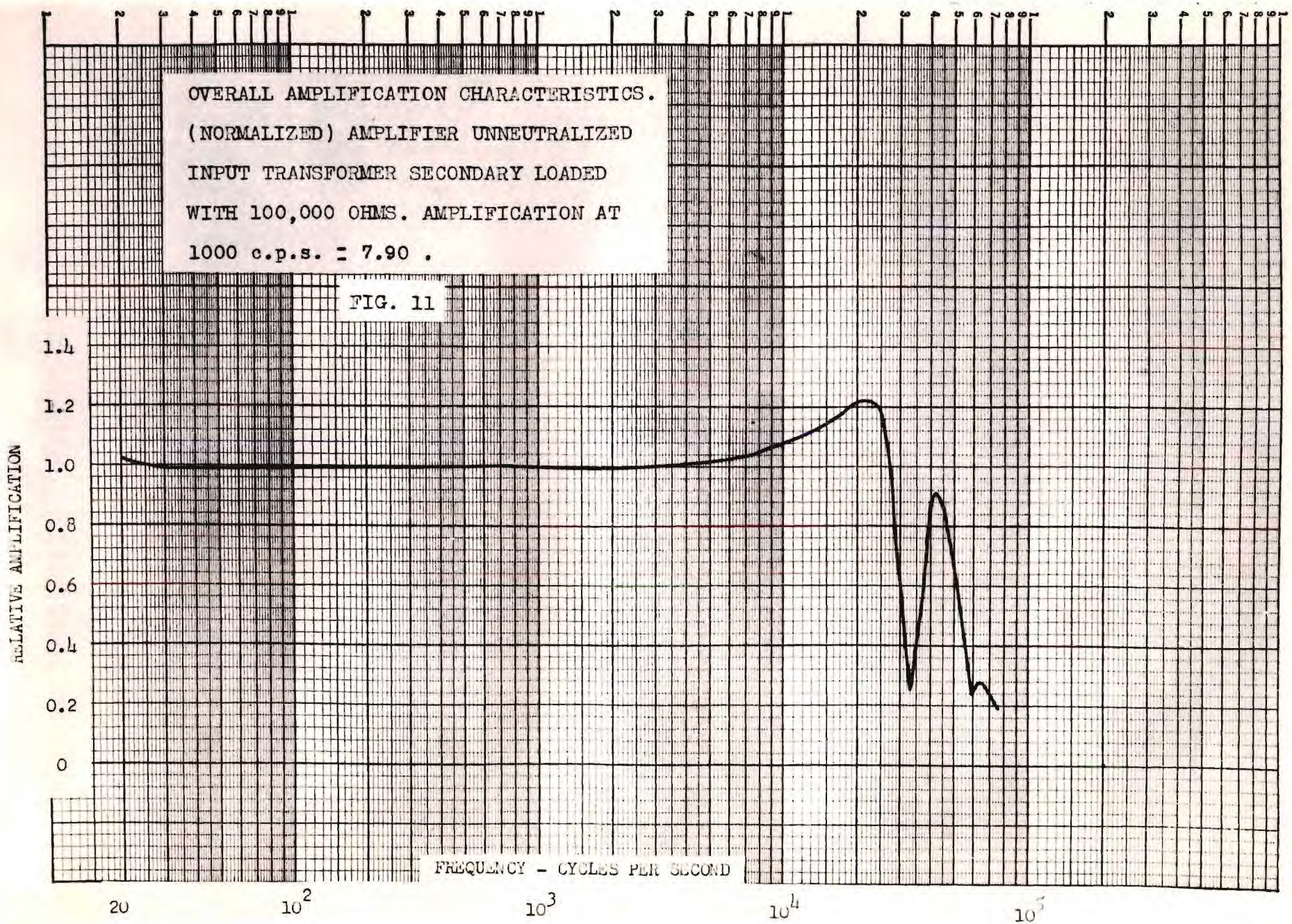
OVERALL AMPLIFICATION CHARACTERISTICS.
(NORMALIZED) AMPLIFIER UNNEUTRALIZED
INPUT TRANSFORMER SECONDARY LOADED
WITH 100,000 OHMS. AMPLIFICATION AT
1000 c.p.s. = 7.90 .
FIG. 11
RELATIVE AMPLIFICATION
1.4
1.2
1.0
0.8
0.6
0.4
0.2
0
FREQUENCY - CYCLES PER SECOND
20
10^2
10^3
10^4
10^5

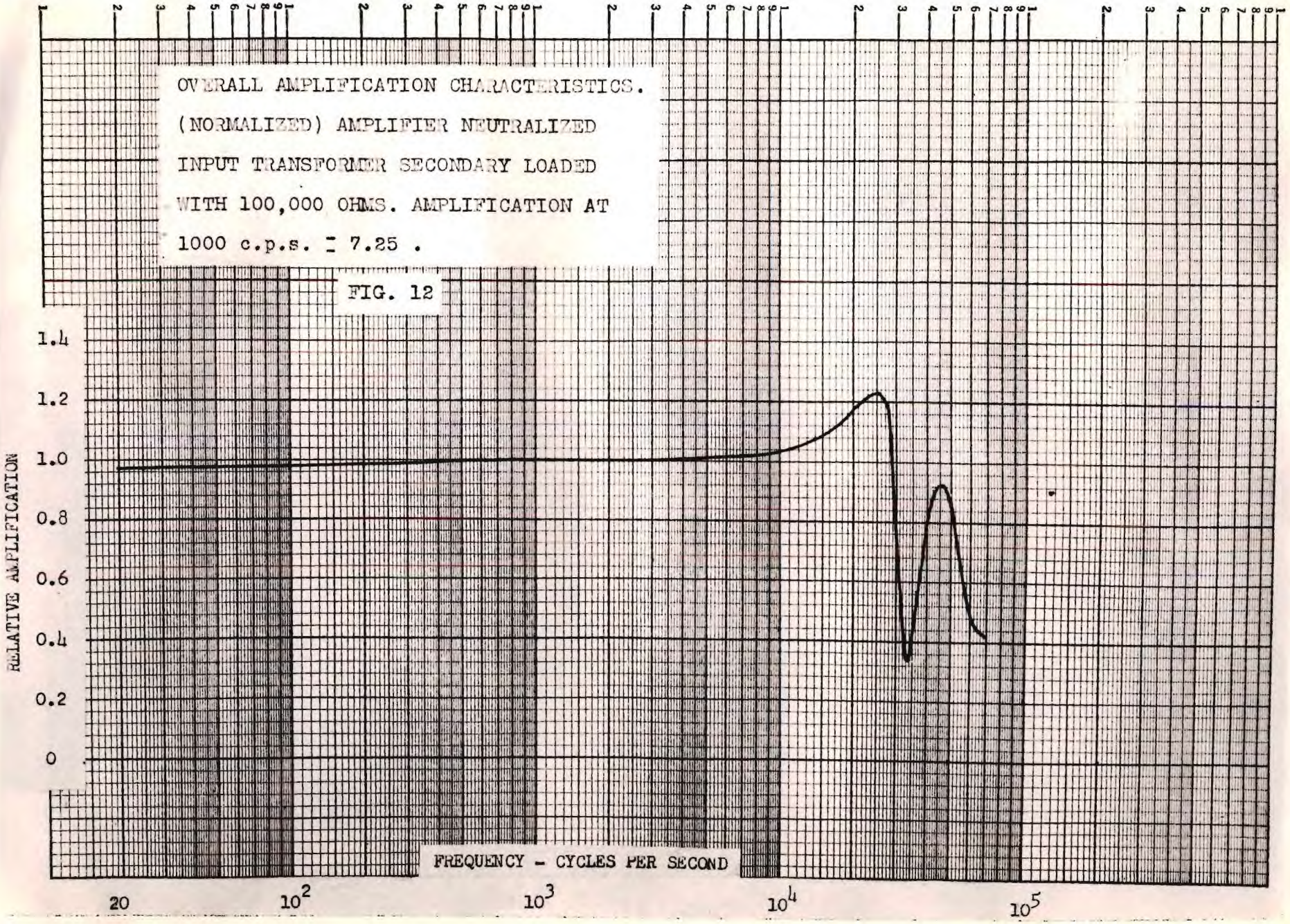
OVERALL AMPLIFICATION CHARACTERISTICS.
(NORMALIZED) AMPLIFIER NEUTRALIZED
INPUT TRANSFORMER SECONDARY LOADED
WITH 100,000 OHMS. AMPLIFICATION AT
1000 c.p.s. = 7.25 .
FIG. 12
RELATIVE AMPLIFICATION
1.4
1.2
1.0
0.8
0.6
0.4
0.2
0
FREQUENCY - CYCLES PER SECOND
20
10^2
10^3
10^4
10^5

condenser set at its minimum value of 7.5 uuf.

By noting Figure 13 and Figure 14, the results of this test can be seen.

The two peaks and the minimum, as shown on the frequency-response curve for this test, are in essentially the same positions as for the preceding test, but the overall amplification is increased slightly.

Once again the phase characteristics remain almost identical in shape as for the preceding test.

The final test of this series was made with the neutralizing condensers set neartheir maximum values. When these condensers were set at their maximum values of 55 uuf, the amplifier broke into strong oscillations at all frequency settings, but with the condensers reset at a value of 50 uuf, the amplifier remained stable up to a frequency of 60 KC, then the amplification increased sharply to 70 KC and at 75 KC the amplifier again developed strong oscillations.

The amplification and phase characteristics for this test are shown on Figure 15 and Figure 16, respectively. These characteristics exhibit pronounced variations from the results of the foregoing tests.

The frequency response is substantially flat to 30 KC. While the second peak remains at the same position as previously, but is considerably reduced in magnitude. The phase characteristic is almost linear to 20 KC, then peaks at 32 KC, drops to a minimum inductive value at 36 KC, and then resumes its gradual rise again.

The results obtained from the conditions, over neutralization, set forth in this test would appear to be the best yet achieved. However, it must be pointed out that the amplifier is on the verge of

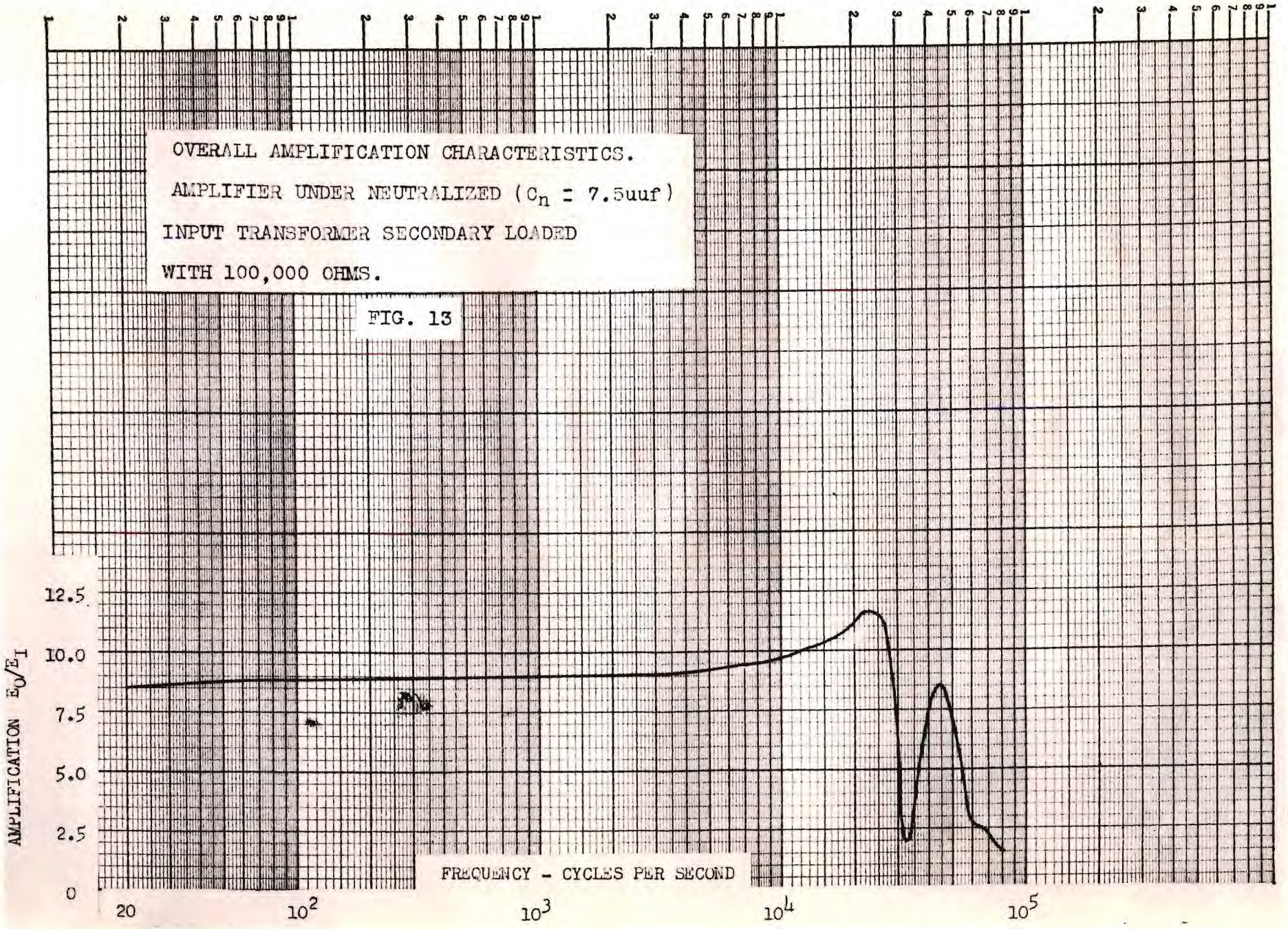
OVERALL AMPLIFICATION CHARACTERISTICS.
AMPLIFIER UNDER NEUTRALIZED (C_n = 7.5uuf)
INPUT TRANSFORMER SECONDARY LOADED
WITH 100,000 OHMS.
FIG. 13
AMPLIFICATION E_O/E_I
12.5
10.0
7.5
5.0
2.5
0
20
10^2
10^3
10^4
10^5
FREQUENCY - CYCLES PER SECOND

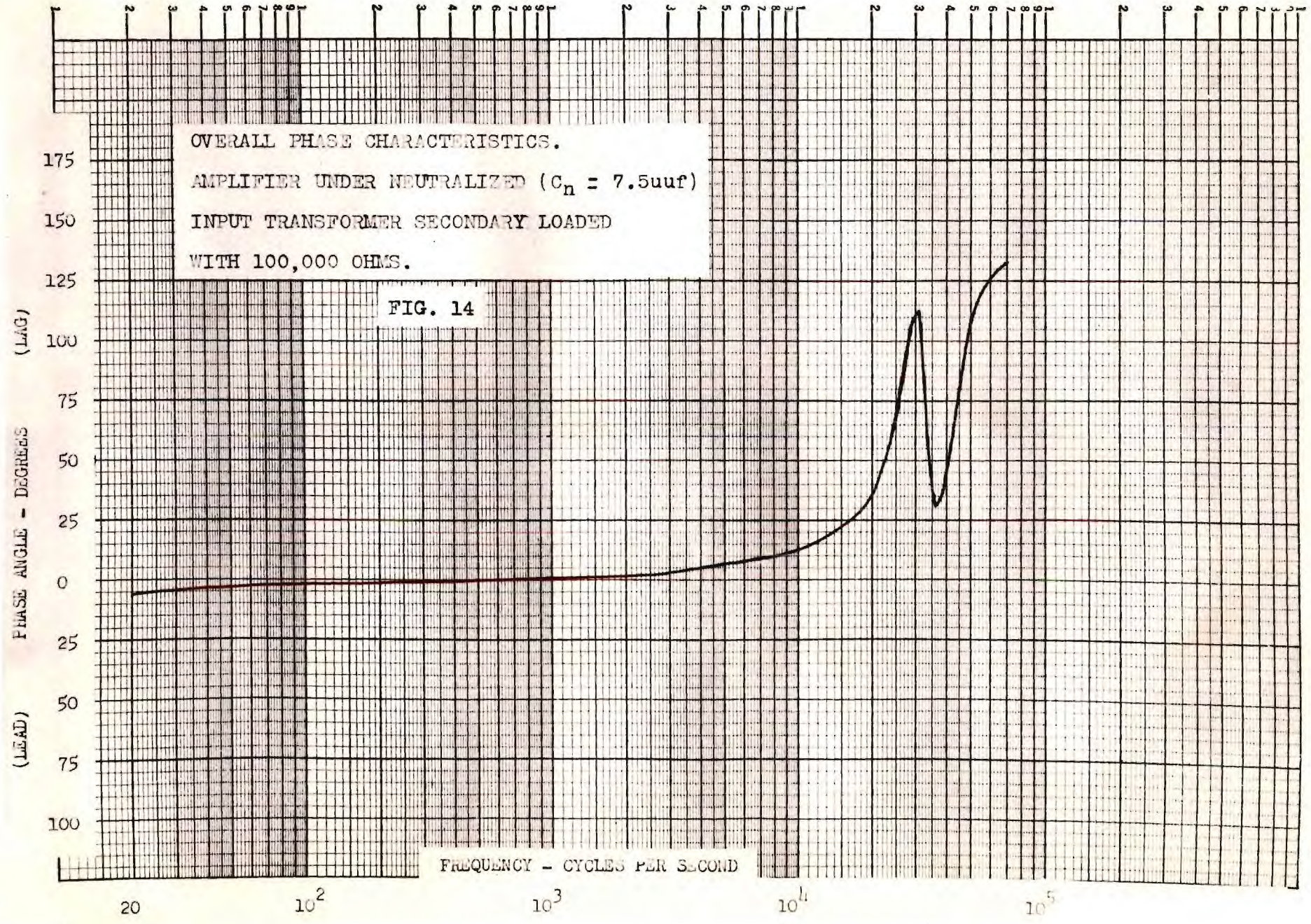
OVERALL PHASE CHARACTERISTICS.
AMPLIFIER UNDER NEUTRALIZED (C_n = 7.5uuf)
INPUT TRANSFORMER SECONDARY LOADED
WITH 100,000 OHMS.
FIG. 14
PHASE ANGLE - DEGREES
(LAG)
(LEAD)
175
150
125
100
75
50
25
0
25
50
75
100
FREQUENCY - CYCLES PER SECOND
20
10^2
10^3
10^4
10^5

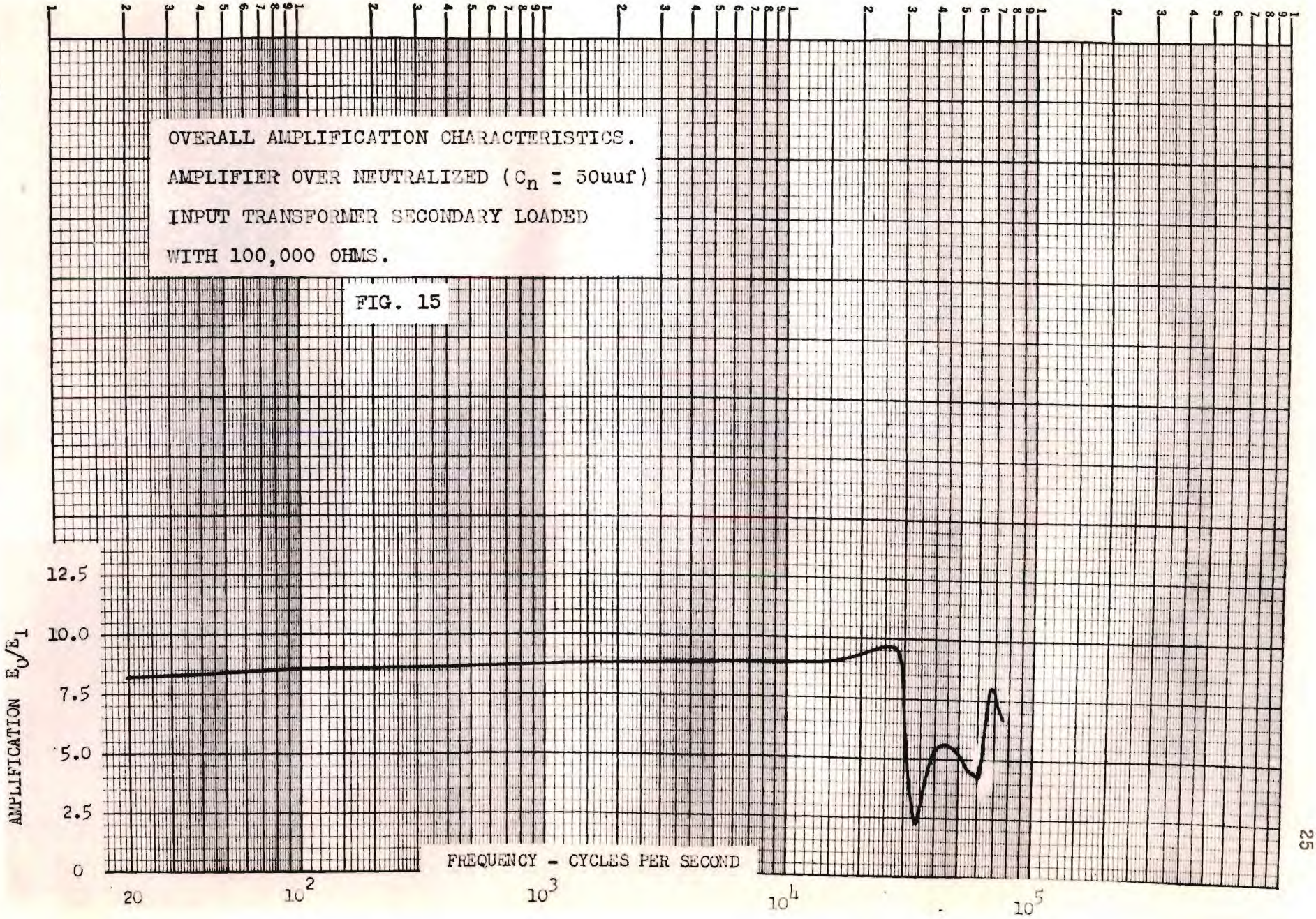
OVERALL AMPLIFICATION CHARACTERISTICS.
AMPLIFIER OVER NEUTRALIZED (C_n = 50uuf)
INPUT TRANSFORMER SECONDARY LOADED
WITH 100,000 OHMS.
FIG. 15
AMPLIFICATION E_0/E_1
12.5
10.0
7.5
5.0
2.5
0
20
10^2
10^3
10^4
10^5
FREQUENCY - CYCLES PER SECOND

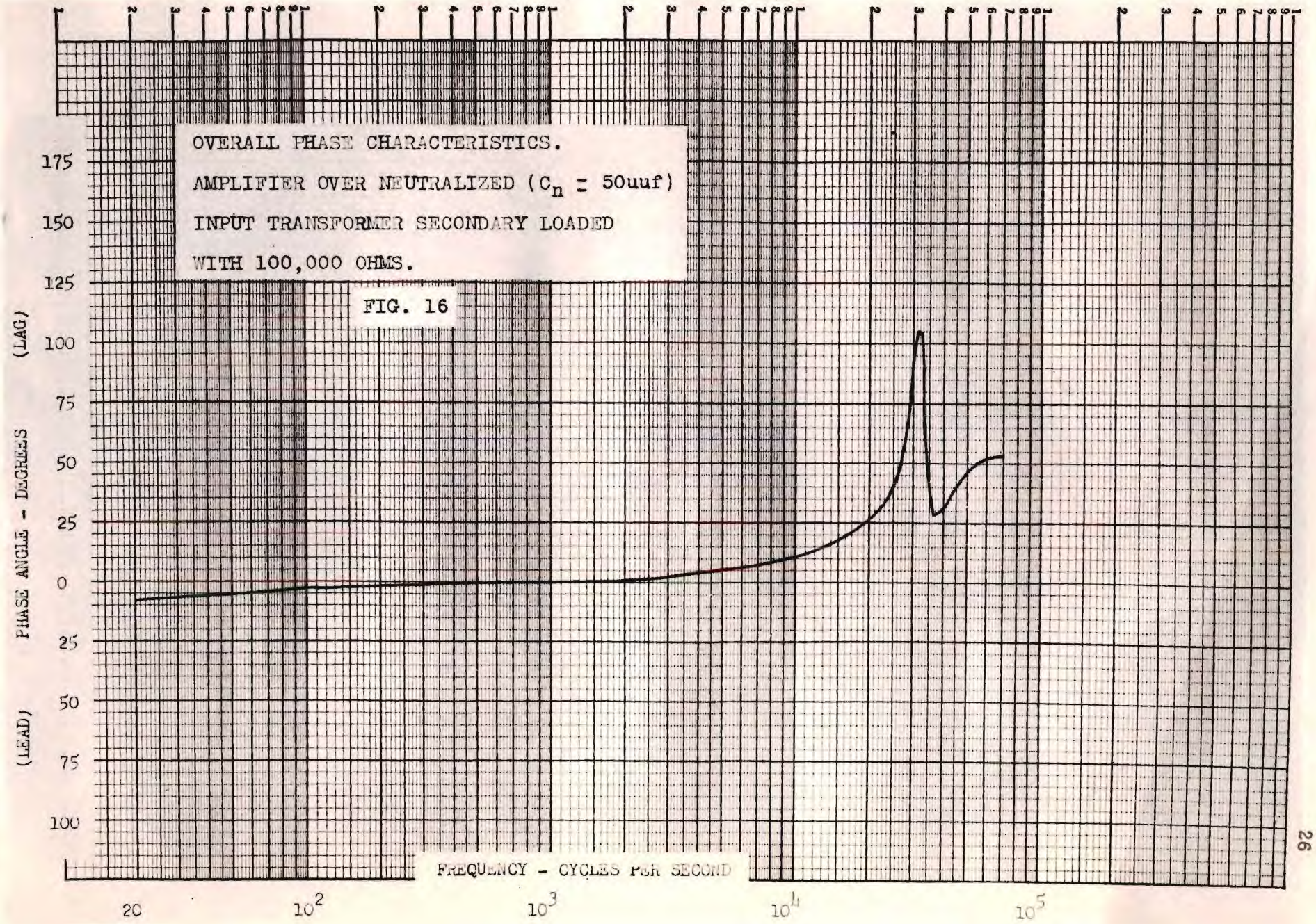
OVERALL PHASE CHARACTERISTICS.
AMPLIFIER OVER NEUTRALIZED (C_n = 50uuf)
INPUT TRANSFORMER SECONDARY LOADED
WITH 100,000 OHMS.
FIG. 16
PHASE ANGLE - DEGREES
(LAG)
(LEAD)
175
150
125
100
75
50
25
0
25
50
75
100
FREQUENCY - CYCLES PER SECOND
20
10^2
10^3
10^4
10^5

oscillating and any transient condition imposed upon the system might cause the amplifier to oscillate. Therefore, this value of neutralizing capacitance must be used with caution to achieve best results.

The next phase was a series of two tests to further determine the effect of neutralization upon an amplifier in which the vacuum tubes had a larger component of grid-to-plate capacitance. To use the basic amplifier already constructed, external capacitances were connected from the grid to the plate of each tube immediately at the pins of the tube sockets. A value of 20 uuf was chosen for each of these added capacitances. Thus a tube which now has an equivalent value of 37 uuf grid-to-plate capacitance was simulated.

The first test of this new series was to readjust the neutralizing condensers, by the same method previously outlined, to achieve neutralization under the newly imposed conditions. This new value of neutralization capacitance was found to be 40 uuf for each condenser.

The results of this test were plotted on Figure 17 and Figure 18.

The second test of this series was made by resetting the neutralizing condensers to their minimum value of 7.5 uuf, with the results shown on Figure 19 and Figure 20.

The overall amplification and phase characteristics for these last two tests are quite similar. Points on the two frequency-response curves coincide closely. The position and magnitude of the peaks coincide, while the overall amplification is almost equal.

The two phase characteristics likewise exhibit a high degree of similarity.

Therefore, it would appear that for the conditions imposed for

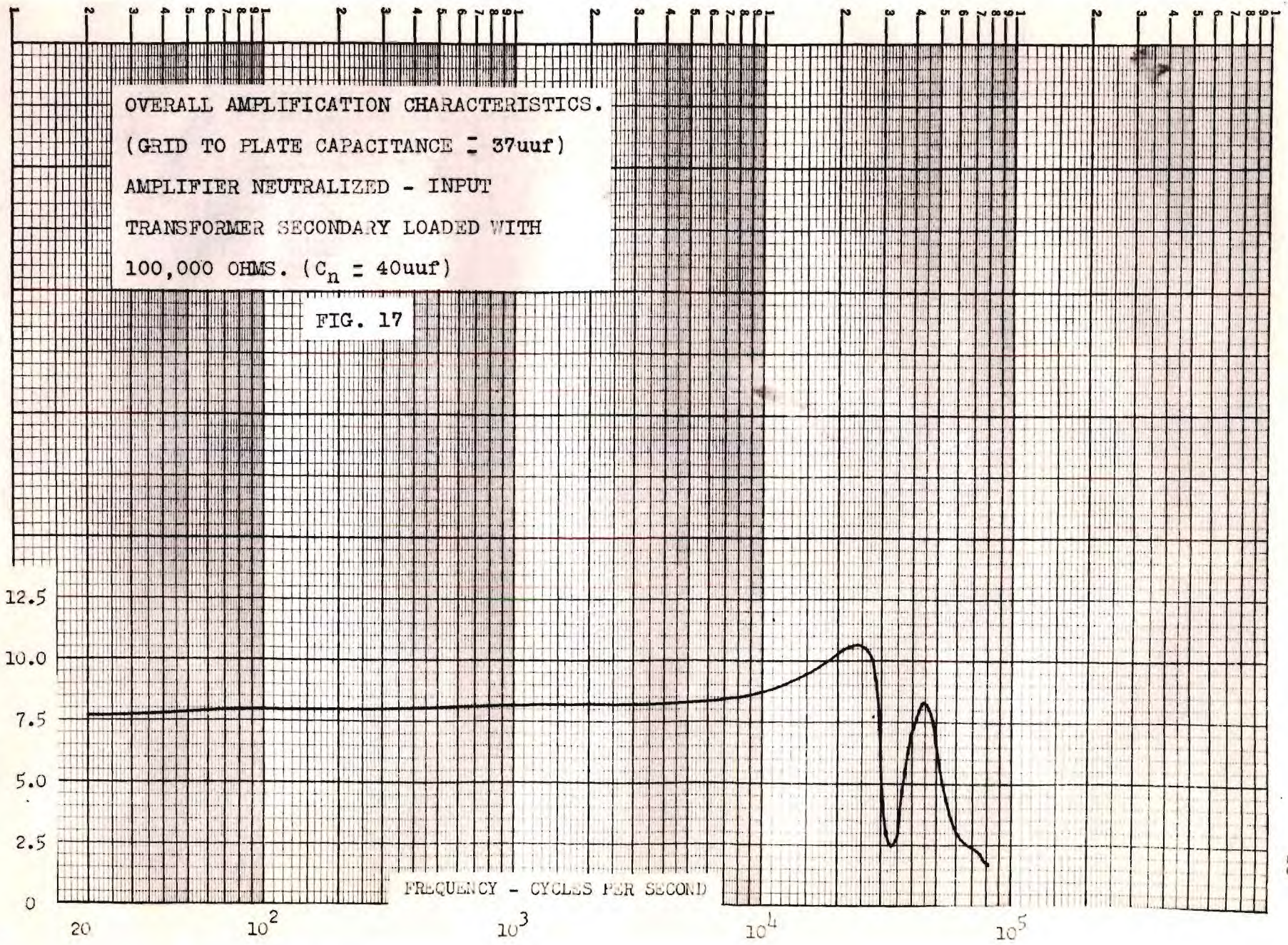
OVERALL AMPLIFICATION CHARACTERISTICS.
(GRID TO PLATE CAPACITANCE = 37uuf)
AMPLIFIER NEUTRALIZED - INPUT
TRANSFORMER SECONDARY LOADED WITH
100,000 OHMS. (C_n = 40uuf)
FIG. 17
AMPLIFICATION E_0/E_1
12.5
10.0
7.5
5.0
2.5
0
20
10^2
10^3
10^4
10^5
FREQUENCY - CYCLES PER SECOND

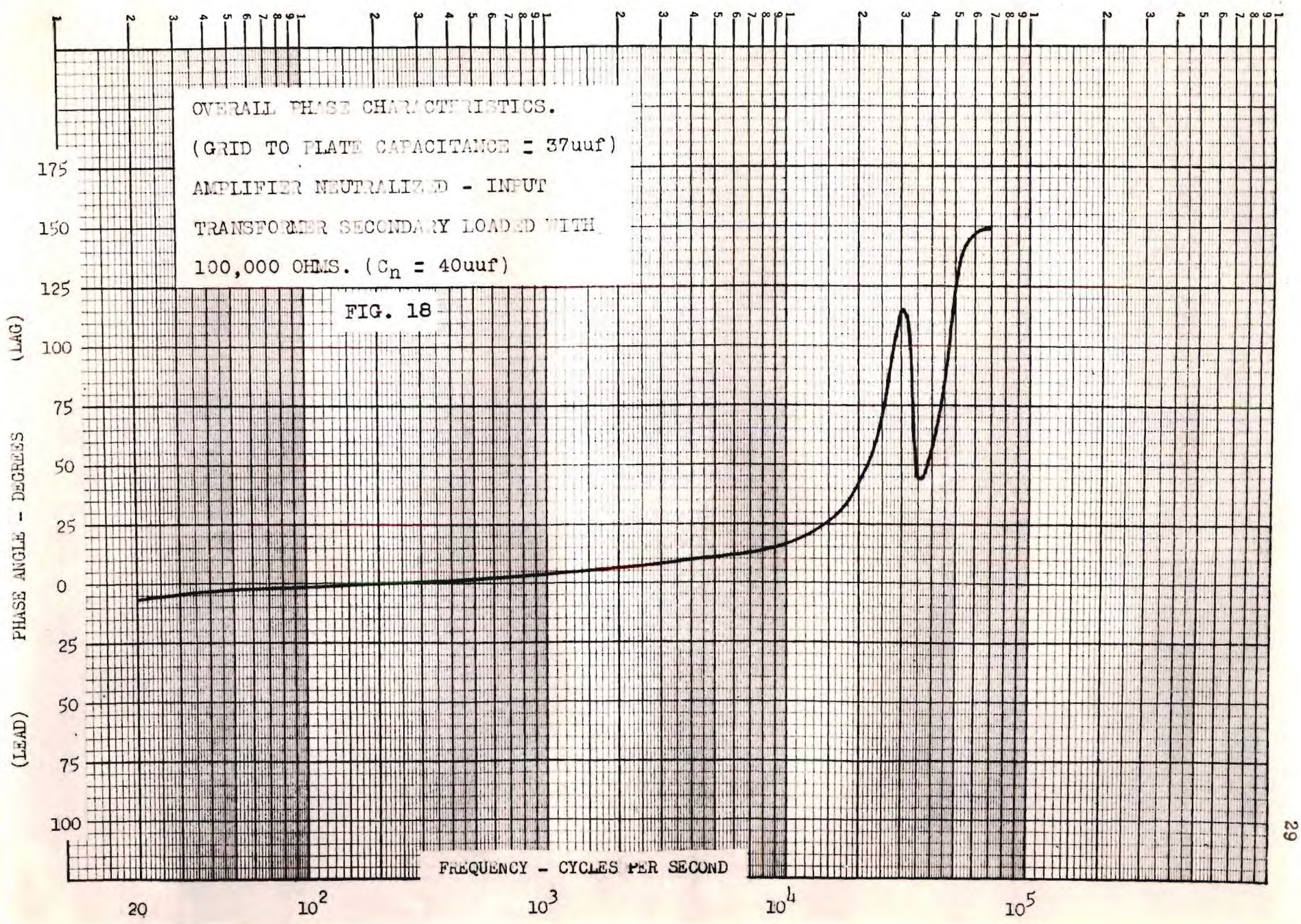
OVERALL PHASE CHARACTERISTICS.
(GRID TO PLATE CAPACITANCE = 37uuf)
AMPLIFIER NEUTRALIZED - INPUT
TRANSFORMER SECONDARY LOADED WITH
100,000 OHMS. (C_n = 40uuf)
FIG. 18
PHASE ANGLE - DEGREES
(LAG)
(LEAD)
175
150
125
100
75
50
25
0
25
50
75
100
FREQUENCY - CYCLES PER SECOND
20
10^2
10^3
10^4
10^5

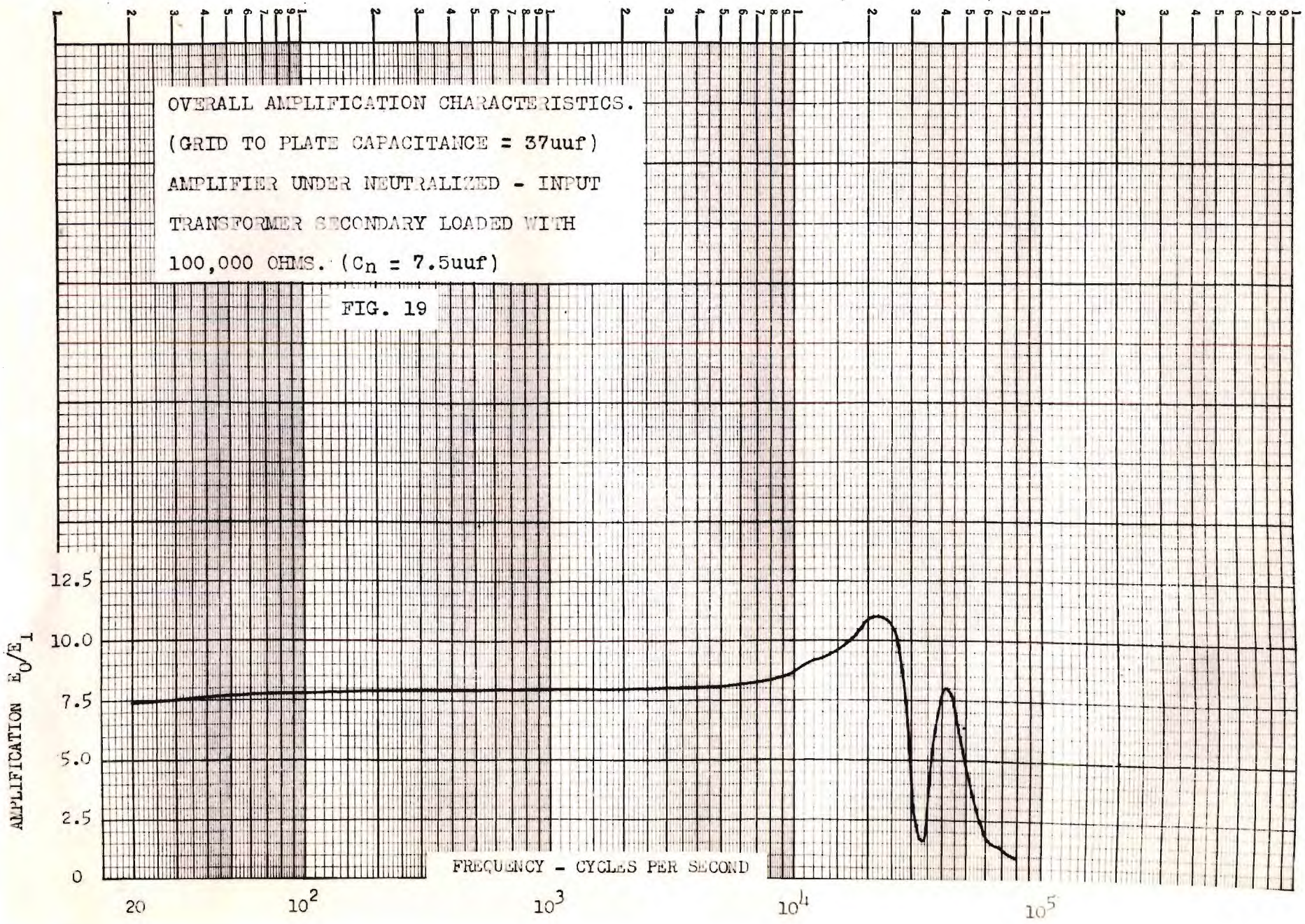
OVERALL AMPLIFICATION CHARACTERISTICS.
(GRID TO PLATE CAPACITANCE = 37uuf)
AMPLIFIER UNDER NEUTRALIZED - INPUT
TRANSFORMER SECONDARY LOADED WITH
100,000 OHMS. (C_n = 7.5uuf)
FIG. 19
AMPLIFICATION E_0/E_1
12.5
10.0
7.5
5.0
2.5
0
20
10^2
10^3
10^4
10^5
FREQUENCY - CYCLES PER SECOND

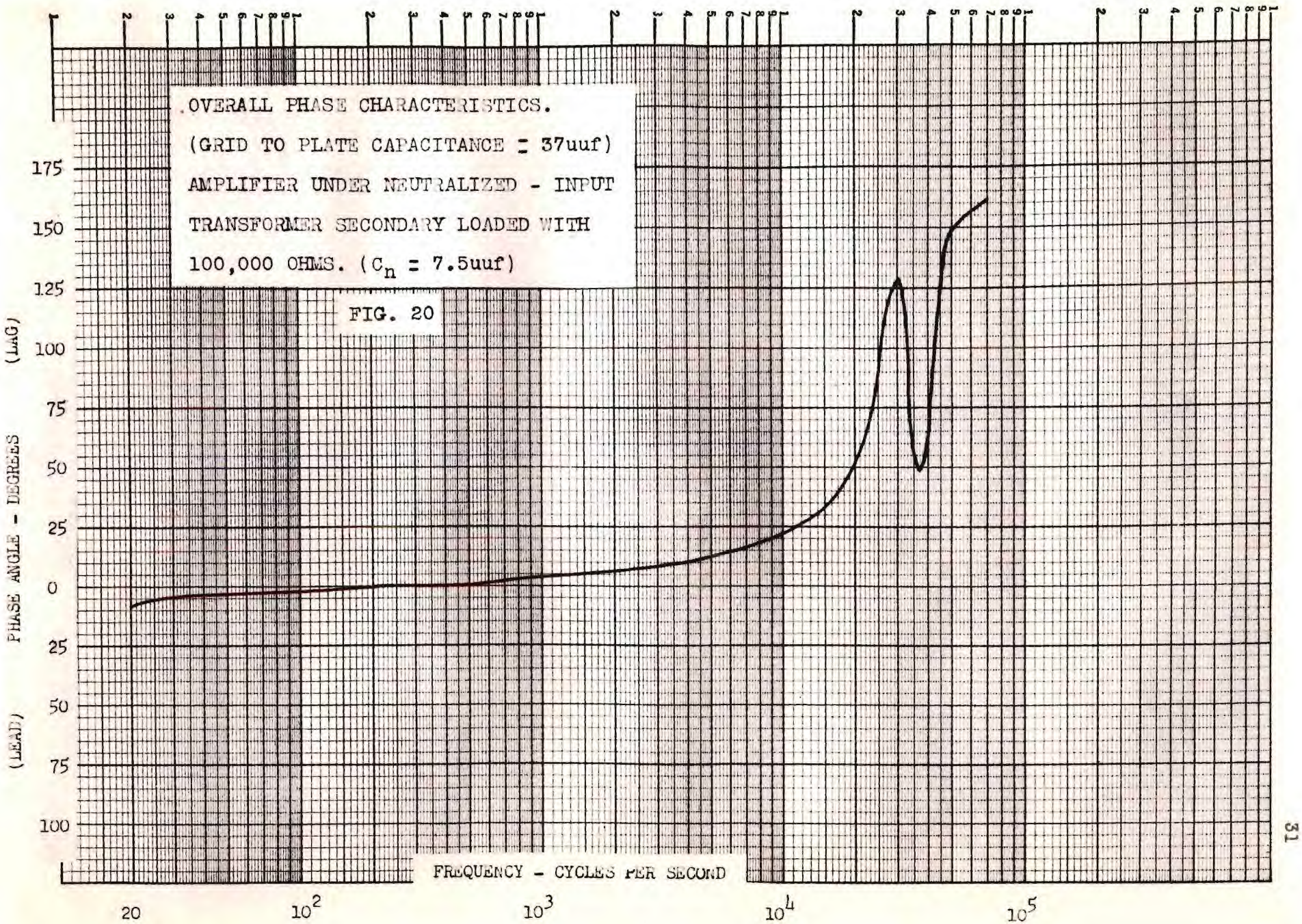
OVERALL PHASE CHARACTERISTICS.
(GRID TO PLATE CAPACITANCE = 37uuf)
AMPLIFIER UNDER NEUTRALIZED - INPUT
TRANSFORMER SECONDARY LOADED WITH
100,000 OHMS. (C_n = 7.5uuf)
FIG. 20
PHASE ANGLE - DEGREES
(LAG)
(LEAD)
175
150
125
100
75
50
25
0
25
50
75
100
FREQUENCY - CYCLES PER SECOND
20
10^2
10^3
10^4
10^5

these last tests, two divergent values of neutralization capacitance do not appreciably alter the overall amplifier characteristics.

The voltage ratio characteristics, E_s/E_p, and the phase characteristics of the input transformer were next measured.

Since it is apparent from the preceding tests that normal values of neutralization do not appreciably alter the overall amplification and phase characteristics of the amplifier, the following tests were made with the amplifier unneutralized.

The first test was performed with the amplifier connected and operating under normal conditions, and with the input transformer secondary unloaded. The frequency response was measured and is shown on Figure 21. It will be noted by referring to this curve that the voltage ratio characteristic for the input transformer follows quite closely the shape of the overall amplification characteristic of the amplifier, with one notable exception. This exception is a minor peak and minimum located at 12 KC and 13.5 KC, respectively.

An attempt to measure the phase characteristics showed a large degree of wave-form distortion on the oscilloscope for the range from 10 KC to 40 KC. It was, therefore, impossible to obtain valid information to plot the phase characteristics from this test.

A second test was made on the transformer with the amplifier connected. This time with a 100,000-ohm resistance connected across the transformer secondary. The frequency-response measurements were made and the results recorded on Figure 22. The two major peaks were reduced in magnitude but unchanged in position. Again there was a minor peak and minimum at the same frequency positions noted in preceding test.

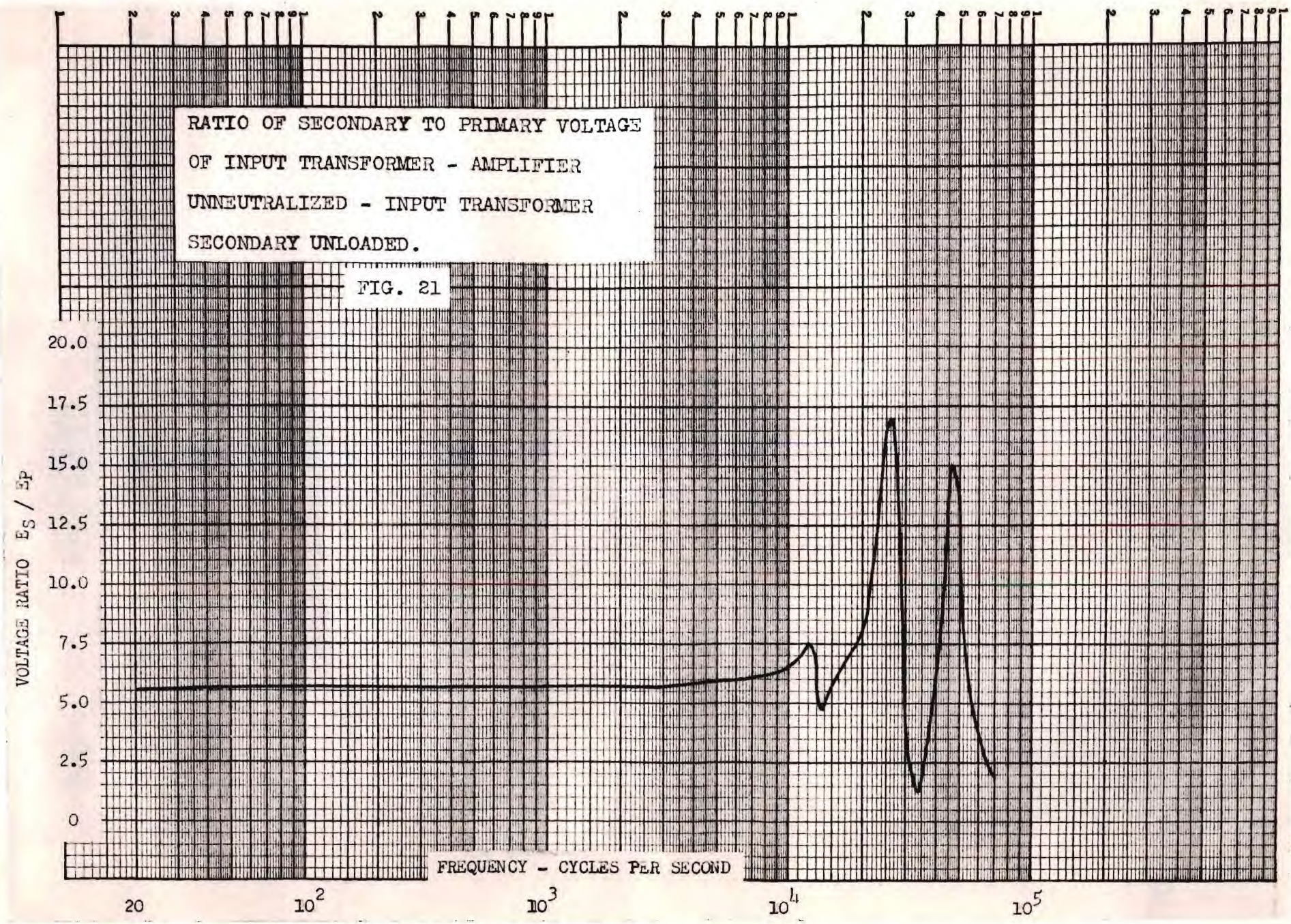
RATIO OF SECONDARY TO PRIMARY VOLTAGE
OF INPUT TRANSFORMER - AMPLIFIER
UNNEUTRALIZED - INPUT TRANSFORMER
SECONDARY UNLOADED.
FIG. 21
VOLTAGE RATIO E_S / E_P
20.0
17.5
15.0
12.5
10.0
7.5
5.0
2.5
0
FREQUENCY - CYCLES PER SECOND
20
10^2
10^3
10^4
10^5

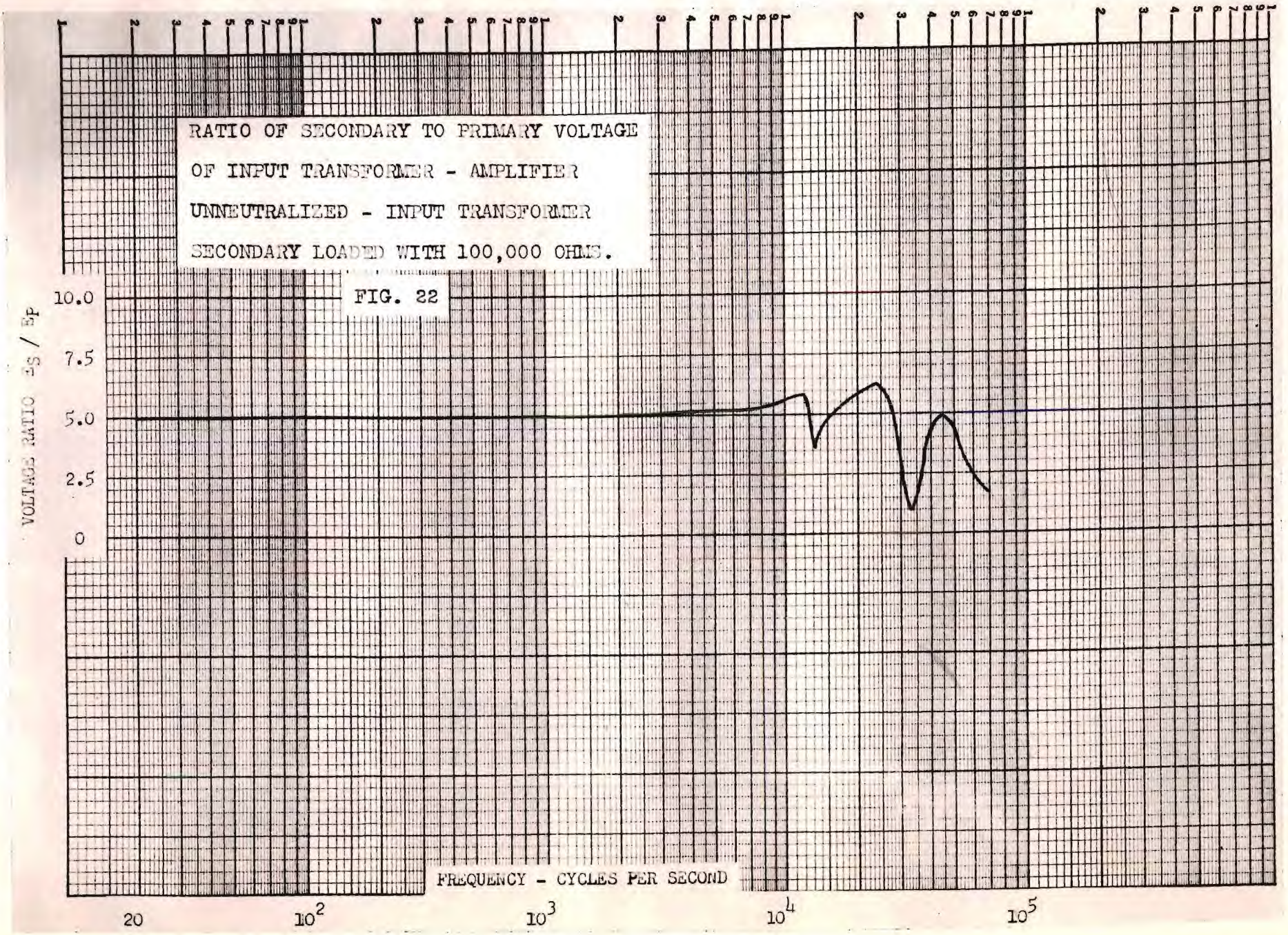
RATIO OF SECONDARY TO PRIMARY VOLTAGE
OF INPUT TRANSFORMER - AMPLIFIER
UNNEUTRALIZED - INPUT TRANSFORMER
SECONDARY LOADED WITH 100,000 OHMS.
FIG. 22
VOLTAGE RATIO Es / Ep
10.0
7.5
5.0
2.5
0
FREQUENCY - CYCLES PER SECOND
20
10^2
10^3
10^4
10^5

For this test it was possible to measure the phase characteristics of the transformer, and the results are shown on Figure 23. The variations of the phase characteristics coincide with the peaks shown on the curve plotted for the frequency response.

The minor variations at 12 KC and 13.5 KC which show up on the frequency-response characteristics of the two preceding tests are not apparent in the overall frequency-response characteristics of the amplifier. Therefore, the input transformer was removed from the circuit and its characteristics were again measured without the amplifier load connected.

The results of this last test are shown on Figure 24 and Figure 25.

It will now be noted that the frequency-response characteristic of the input transformer does not show a minor peak and minimum in the 12 KC and 13.5 KC region, as was previously observed.

Since the impedance that the transformer secondary works into is a function of the frequency and is dependent upon the tube plate load impedance which is reflected back into the grid circuit, it would appear likely that the vacuum tube input impedance variations cause the minor peak and minimum.

An additional fact gathered from this last frequency-response curve is that the input transformer characteristic shows a minor peak at 85 KC. This minor peak is verified by the transformer secondary short-circuit impedance locus plot shown in Figure 37 in a later section.

This peak at 85 KC does not manifest itself in the overall frequency-response characteristic of the amplifier. This fact is

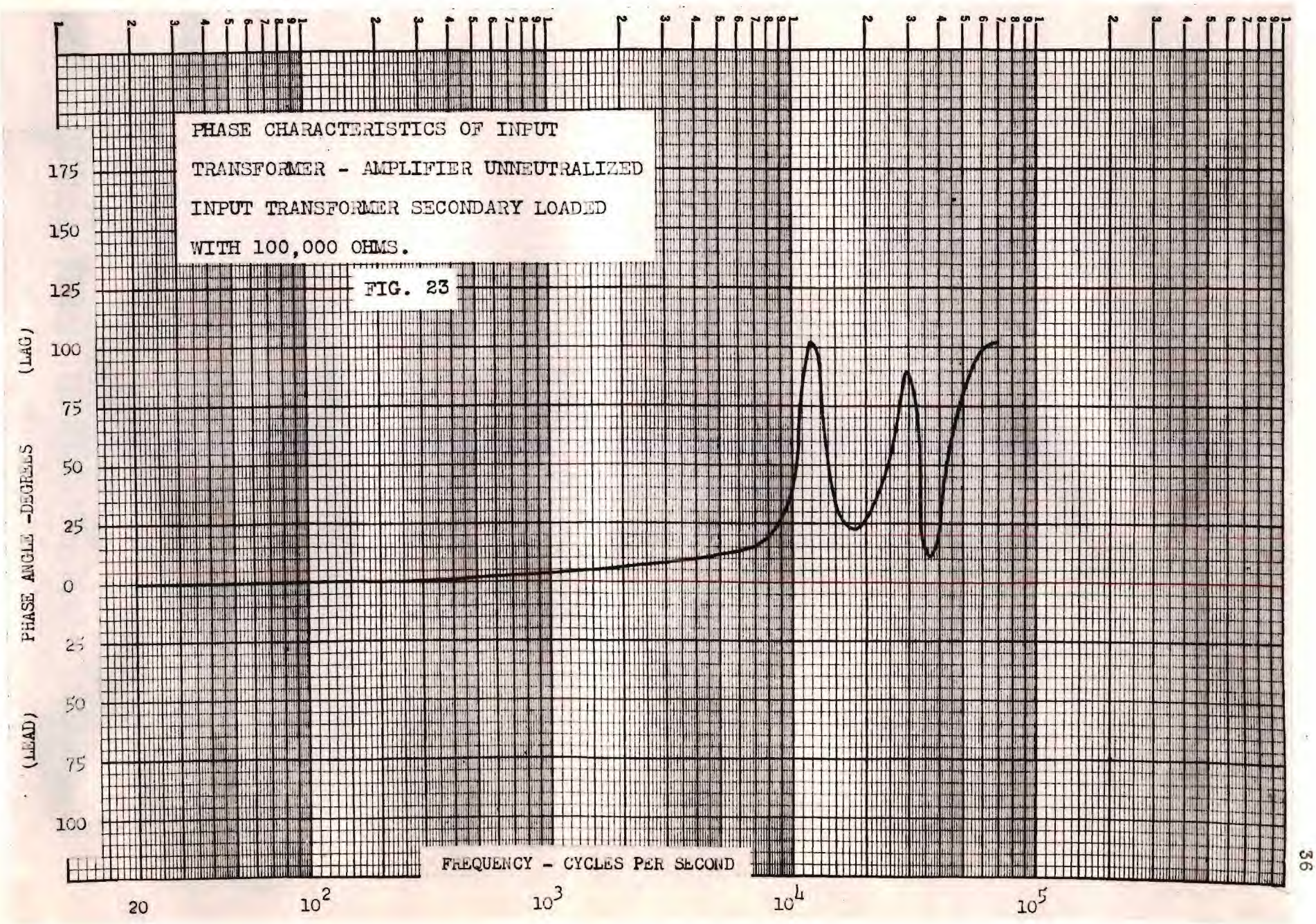
PHASE CHARACTERISTICS OF INPUT
TRANSFORMER - AMPLIFIER UNNEUTRALIZED
INPUT TRANSFORMER SECONDARY LOADED
WITH 100,000 OHMS.
FIG. 23
PHASE ANGLE -DEGREES
(LAG)
(LEAD)
175
150
125
100
75
50
25
0
25
50
75
100
FREQUENCY - CYCLES PER SECOND
20
10^2
10^3
10^4
10^5

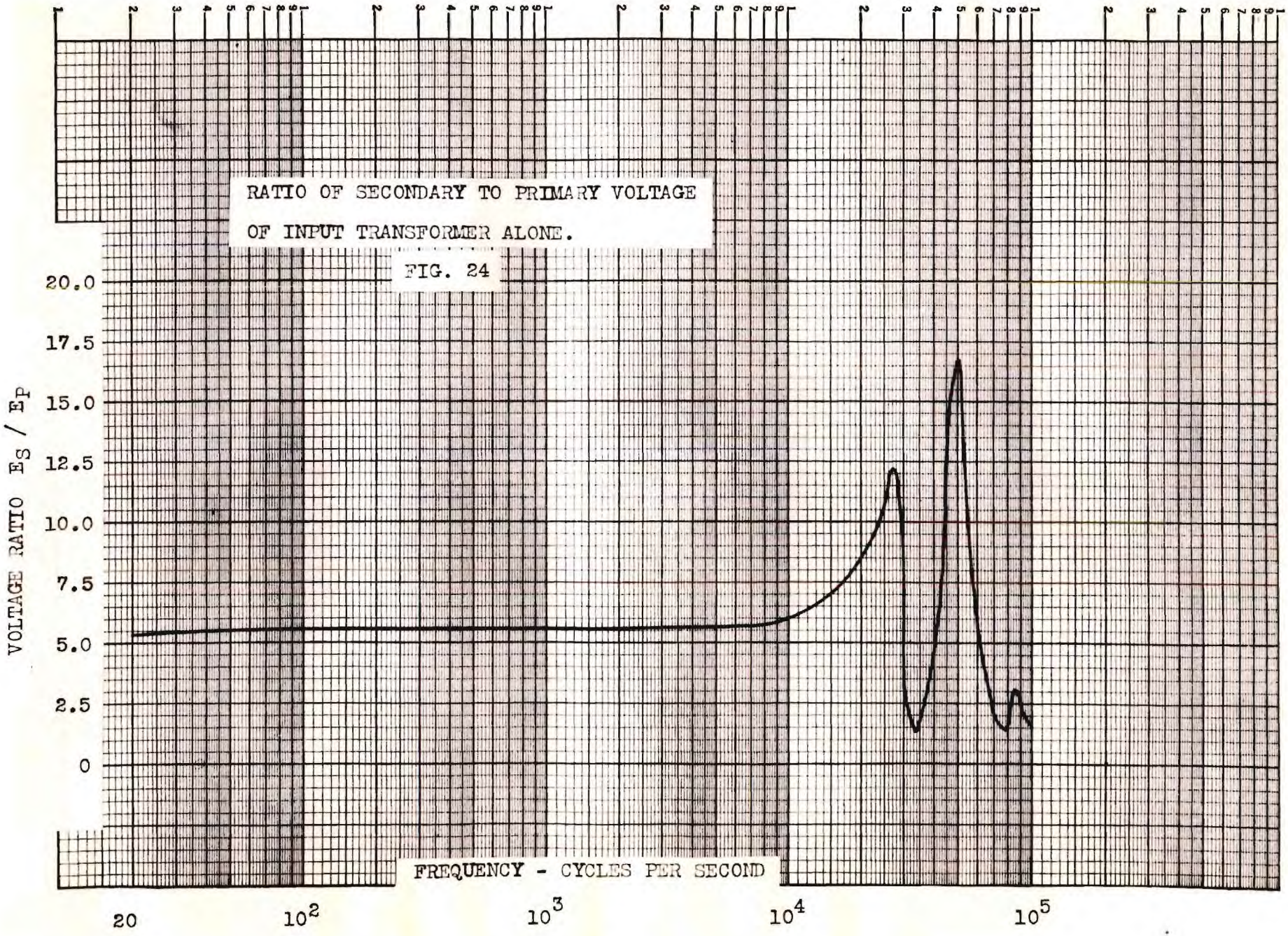
RATIO OF SECONDARY TO PRIMARY VOLTAGE
OF INPUT TRANSFORMER ALONE.
FIG. 24
VOLTAGE RATIO E_S / E_P
20.0
17.5
15.0
12.5
10.0
7.5
5.0
2.5
0
FREQUENCY - CYCLES PER SECOND
20
10^2
10^3
10^4
10^5

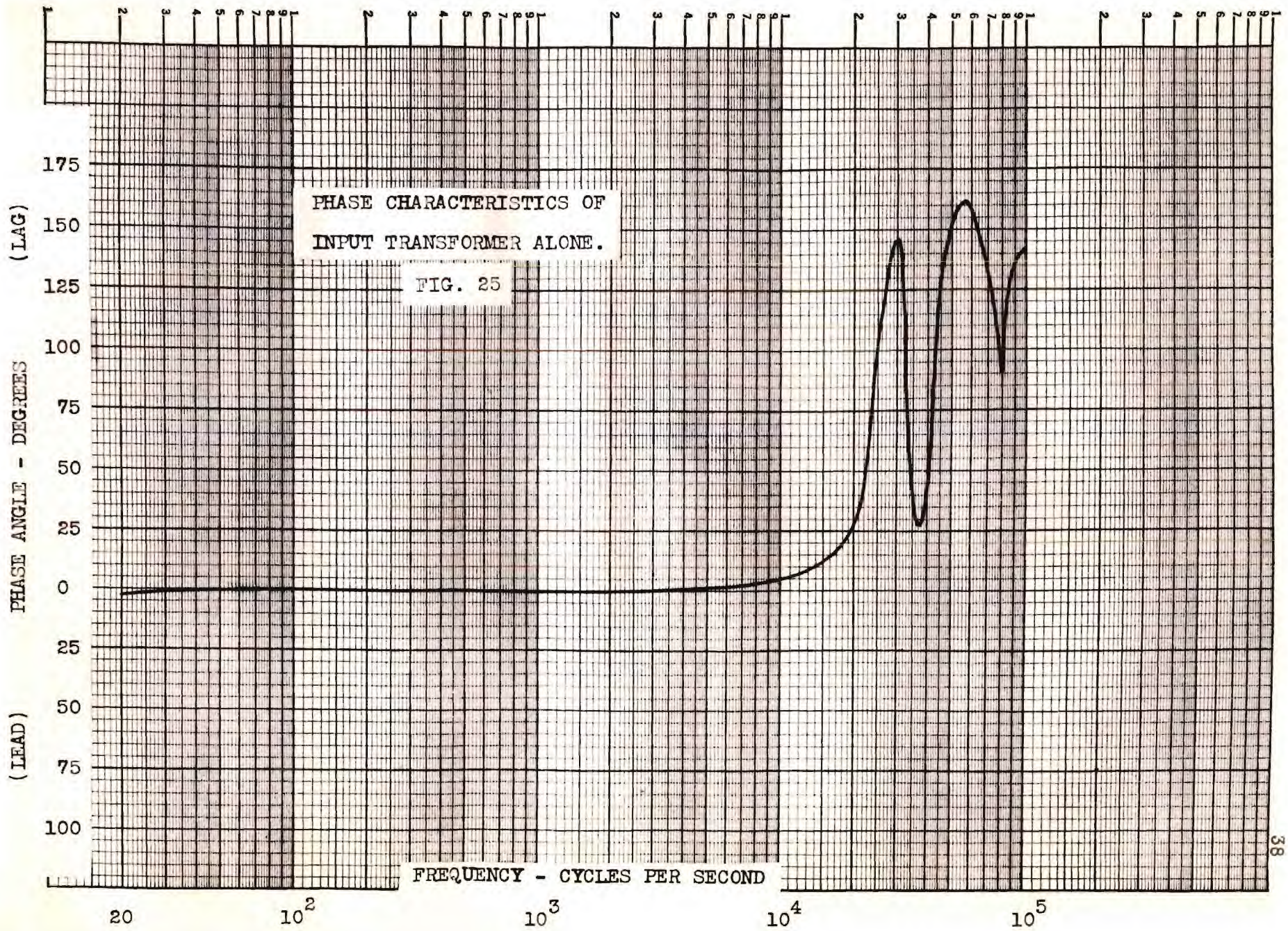
PHASE CHARACTERISTICS OF
INPUT TRANSFORMER ALONE.
FIG. 25
PHASE ANGLE - DEGREES
(LAG)
(LEAD)
175
150
125
100
75
50
25
0
25
50
75
100
FREQUENCY - CYCLES PER SECOND
20
10^2
10^3
10^4
10^5

probably due to the frequency-response characteristic of the output transformer which drops off gradually above 20 KC, since its secondary is heavily loaded with a 500-ohm non-inductive resistance.

The excursions of the phase characteristics of the input transformer again show the variations to be expected from the results of the corresponding frequency-response curve.

It is apparent from the results of this last test on the input transformer that its characteristics exert the primary controlling influence on the overall amplifier characteristics.

The amplifier characteristics exhibited in all of the tests previously described are widely different from the characteristics usually associated with transformer-coupled audio amplifiers found in the standard literature.

To check on the validity of the experiments thus far performed, similar tests were made on two separate and different amplifiers to determine their overall amplification and phase characteristics.

One amplifier used 6L6 tubes, triode connected, Class A operation, in a push-pull arrangement with a medium-quality Stancor transformer. The other amplifier used 6L6 tubes, tetrode connected, Class B operation, in a push-pull arrangement with a high-quality UTC transformer. Both amplifiers when tested exhibited frequency response phenomena similar to those observed for the amplifier previously tested and described.

Thus it would appear that additional peaks in the frequency-response characteristics are possible in transformer-coupled audio amplifiers, but are probably neglected in the usual case since they normally appear at a frequency above the specified pass band of the

transformer.

Data on the tests performed on the two additional amplifiers was not included, since it was the primary purpose of this thesis to examine and study in some detail only the single amplifier previously mentioned.

However, these last tests strongly indicate that additional peaks in the frequency-response characteristic are possibly the rule rather than the exception for transformer-coupled audio amplifiers.

Transient Response of the Amplifier

To investigate the transient response of the amplifier under different conditions, a square-wave signal was fed into the amplifier input terminals by a Measurements Corporation Square-Wave Generator, Model 71, and the output wave shape was recorded on an oscilloscope.

Prior to recording the output wave shape of the amplifier, the square wave fed into the amplifier input terminal was recorded. In this test, as in all of the tests to be described later, the results were photographed with a Dumont Oscillographic Camera.

The input test signal is not a perfect square wave, but it was believed to be similar enough in shape to a true square wave to indicate the transient response of the amplifier.

The input wave shape is shown on Figure 26. This wave shape is quite good up to a frequency of 1000 (PRF = Pulse Repetition Frequency), but above this frequency there is some distortion due to the fact that the square-wave generator is not feeding into the proper terminating impedance.

Figure 27 and Figure 28, respectively, show the transient

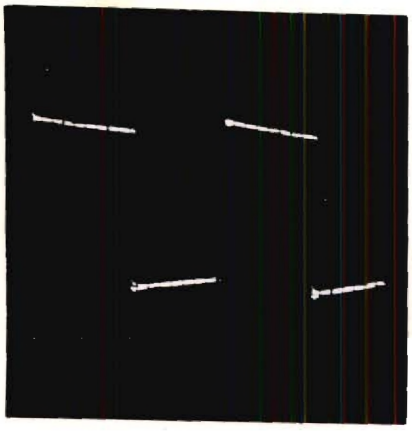

f = 500 (PRF)

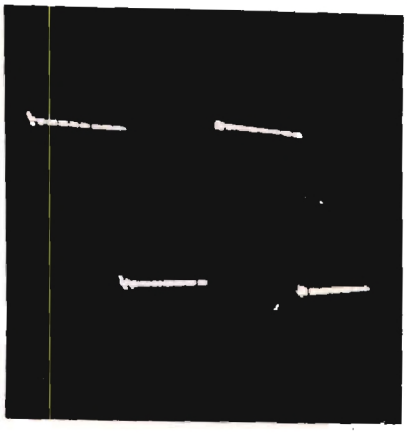

f = 1000 (PRF)

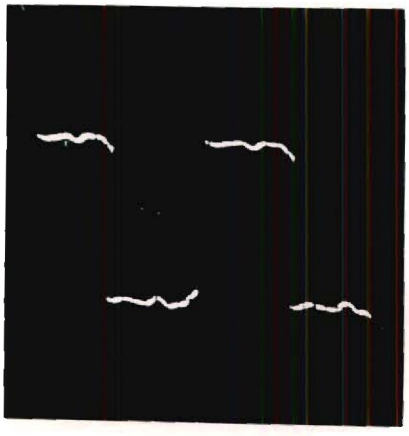

f = 5000 (PRF)

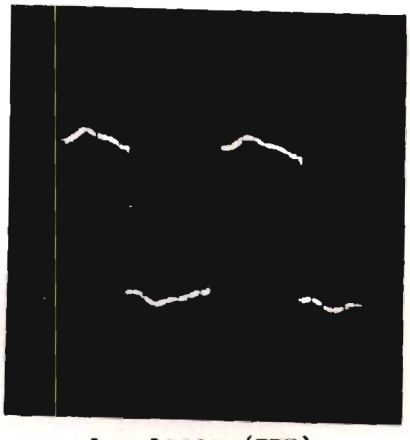

f = 10000 (PRF)

f = 20000 (PRF)

SQUARE-WAVE INPUT TO AMPLIFIER AT

PRIMARY OF INPUT TRANSFORMER.

FIG. 26

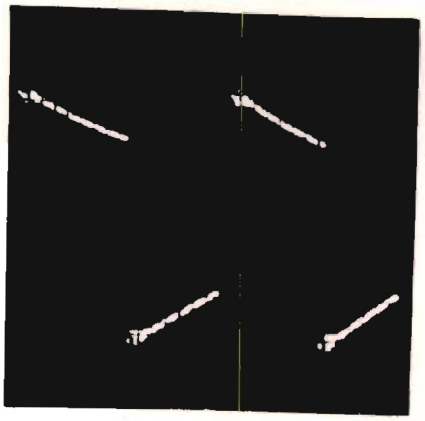

f = 500 (PRF)

f = 1000 (PRF)

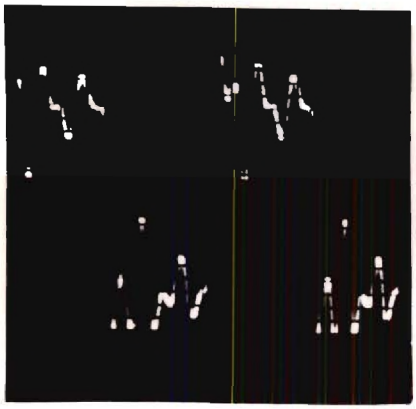

f = 5000 (PRF)

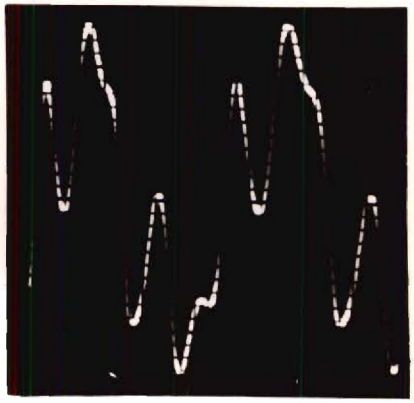

f = 10000 (PRF)

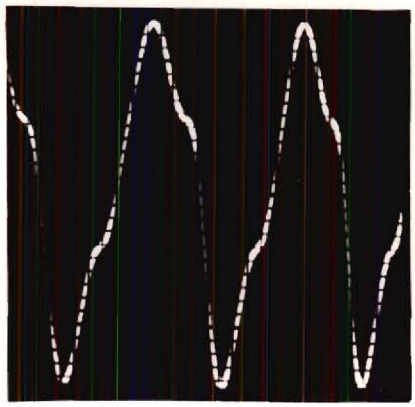

f = 20000 (PRF)

TRANSIENT RESPONSE OF AMPLIFIER TO A SQUARE WAVE - AMPLIFIER UNNEUTRALIZED INPUT TRANSFORMER SECONDARY UNLOADED.

FIG. 27

f = 500 (PRF)

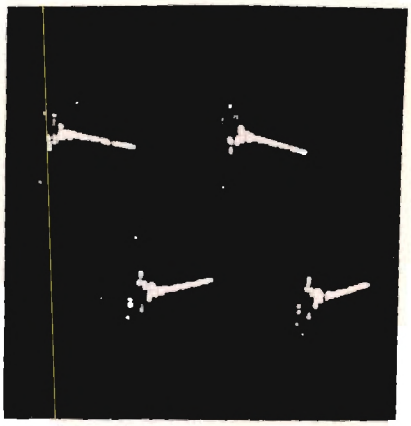

f = 1000 (PRF)

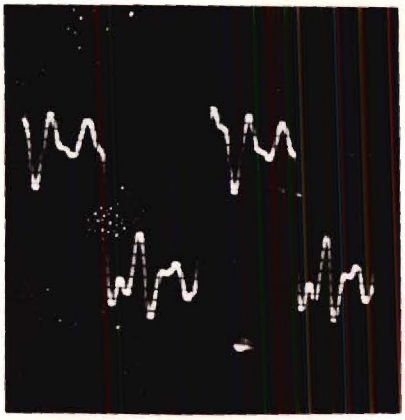

f = 5000 (PRF)

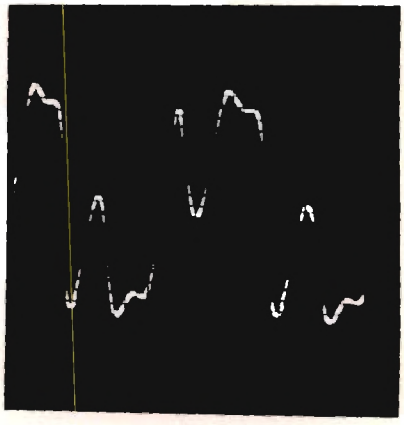

f = 10000 (PRF)

f = 20000 (PRF)

TRANSIENT RESPONSE OF AMPLIFIER TO A SQUARE WAVE - AMPLIFIER NEUTRALIZED (C_n = 20uuf) INPUT TRANSFORMER SECONDARY UNLOADED.

FIG. 28

response, first, with the amplifier unneutralized, and second, with the amplifier neutralized. In both cases the input transformer secondary is unloaded.

In each case, the transient response of the amplifier at five different frequencies was recorded. The significant characteristic of these output wave forms is the slope of the horizontal portion of the wave. This slope is due primarily to phase distortion at low frequencies. It can be noted for the first case, as shown on Figure 27, at the frequencies of 500 (PRF) and 1000 (PRF), that the slopes are respectively 39% and 22%. At a frequency of 5,000 (PRF) and 10,000 (PRF) the amplifier oscillates strongly under the influence of a square wave.

For the second case, Figure 28, a study of the recorded results indicates very little change at the lower frequencies when the amplifier is neutralized. However, at the higher frequencies there is a noticeable change caused by neutralization. The magnitude of the positive part of the oscillation cycle is reduced considerably.

The next step was a study of the transient response of the amplifier when operated under two more different conditions. First, the amplifier was unneutralized, and second, the amplifier was neutralized. In both cases the input transformer secondary was loaded with 100,000-ohm resistance.

The results are shown on Figure 29 and Figure 30, respectively.

For both of these last two cases, the results are quite identical. However, there is a decided difference between the cases when the transformer secondary was loaded and when the transformer secondary was unloaded, particularly at the higher frequencies.

f = 500 (PRF)

f = 1000 (PRF)

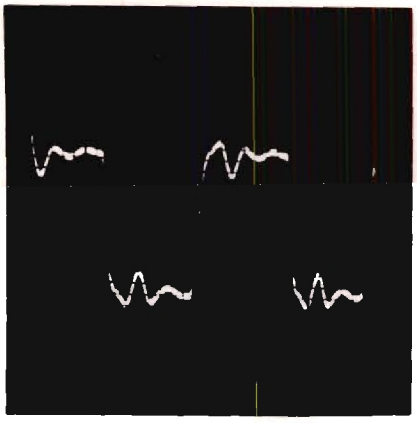

f = 5000 (PRF)

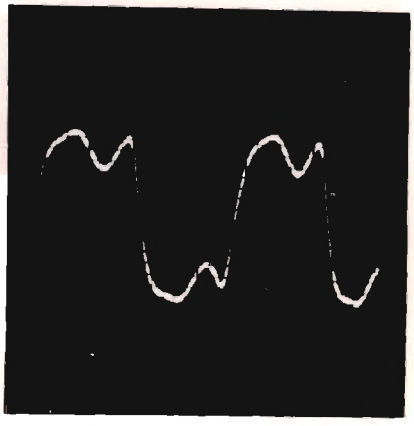

f = 10000 (PRF)

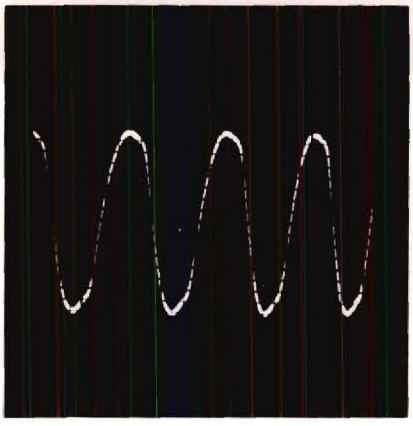

f = 20000 (PRF)

TRANSIENT RESPONSE OF AMPLIFIER TO A SQUARE WAVE - AMPLIFIER UNNEUTRALIZED INPUT TRANSFORMER SECONDARY LOADED WITH 100,000 OHMS.

FIG. 29

f = 500 (PRF)

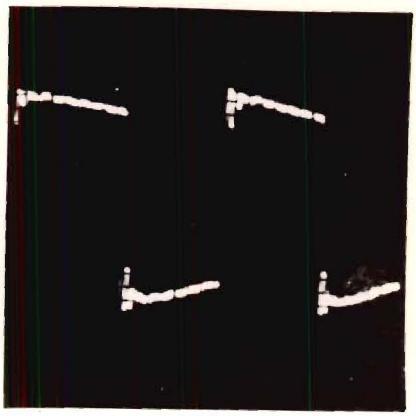

f = 1000 (PRF)

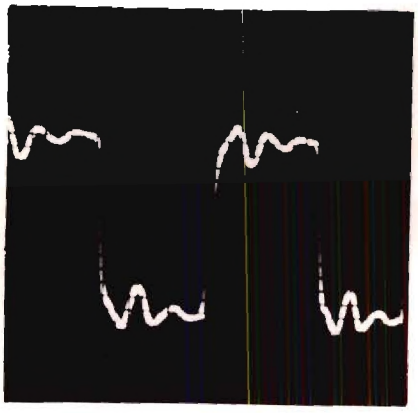

f = 5000 (PRF)

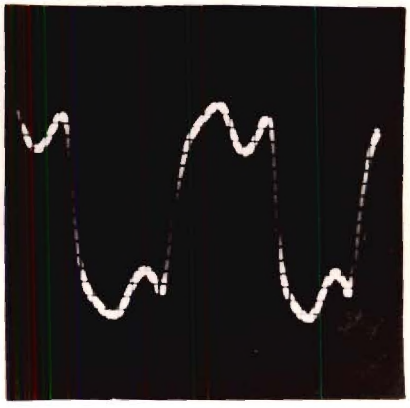

f = 10000 (PRF)

f = 20000 (PRF)

TRANSIENT RESPONSE OF AMPLIFIER TO A SQUARE WAVE - AMPLIFIER NEUTRALIZED (C_n = 20uuf) INPUT TRANSFORMER SECONDARY LOADED WITH 100,000 OHMS.

FIG. 30

These last two sets of photographs would indicate that the value of loading resistance chosen causes the amplifier to be under-damped at certain frequencies.

Resonant circuits with less than critical damping act as shown in the photographs for the frequencies, 5000 (PRF) and 10,000 (PRF), Figure 29 and Figure 30, when the resonant frequency is somewhat higher than the fundamental frequency of the square wave. The vertical part of the square wave has been rounded off somewhat, and a damped oscillation appears. The ratio of the resonant frequency to the square-wave fundamental is equal to the number of half-cycles of oscillations that occur in one-half cycle of the square wave. The damping of the resonant circuit is indicated by the rate at which the oscillations die out.[2]

Another method of determining the resonant frequencies of the amplifier circuit is to increase the frequency of the square-wave input until a sine wave appears in the amplifier output.

It would appear from the transient-response characteristics of the amplifier, as it did for the amplification and phase characteristics, that the neutralized condition causes a slight improvement over the unneutralized condition, while the transformer secondary loading effect causes a marked improvement over the unloaded effect.

During all of the transient-response tests, the oscilloscope amplifier gain control was set at one position and kept constant so that exact magnitude comparisons of the output wave shapes could be made.

---

[2]F. E. Terman, Radio Engineers' Handbook, First Edition, p. 969, McGraw-Hill Book Company.

As a corollary to the above tests, the sine-wave response of the amplifier was recorded for one set of operating conditions. The amplifier was neutralized, and the input transformer secondary was loaded. The results of this test are shown on Figure 31.

The sine-wave response of the amplifier is excellent at the frequencies checked, with only a slight amount of distortion noted at the lowest frequency measured, 30 c.p.s.

Amplifier Input Impedance Measurements

With the aid of a Western Electric Impedance Bridge, Type 4-A, the input impedance of the amplifier was measured.

First the input impedance was measured with the amplifier unneutralized and the input transformer secondary unloaded. The results obtained from this test are first shown on Figure 32 and Figure 33, on which the resistive and reactive components of the input impedance are plotted separately as a function of frequency. These same results are shown in a different form on Figure 34. This latter curve shows partially why the overall frequency response characteristics of the amplifier are of an unusual shape, since the input signal is feeding into a complex circuit that passed through several poles and zeros in the frequency spectrum considered.

Next, the input impedance was measured, by the same means, with the amplifier unneutralized and a 100,000-ohm resistance connected across the input transformer secondary.

As in the first case, the results are shown in two different forms on Figure 35 and Figure 36. The curve of Figure 36 indicates the effect

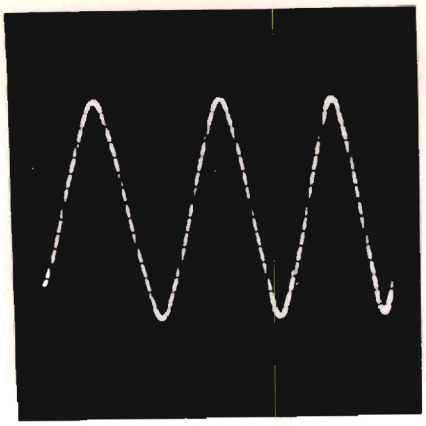

f = 30 c.p.s.

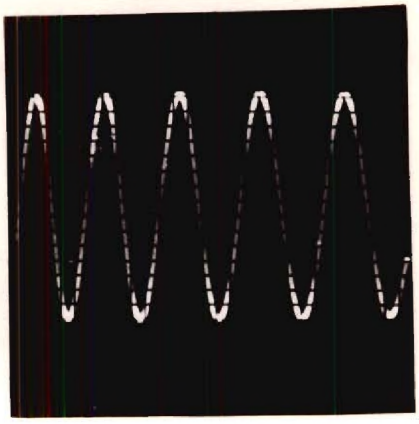

f = 1000 c.p.s.

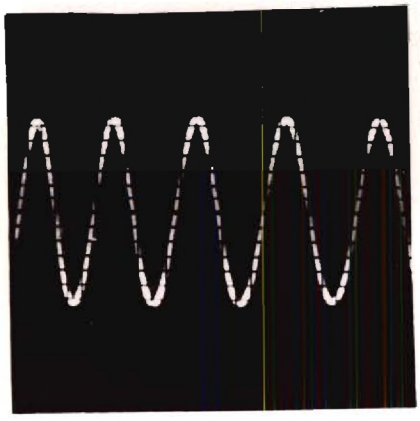

f = 10000 c.p.s.

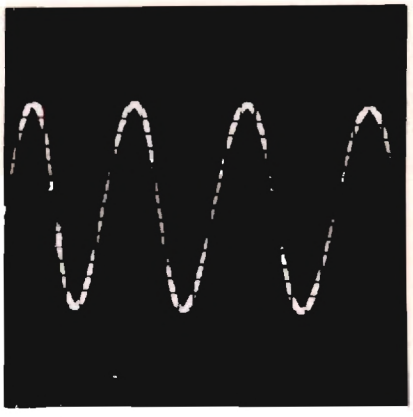

f = 20000 c.p.s.

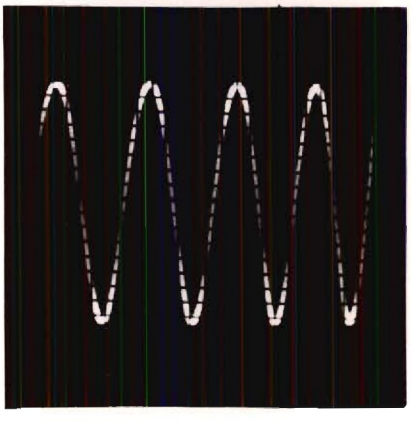

f = 50000 c.p.s.

SINE-WAVE RESPONSE OF AMPLIFIER.

AMPLIFIER NEUTRALIZED (C_n = 20uuf)

INPUT TRANSFORMER SECONDARY LOADED

WITH 100,000 OHMS.

FIG. 31

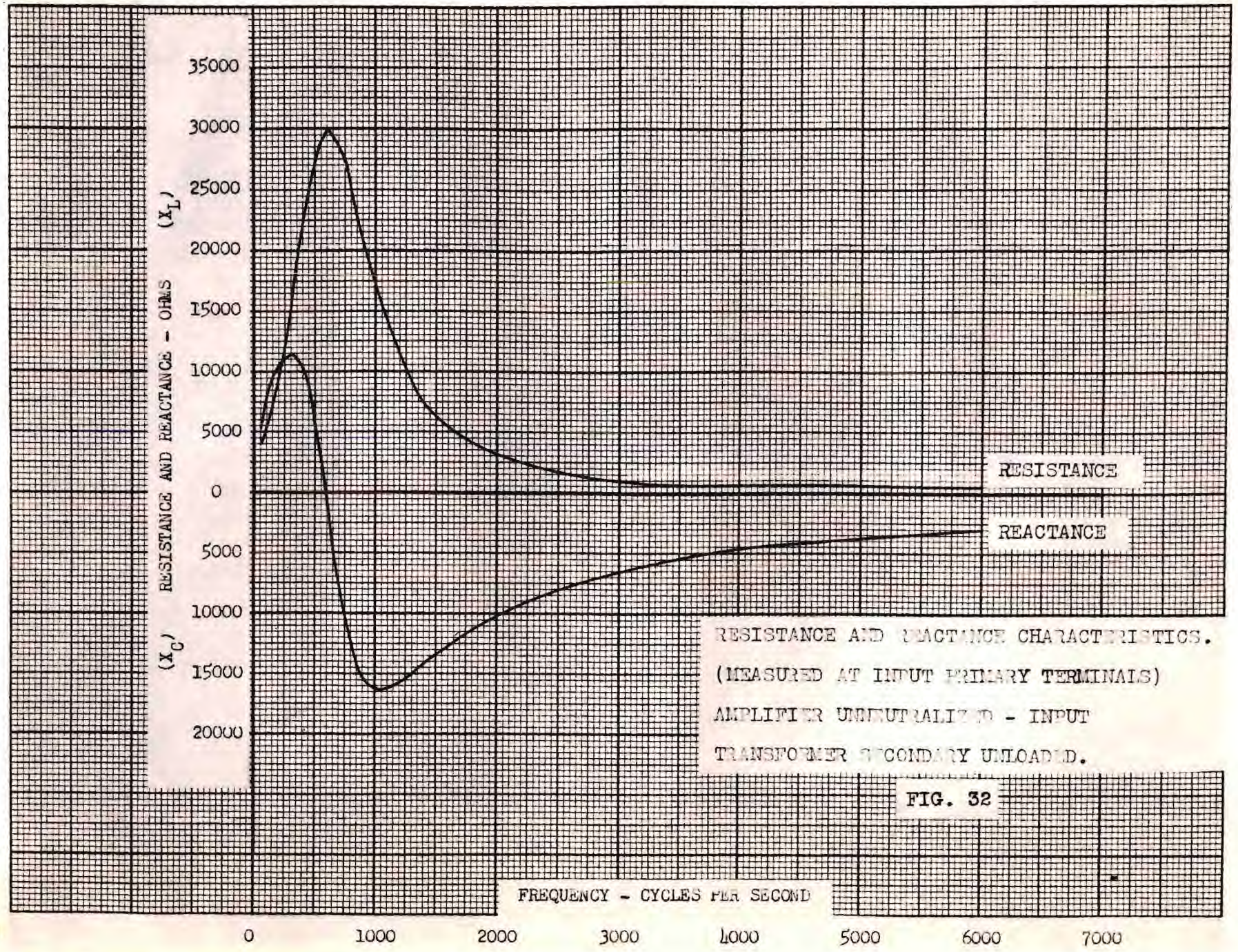

RESISTANCE AND REACTANCE CHARACTERISTICS.
(MEASURED AT INPUT PRIMARY TERMINALS)
AMPLIFIER UNNEUTRALIZED - INPUT
TRANSFORMER SECONDARY UNLOADED.

FIG. 32

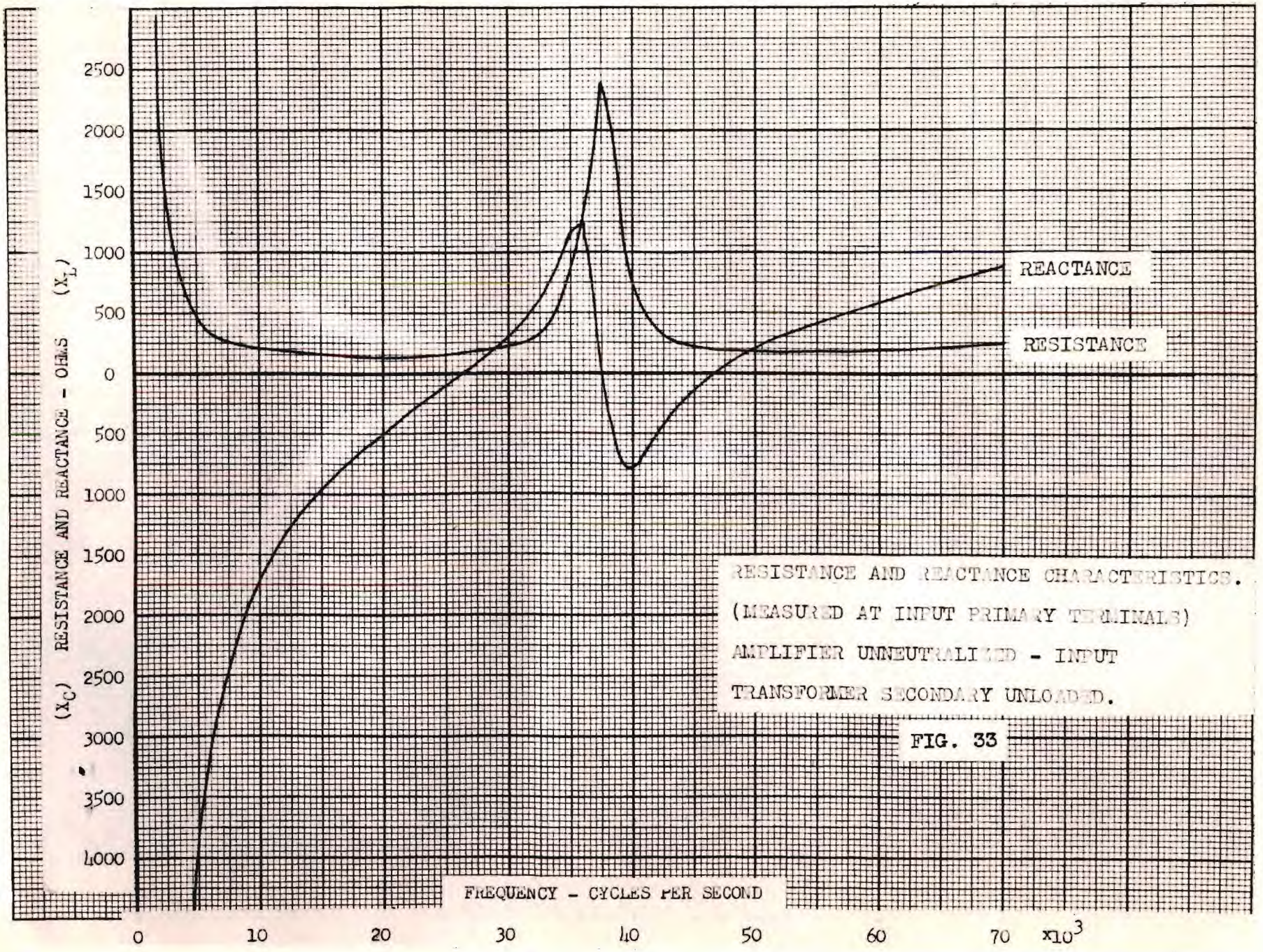

RESISTANCE AND REACTANCE CHARACTERISTICS.
(MEASURED AT INPUT PRIMARY TERMINALS)
AMPLIFIER UNNEUTRALIZED - INPUT
TRANSFORMER SECONDARY UNLOADED.

FIG. 33

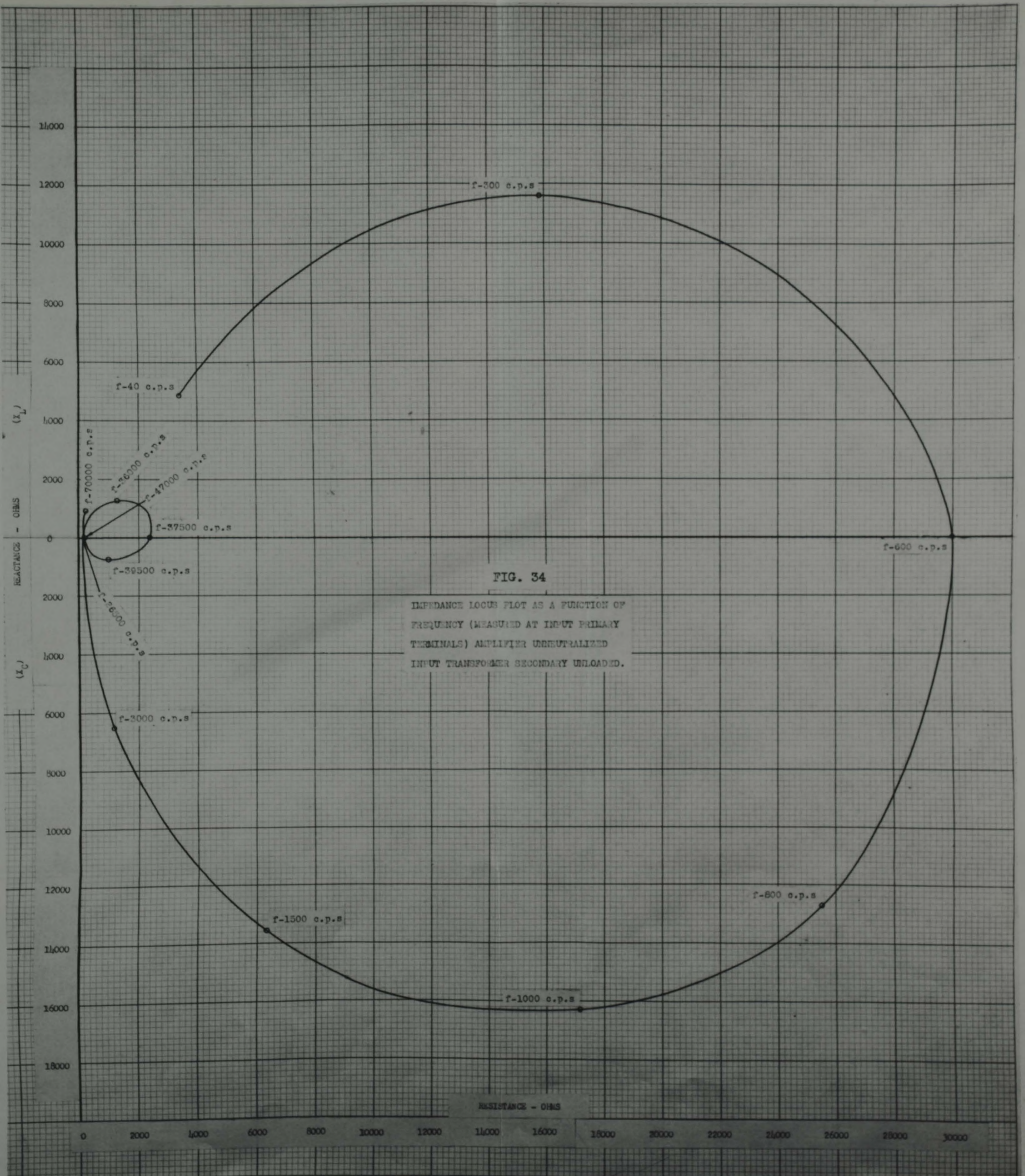

FIG. 34

IMPEDANCE LOCUS PLOT AS A FUNCTION OF FREQUENCY (MEASURED AT INPUT PRIMARY TERMINALS) AMPLIFIER UNNEUTRALIZED INPUT TRANSFORMER SECONDARY UNLOADED.

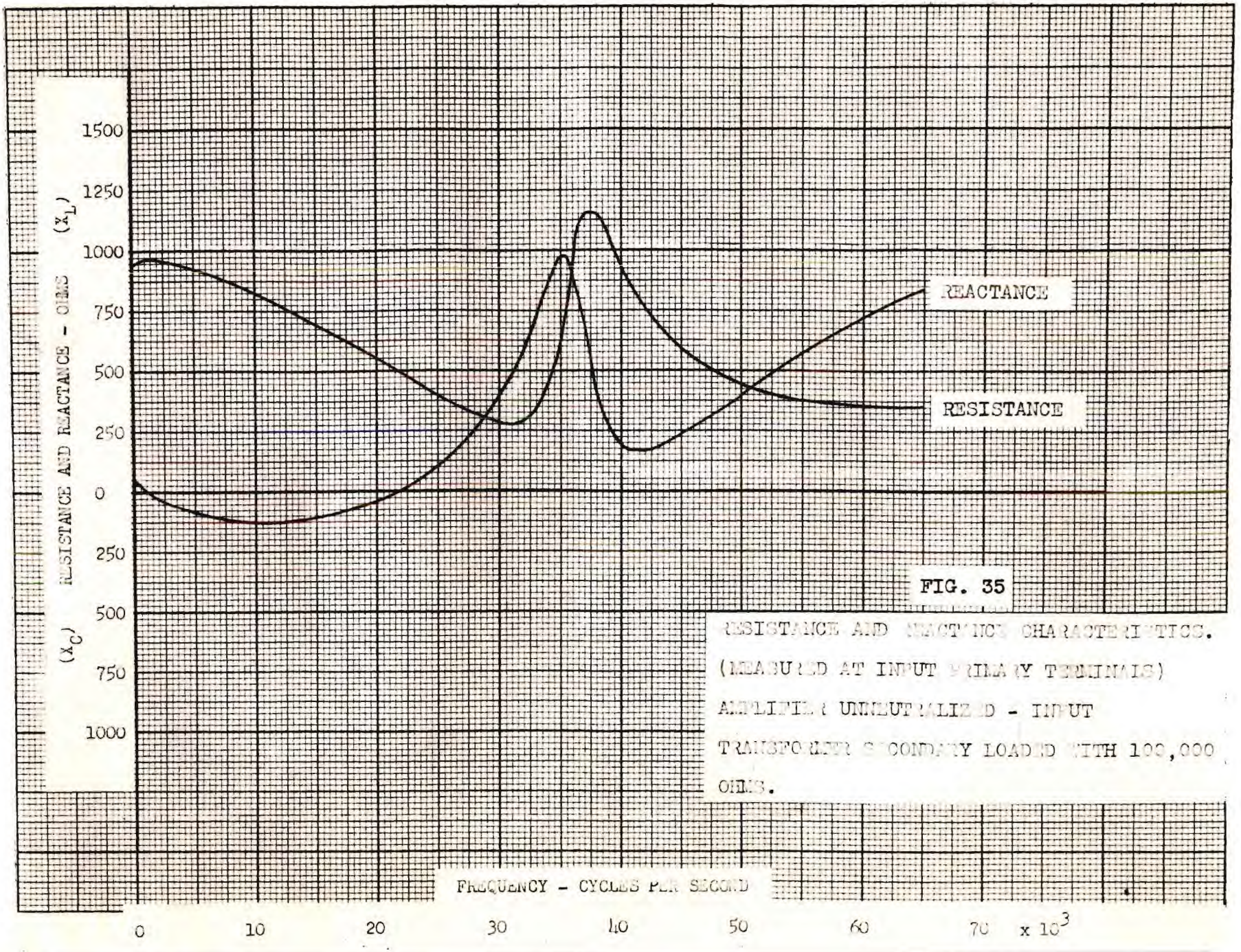

FIG. 35

RESISTANCE AND REACTANCE CHARACTERISTICS.
(MEASURED AT INPUT PRIMARY TERMINALS)
AMPLIFIER UNNEUTRALIZED - INPUT
TRANSFORMER SECONDARY LOADED WITH 100,000
OHMS.

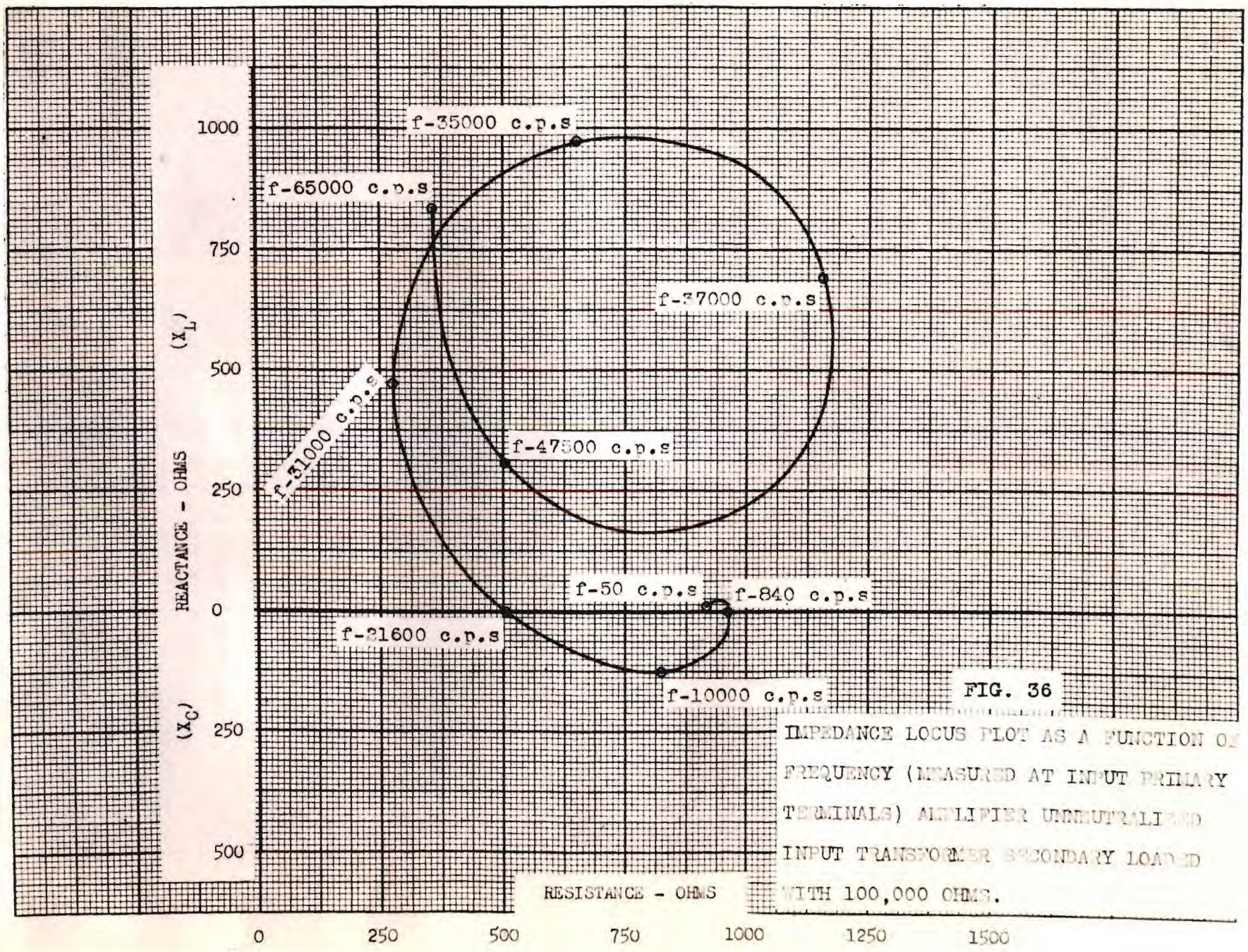

FIG. 36

IMPEDANCE LOCUS PLOT AS A FUNCTION OF FREQUENCY (MEASURED AT INPUT PRIMARY TERMINALS) AMPLIFIER UNNEUTRALIZED INPUT TRANSFORMER SECONDARY LOADED WITH 100,000 OHMS.

of a resistive load across the transformer secondary upon the input-impedance characteristics. Above 21.6 KC the reactive component lies entirely in the inductive region. In this latter case, the complex circuit into which the input signal is fed does not pass through true poles and zeros above 21.6 KC but rather through quasi (or pseudo) poles and zeros.

Further significance of similar types of impedance locus plots will be discussed more fully in the following section which deals with the synthesis of the input transformer equivalent circuit.

Synthesis of the Input Transformer Equivalent Circuit

The results obtained from the numerous preceding tests on the amplifier clearly indicate that the input transformer characteristics control the overall frequency-response and phase characteristics of the amplifier. Therefore, a determination of the equivalent circuit for the input transformer above would show why the overall frequency-response and phase characteristics of the amplifier assume their respective shapes.

That the equivalent circuit for the interstage transformer used in this amplifier is more complex than the ones normally representative of a transformer-coupled audio amplifier has become apparent from all of the data thus far collected.

Since, as was previously mentioned, the output transformer does not exert an appreciable influence on the overall amplifier characteristics, its characteristics were not measured. However, the method outlined in this section of the report could undoubtedly be used to determine the output transformer equivalent circuit in a like manner.

An extensive search was made of the available literature in an effort to ascertain whether any information had been published from work done in this country on the analysis of a more complete equivalent circuit for an interstage transformer than is indicated in standard textbooks and publications.

This search through American literature did not prove fruitful. But an abstract from The Wireless Engineer did indicate that a German writer, Von H. Knapp of Siemens and Halske Company, Berlin, had done some work along this line. The results of this work had been published in a German publication, Elektrische Nachrichten Technik, Volume 20, Issue 8, August 1943. After a detailed examination of this article in its original form, it appeared that the information contained therein would be very useful, and a translation was made. The complete translation is included in this thesis in Appendix III.

The following work is largely based on the methods clearly outlined by Mr. Von H. Knapp in his article, and consequently, a detailed explanation of each step-by-step analysis will not be repeated in this section of the thesis.

As a preliminary step to the equivalent circuit determination, certain necessary transformer parameters were measured.[3]

These parameters are listed below:

Incremental Primary Inductance, L_1, - - - - - - - - - - - - - - - - - 8.25 h

Total Leakage Inductance referred to the primary, L_{s_1}, - - - - - 3.0 mh

Total Leakage Inductance referred to the secondary, L_{s_2}, - - - - 370 mh

---

[3]F. E. Terman, Measurements in Radio Engineering, First Edition, McGraw-Hill Book Company.

D-C Resistance of Primary, R_1, - 69Ω

D-C Resistance of Secondary, R_2, - - - - - - - - - - - - - - - - - - 2280Ω

Turns Ratio - Primary to full Secondary, $\frac{N_1}{N_2}$, - - - - - - - - - - - 1:11.2

The next step in the determination of the transformer equivalent circuit was the measurement of the secondary short-circuit impedance, and the primary short-circuit impedance. These measurements were made with a Western Electric Impedance Bridge, Type 4-A. To insure the validity of the bridge readings in the higher frequency range, from 40 KC upward to 100 KC, standard inductances, capacitances, and decade resistances were measured singly, and in series and parallel combinations. The bridge checked very closely the values expected over the entire frequency range considered.

The results of the secondary and primary short-circuit impedance measurements are shown on Figure 37 and Figure 38, respectively. From these two diagrams, the equivalent circuit for the primary and secondary can be synthesized with the aid of the parameters already evaluated.

From the secondary short-circuit impedance locus plot, it can be seen that the circuit which it represents traverses three poles, namely at 30 KC, 63 KC, and 81 KC, and two zeros, namely at 34.5 KC and 79 KC.

However, only the frequency range up to and including the pole at 63 KC will be considered for the determination of the secondary equivalent circuit. The circuit complexity and mathematical manipulations associated with it are greatly increased by utilizing the complete information obtainable by considering the full frequency range up to 95 KC. Since the zero and pole at 79 KC and 81 KC are of a minor nature, and account for the minor peak noted on Figure 24, the above-mentioned

f = 97500 c.p.s

f = 17000 c.p.s

f = 5000 c.p.s

f = 34500 c.p.s

f = 30000 c.p.s

f = 63000 c.p.s

f = 95000 c.p.s

f = 81000 c.p.s

f = 79000 c.p.s

f = 67500 c.p.s

REACTANCE - OHMS (x 10^3) (X_L)

RESISTANCE - OHMS (x 10^3)

IMPEDANCE LOCUS PLOT AS A FUNCTION OF FREQUENCY MEASURED AT SECONDARY OF INPUT TRANSFORMER WITH PRIMARY SHORT-CIRCUITED.

FIG. 37

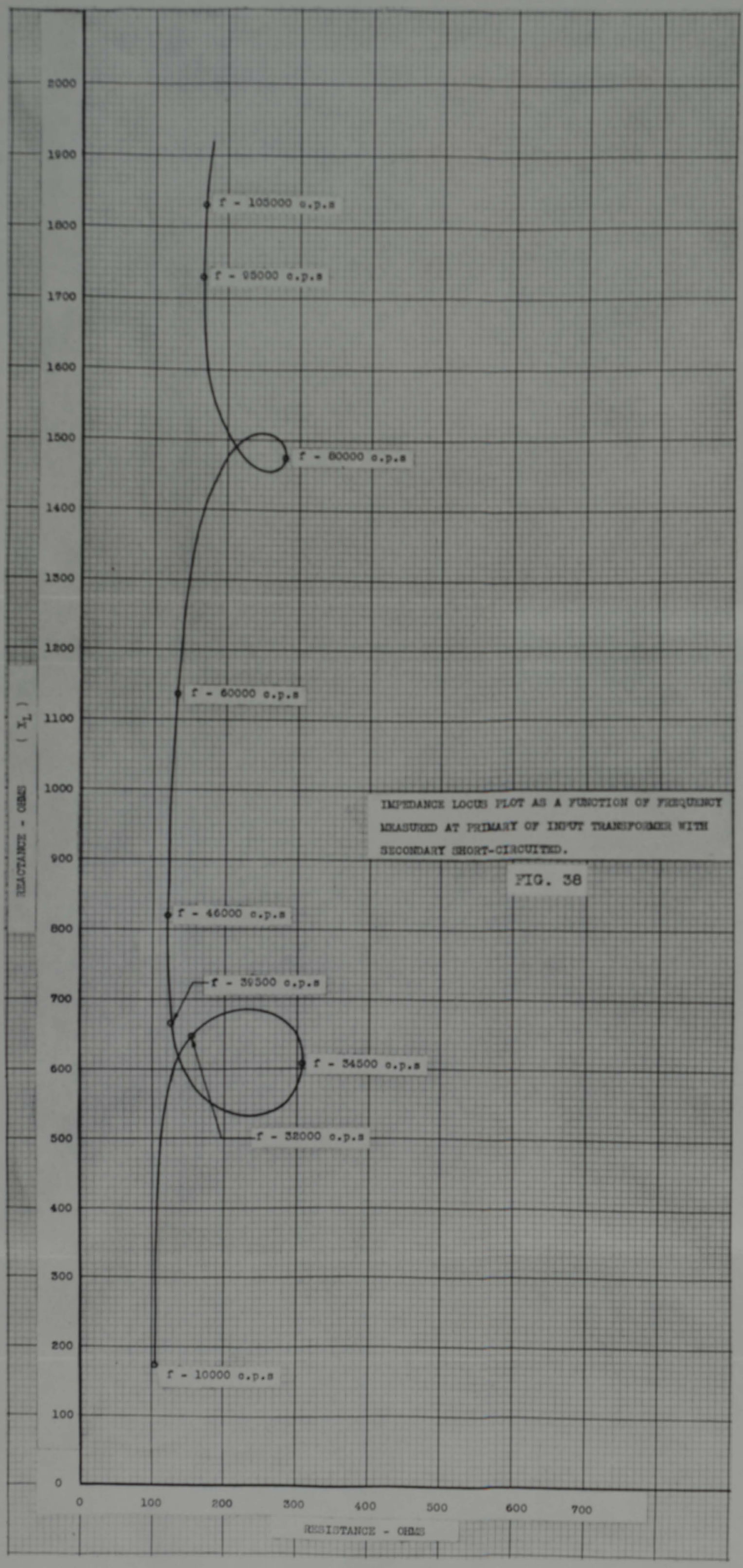

IMPEDANCE LOCUS PLOT AS A FUNCTION OF FREQUENCY MEASURED AT PRIMARY OF INPUT TRANSFORMER WITH SECONDARY SHORT-CIRCUITED.

FIG. 38

frequency range was chosen, as it will still result in an equivalent circuit valuable up to 80 KC for the secondary side.

The impedance plot of Figure 37, for the frequency range considered, will result from a circuit of the type shown on Figure 39.[4]

The impedance, R_2^K, looking into the terminals 3-4 of Figure 39 is:

$$R_2^K = jwL_{s_2} \cdot \frac{1 - w^2L_oK_2}{w^4\left[L_{s_2}L_oC_6K_2\right] - w^2\left[L_{s_2}(K_2+C_6) + L_oK_2\right] + 1} \qquad (1)$$

This function has one zero at the real angular frequency, w_1, which can be found by equating the second term of the numerator to zero. For which we have:

$$w_1 = \frac{1}{\sqrt{L_oK_2}} \qquad (2)$$

Equation (1) also has two poles at the real angular frequencies, w_2 and w_3, which can be found by equating the denominator to zero. We then obtain,

$$w_2^2 = \frac{\left[L_{s_2}(K_2+C_6) + L_oK_2\right] + \sqrt{\left(L_{s_2}(K_2+C_6) + L_oK_2\right)^2 - 4\left(L_{s_2}L_oC_6K_2\right)}}{2\left[L_{s_2}L_oC_6K_2\right]} \qquad (3)$$

$$w_3^2 = \frac{\left[L_{s_2}(K_2+C_6) + L_oK_2\right] - \sqrt{\left(L_{s_2}(K_2+C_6) + L_oK_2\right)^2 - 4\left(L_{s_2}L_oC_6K_2\right)}}{2\left[L_{s_2}L_oC_6K_2\right]} \qquad (4)$$

From these two equations the following relationships can be easily determined:

---

[4]T. E. Shea, Transmission Networks and Wave Filters, D. Van Nostrand Co., Inc.

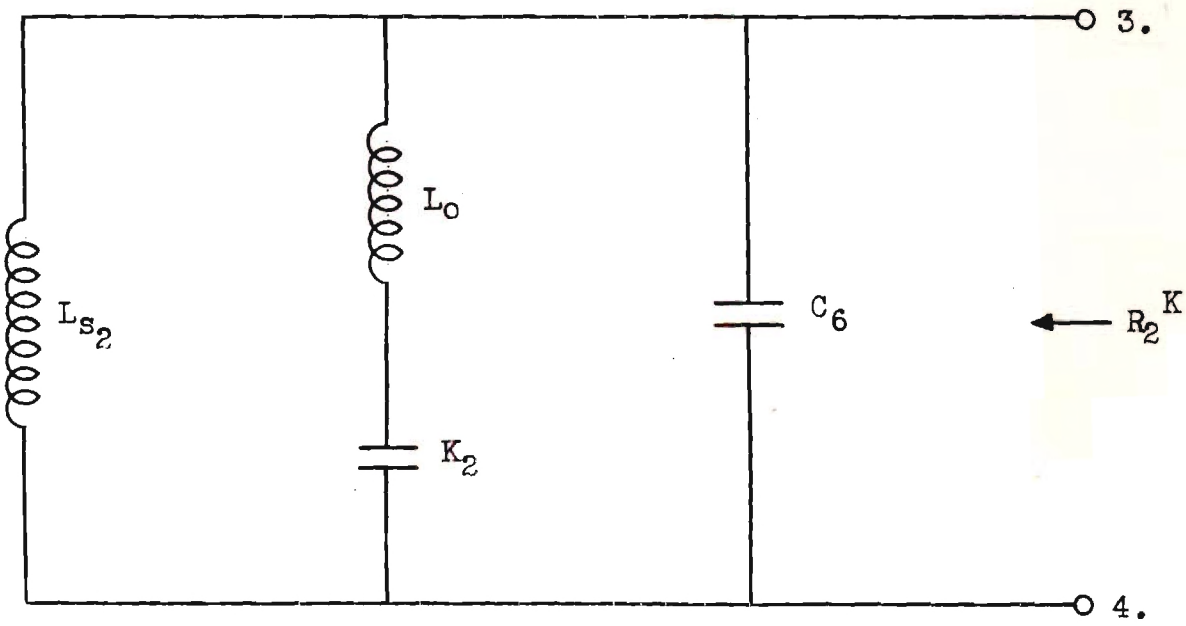

SYNTHESIZED EQUIVALENT CIRCUIT DIAGRAM FOR THE SECONDARY OF THE INPUT TRANSFORMER DEVELOPED FROM THE IMPEDANCE LOCUS PLOT OBTAINED WITH THE TRANSFORMER PRIMARY SHORT CIRCUITED.

FIG. 39

$$w_2^2 \cdot w_3^2 = \frac{1}{L_{s_2} L_o C_6 K_2} \tag{5}$$

and

$$w_2^2 + w_3^2 = \frac{L_{s_2}(K_2 + C_6) + L_o K_2}{L_{s_2} L_o C_6 K_2} \tag{6}$$

Also, from the two equations above the following relationships can be derived. This derivation is shown in Appendix II.

$$L_{s_2}(K_2 + C_6) = \left[\frac{1}{w_2^2} + \frac{1}{w_3^2}\right] - \left[\frac{1}{w_1^2}\right] \tag{7}$$

$$\frac{K_2}{C_6} = \left[\left(\frac{w_2}{w_1}\right)^2 + \left(\frac{w_3}{w_1}\right)^2 - \left(\frac{w_2}{w_1}\right)^2 \left(\frac{w_3}{w_1}\right)^2 - 1\right] \tag{8}$$

The value of L_{s_2} has previously been determined, and we can now solve for C_6 and K_2, since we have two equations and two unknowns.

The values are:

$$C_6 = 23 \text{ uuf}$$

$$K_2 = 13 \text{ uuf}$$

The circuit of Figure 39 goes through one zero, which will occur when L_o and K_2 are in series resonance at 34.5 KC. Therefore, it is quite simple to solve for the value of L_o.

$$L_o = \frac{1}{(2\pi f)^2 \times K_2} \tag{9}$$

Therefore, $L_o = 1.61h$

Thus we now have all of the values of components shown in the circuit of Figure 39.

In a similar manner, from the primary short-circuit impedance locus plot, Figure 38, it can be seen that the circuit which it represents

traverses two poles, namely at 34.5 KC and 80.0 KC, and two zeros, namely at 46 KC and 95 KC. The impedance plot of Figure 38 will result from a circuit of the type shown on Figure 40.

The impedance, R_1^K, looking into the terminals 1-2 of Figure 40 is:

$$R_1^K = jwL_{s_1} \cdot \frac{1 - w^2L'K_1 - w^2L''C_5 + w^4L'L''C_5K_1}{w^4C_5K_1\left[L'L''+L_{s_1}(L'+L'')\right] - w^2\left[L'K_1+L''C_5+L_{s_1}(K_1+C_5)\right] + 1} \tag{10}$$

The above function has two zeros at the real angular frequencies, w_1 and w_2, which can be found by equating the second term of the numerator to zero. For which we have:

$$w_1 = \frac{1}{\sqrt{L'K_1}} \tag{11}$$

and

$$w_2 = \frac{1}{\sqrt{L''C_5}} \tag{12}$$

This function also has two poles at the real angular frequencies, w_3 and w_4, which can be found by equating the denominator to zero. For which we have:

$$w_3^2 = \frac{L'K_1+L''C_5+L_{s_1}(K_1+C_5) + \sqrt{\left(L'K_1+L''C_5+L_{s_1}(K_1+C_5)\right)^2 - 4\left(C_5K_1(L'L''+L_{s_1}(L'+L'')\right)}}{2\left[C_5K_1(L'L'' + L_{s_1}(L' + L''))\right]} \tag{13}$$

and

$$w_4^2 = \frac{L'K_1+L''C_5+L_{s_1}(K_1+C_5) - \sqrt{\left(L'K_1+L''C_5+L_{s_1}(K_1+C_5)\right)^2 - 4\left(C_5K_1(L'L''+L_{s_1}(L'+L'')\right)}}{2\left[C_5K_1(L'L'' + L_{s_1}(L' + L''))\right]} \tag{14}$$

By the use of equations (13) and (14) the following relationships

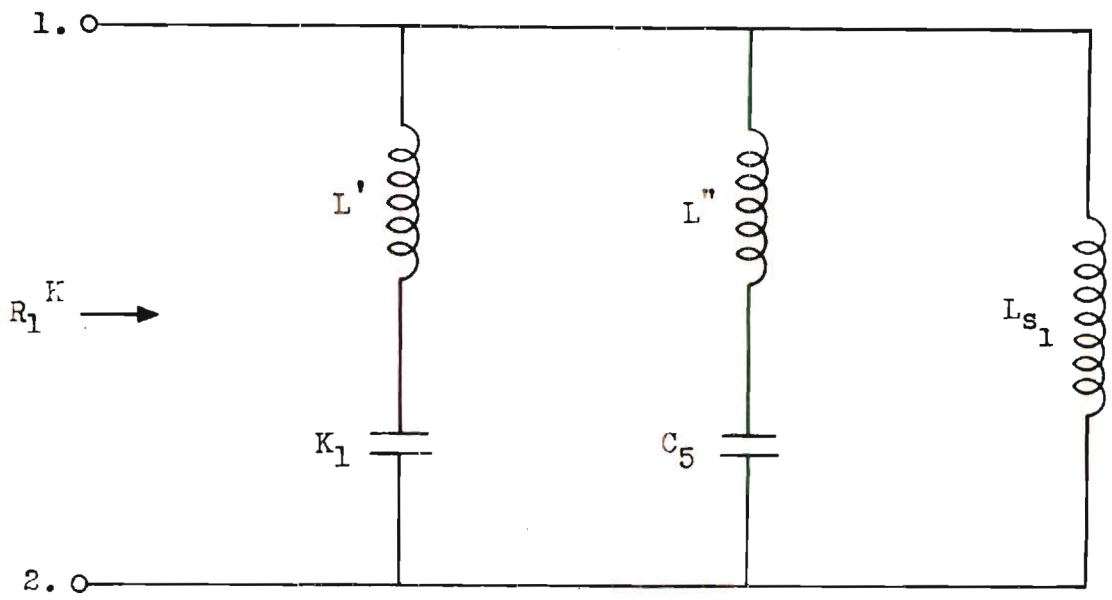

SYNTHESIZED EQUIVALENT CIRCUIT DIAGRAM FOR THE PRIMARY OF THE INPUT TRANSFORMER DEVELOPED FROM THE IMPEDANCE LOCUS PLOT OBTAINED WITH THE TRANSFORMER SECONDARY SHORT CIRCUITED.

FIG. 40

are derived.

$$w_3^2 \cdot w_4^2 = \frac{1}{C_5K_1\left[L'L'' + L_{s1}(L' + L'')\right]} \tag{15}$$

and

$$w_3^2 + w_4^2 = \frac{L'K_1 + L''C_5 + L_{s1}(K_1 + C_5)}{C_5K_1\left[L'L'' + L_{s1}(L' + L'')\right]} \tag{16}$$

From equations (15) and (16) the following equations are derived in a similar manner as is shown in Appendix II.

$$L_{s1}(K_1 + C_5) = \left[\frac{1}{w_3^2} + \frac{1}{w_4^2}\right] - \left[\frac{1}{w_1^2} + \frac{1}{w_2^2}\right] \tag{17}$$

and

$$\frac{K_1}{C_5} = \frac{\left[1 - \left(\frac{w_3}{w_2}\right)^2\right]\left[\left(\frac{w_4}{w_1}\right)^2 - 1\right]}{\left[1 - \left(\frac{w_3}{w_2}\right)^2\right]\left[1 - \left(\frac{w_4}{w_2}\right)^2\right]} \tag{18}$$

Since the value of L_{s_1} has already been determined, we now solve for the values of C_5 and K_1 from equations (17) and (18). These values are:

$$C_5 = 779 \text{ uuf}$$

$$K_1 = 2734 \text{ uuf}$$

The circuit of Figure 40 goes through two zeros, one when L' and K_1, are in series resonance at 46 KC, and another when L" and C_5 are in series resonance at 95 KC.

From the preceding information, the values of L' and L" are determined.

$$L' = 4.38 \text{ mh}$$

$L'' = 3.59$ mh

We have now evaluated all of the components shown in the circuit diagram of Figure 40.

As a check of the values determined for the primary and secondary equivalent circuits of the transformer, the appropriate values of capacitance and inductance were substituted in equations (3), (4), (13) and (14). The values of frequencies for the poles were then solved for and found to give very close agreement with the pole frequencies as found from the impedance locus plots of Figure 37 and Figure 38.

The last step necessary for the equivalent circuit determination is to calculate the value of K. The nature of K and its derivation are explained in detail in Appendix III, and the explanation will not be repeated at this point.

In order to arrive at the value of K, we first must determine the value of C_o which is summarily designated as the "self-capacitance." This value of C_o is found by locating the frequency at which it and the primary inductance, L_1, are in resonance. This resonant condition occurs at a relatively low frequency, and is found from the primary open-circuit impedance plot shown on Figure 41.

From this resonant frequency, f_1, of 1000 c.p.s. and a knowledge of the value of L_1, C_o can be easily calculated.

$$C_o = \frac{1}{(2\pi f_1)^2 \times L_1} \qquad (19)$$

Therefore

$C_o = 3080$ uuf

As is shown by the article in Appendix III,

f = 700 c.p.s

f = 100 c.p.s

f = 40000 c.p.s

f = 59000 c.p.s

f = 45000 c.p.s

f = 70000 c.p.s

f = 47000 c.p.s

f = 5000 c.p.s

f = 1000 c.p.s

f = 1500 c.p.s

REACTANCE - OHMS (x 10^3)

(X_L)

(X_C)

RESISTANCE - OHMS (x 10^3)

0 5 10 15 20 25 30 35 40 45 50 55 60 65 70 75 80 85 90

10 15 20 25 30 35 40 45 50

IMPEDANCE LOCUS PLOT AS A FUNCTION OF FREQUENCY MEASURED AT PRIMARY OF INPUT TRANSFORMER WITH SECONDARY OPEN-CIRCUITED.

FIG. 41

$$C_o = K_1 + C_5 + \ddot{u}^2 (K_2 + C_6) - 2\ddot{u}K \qquad (20)$$

From this function K is found to be:

$$K = \frac{K_1 + C_5 + \ddot{u}^2 (K_2 + C_6) - C_o}{2\ddot{u}} \qquad (21)$$

Since all of the values on the right hand side of the above equation have already been measured, or calculated, the numerical value of K is readily solved for.

K = 230 uuf

We have now determined all of the values necessary to set up the complete equivalent circuit for the input transformer. This circuit with all of the values referred to the primary side and the potential transformation considered by use of an ideal transformer, is shown on Figure 42.

No attempt was made to solve for the very complex impedance relationships of the final complete equivalent circuit.

However, a few of the simple apparent zeros and poles are listed below.

L' and K_1 are in series resonance at 46 KC

L" and C_5 are in series resonance at 95 KC

$\ddot{u}K$ and L_{s_1} are in parallel resonance at 58 KC

$\frac{L_o}{\ddot{u}^2}$ and $\ddot{u}K_2$ are in series resonance at 34.5 KC

By comparison of the primary open-circuit impedance locus plot of Figure 41 and the amplifier input-impedance locus plot of Figure 34, the loading effect of the input admittance of the vacuum tubes upon the input transformer can be noted. The two curves are identical in shape but the pole and zero frequencies of the amplifier input-impedance locus plot, Figure 34, have been lowered slightly by the input-admittance

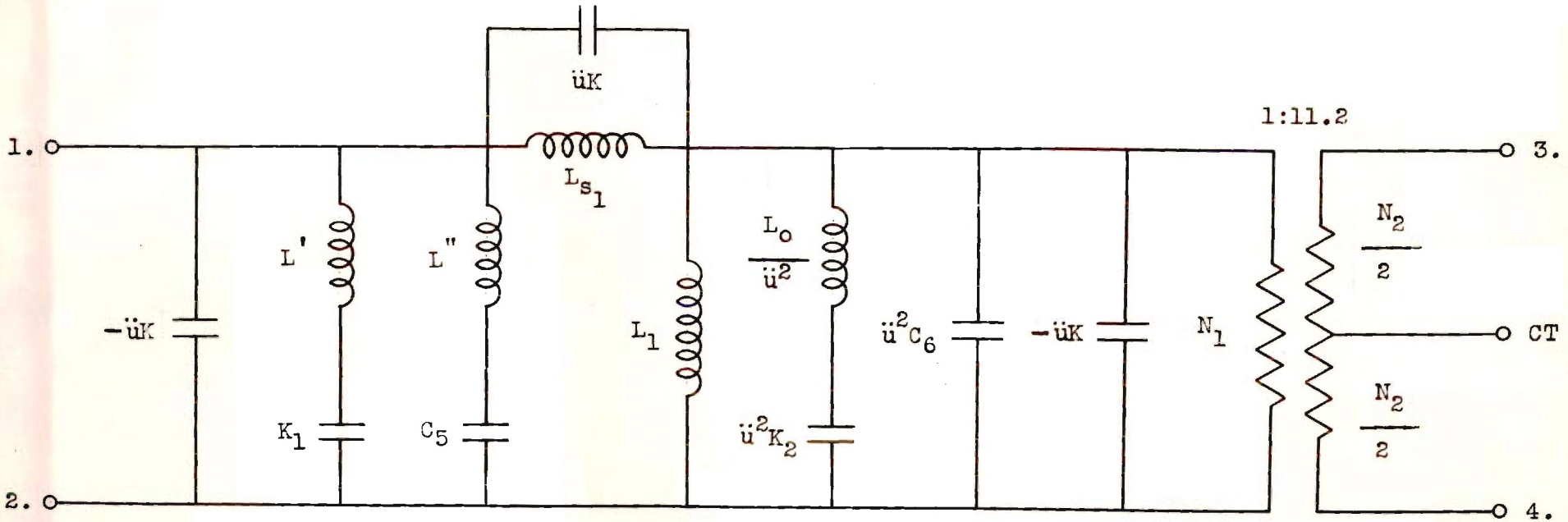

COMPLETE SYNTHESIZED EQUIVALENT CIRCUIT DIAGRAM FOR THE INPUT TRANSFORMER USING AN IDEAL TRANSFORMER. ALL VALUES ARE REFERRED TO THE PRIMARY.

FIG. 42

effect of the vacuum tubes.

Along this same line, the effect of externally added capacity was studied in the following manner. An audio-frequency oscillator was connected to the secondary terminals of the input transformer through a one-megohm resistor with the primary terminals short-circuited. Different values of external capacitance were connected across the secondary terminals, and as the frequency of the audio oscillator was varied, the series and parallel resonances of the secondary were found with the aid of a vacuum-tube voltmeter also connected across the secondary terminals. The results of this test are shown on Figure 43, where the resonant frequencies are plotted as a function of the externally added capacitance. From a study of this chart the effect of the capacitive component of the input admittance of the vacuum tubes upon the resonant frequencies of the transformer can be observed.

In the equivalent circuit for an interstage transformer as is normally represented, all capacitive effects are considered by a single lumped capacitance parallel with the primary incremental inductance and in series with the leakage inductance. This approximation will give adequate results in most cases, but it is sometimes found that the resonant frequency determined from the leakage inductance and this single lumped value of capacitance does not correspond with the one actually measured. Therefore, the last section of this thesis was an attempt to derive a more truly representative equivalent circuit for an interstage transformer.

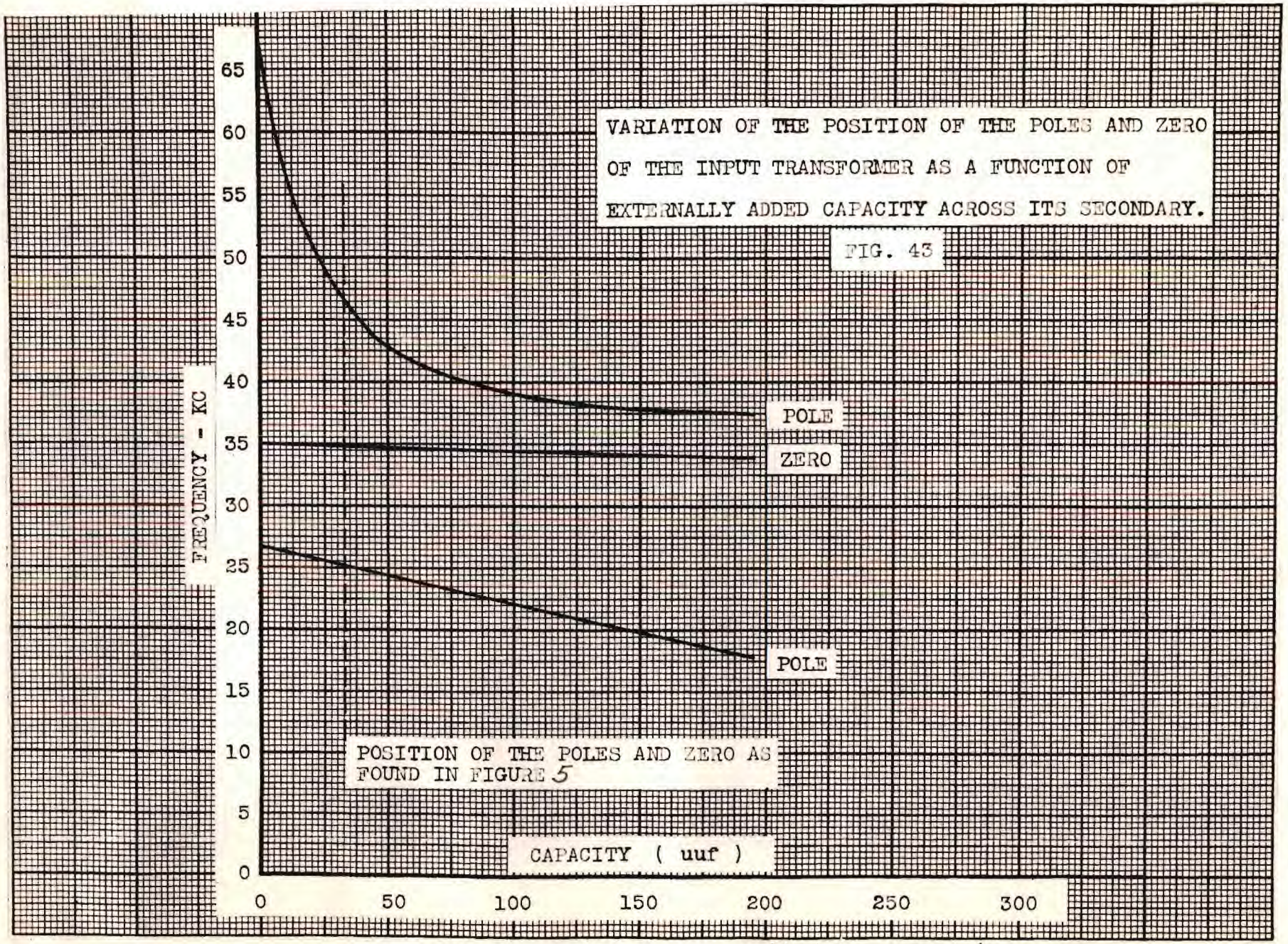
VARIATION OF THE POSITION OF THE POLES AND ZERO OF THE INPUT TRANSFORMER AS A FUNCTION OF EXTERNALLY ADDED CAPACITY ACROSS ITS SECONDARY.
FIG. 43
FREQUENCY - KC
65
60
55
50
45
40
35
30
25
20
15
10
5
0
POLE
ZERO
POLE
POSITION OF THE POLES AND ZERO AS FOUND IN FIGURE 5
CAPACITY (uuf)
0
50
100
150
200
250
300

SUMMARY

Symmetrical neutralization does not produce any astounding changes in the overall amplification and phase characteristics of the amplifier tested as compared with the unneutralized condition. It is probable that properly arranged feedback around the input transformer would have produced a flatter overall frequency response of the amplifier up to a higher frequency. However, it was the purpose of this thesis to examine the effect of the simpler form of feedback (or neutralization) as it applied to the vacuum tubes alone.

Neutralization of the effect of the grid-to-plate capacitance does make minor improvements. But, since the input-capacitance value of the vacuum tubes was found to be small in comparison with the values of capacitances associated with the input transformer, it can be readily seen that cancellation of the effect of the grid-to-plate capacitance of the tubes alone would not make pronounced changes in the overall amplification and phase characteristics of the amplifier.

The input-admittance load of the vacuum tubes causes some minor variations of the input transformer characteristics when the vacuum tubes are connected to the transformer. However, these minor variations are swamped out when the overall amplifier characteristics are considered.

Since the input transformer characteristics are the principal factors that control what form the overall amplifier characteristics are to take, a new method of determining a more complete equivalent circuit for an interstage transformer is outlined in this report.

While the method used for this determination was based on the work originally done by Mr. Von H. Knapp, the final equivalent circuit

diagram derived for the interstage transformer actually measured was somewhat more elaborate than the one evaluated by Mr. Knapp. This method of transformer analysis takes into account the effect of capacitances associated with the transformer which are normally neglected or considered to be inconsequential. Therefore, it is obvious that a more complete circuit could be derived by a method which takes into account all of these capacitances.

It is to be emphasized, however, that this equivalent circuit neglects winding resistances and core losses. These losses are considered to be of secondary importance, since they affect the magnitude of impedance variations, but have little effect upon the positions of the zeros and poles.

Furthermore, two methods of observing and determining experimentally the effect of the vacuum tube admittance load upon the input transformer characteristics, and thus consequently upon the overall amplifier characteristics, were evolved.

The first method was to measure the amplifier input impedance at the primary terminals of the input transformer with the vacuum tubes connected and operating. The second part of this first method was to measure the primary open-circuit impedance of the transformer alone. By comparing the impedance locus plots obtained under these conditions, the effect of the input admittance of the vacuum tubes can be noted.

The second method was to connect external capacitance to the secondary of the input transformer, and to measure the resonant points of the transformer as a function of externally added capacitance. From these results the value of the capacitive component of the input admittance of the vacuum tubes can be determined experimentally.

CONCLUSIONS

A simple form of neutralization when applied to a properly designed transformer-coupled audio amplifier using high-quality component parts does not greatly improve the overall frequency-response and phase characteristics of the amplifier.

It was found that additional peaks are present in the overall frequency-response characteristics of the transformer-coupled audio amplifiers, but these peaks are probably neglected for the usual cases since they normally occur at a frequency above the specified pass band of the transformer.

The input admittance of the vacuum tubes is in effect connected across the secondary of the input transformer. Since the value of this admittance will vary as a function of the frequency, these load variations, which are reflected into the transformer secondary, will, therefore, cause some deviations in the transformer characteristics, when these characteristics are measured with the vacuum tube load connected. However, this input admittance loading effect is not apparent when the overall frequency-response characteristic of the amplifier is considered. This effect would undoubtedly be more pronounced if the vacuum tubes used had a larger value of mu and G_m and a reactive load in the plate circuit.

It was also shown that a more complete equivalent circuit for an interstage transformer can be derived by appropriate impedance measurements made upon the transformer. This transformer equivalent circuit is proven valid since the pole and zero frequencies determined by the impedance measurements will account for the peaks and minima which

appear on the frequency-response curves. For the simple transformer-coupled audio amplifier the additional work required to evaluate a more complete equivalent circuit would not be justified. However, it has been found by other writers that in many cases an audio amplifier using feed-back will oscillate in the 40 KC to 50 KC region. For this case a more complete equivalent circuit would indicate the amplitude and phase changes that occur over the frequency range under consideration. Consequently, a more accurate equivalent circuit would enable a more complete analysis of the feed-back amplifier to be made.

BIBLIOGRAPHY

Bode, H. W., Network Analysis and Feedback Amplifier Design, D. Van Nostrand Company, 1945, 551 pp.

Everitt, W. L., Communication Engineering, McGraw-Hill Book Company, 1937, 727 pp.

Klipsch, P. W., "Design of Audio-frequency Amplifier Circuits using Transformers," Proc. I.R.E., Vol. 24, p. 219, February, 1936.

_____, "Applying Neutralization to A-F Amplifiers," Electronics, Vol. 7, p. 252, August, 1934.

Knapp, Von H., "The Influence of Capacitances between the Windings of a Transformer on its Characteristics," Elektrische Nachrichten Technik, Vol. 20, No. 8, p. 192, August, 1943.

Koehler, Glenn, "The Design of Transformers for Audio-frequency Amplifiers with Preassigned Characteristics," Proc. I.R.E., Vol. 16, No. 12, p. 1742, December, 1928.

Lee, Reuben, Electronic Transformers and Circuits, John Wiley and Sons, Inc., 1947, 282 pp.

M.I.T., Staff Members of Electrical Engineering Department, Magnetic Circuits and Transformers, John Wiley and Sons, Inc., 1943, 718 pp.

_____, Applied Electronics, John Wiley and Sons, Inc., 1943, 772 pp.

Sah, A Pen-Tung, "Quasi Transients in Class B Audio-frequency Push-pull Amplifiers," Proc. I.R.E., Vol. 24, No. 11, p. 1522, November, 1936.

Shea, T. E., Transmission Networks and Wave Filters, D. Van Nostrand Company, 1929, 470 pp.

Story, J. G., "Design of Audio-frequency Input and Intervalve Transformers," The Wireless Engineer, Vol. 15, p. 69, February, 1938.

Terman, F. E. and R. E. Ingebretsen, "Output Transformer Response," Electronics, Vol. 9, p. 30, January, 1936.

Terman, F. E., Measurements in Radio Engineering, McGraw-Hill Book Company, 1935, 400 pp.

_____, Radio Engineers' Handbook, Mc-Graw-Hill Book Company, 1943, 1019 pp.

Wrathall, E. T., "Audio-frequency Transformers," The Wireless Engineer, Vol. 14, p. 293-363-414, June-August, 1937.

APPENDIX I

TABLES

TABLE I

Linear Standard Audio Transformer Features

(Furnished by Manufacturer)

1. True Hum Balancing Coil Structure - maximum neutralization of stray fields.

2. Balanced Variable Impedance Line - permits highest fidelity on every tap of a universal unit - no line reflections or transverse coupling.

3. Reversible Mounting - permits above chasis or subchasis mounting.

4. Alloy Shields - maximum shielding from inductive pickup.

5. Multiple Coil, Semi-Toroidal Coil Structure - minimum distributed capacity and leakage reactance.

6. Precision Winding - accuracy of winding 0.1%, perfect balance of inductance and capacitance; exact impedance reflection.

7. Hiperm-Alloy - a stable high permeability nickel - iron core material.

8. High Fidelity - guaranteed uniform response, from 30 to 20,000 cycles $\pm$ 1 db.

TABLE II

Values and Ratings of Component Parts shown on the Schematic Diagram. (Figure 2)

T - 1	Input Transformer	UTC, LS - 10
T - 2	Output Transformer	UTC, LS - 55
R - 1	10,000 ohms	10 watts
R - 2	100,000 ohms	1 watt
P - 1	Potentiometer	0-15,000 ohms
P - 2	Potentiometer	0-15,000 ohms
C - 1	0.1 uf	550 WVDC
C - 2	0.1 uf	550 WVDC
C - 3	Air Trimmer	7.5 to 55 uuf
C - 4	Air Trimmer	7.5 to 55 uuf
C - 5	0.1 uf	550 WVDC
C - 6	0.1 uf	550 WVDC
C - 7	1.0 uf	550 WVDC

TABLE III

Overall Amplification and Phase Characteristics. Amplifier Unneutralized and Input Transformer Unloaded. E_I = 2 volts (Constant).

Values are Plotted on Figure 5 and Figure 6.

Amplification E_o/E_I	Phase Angle ϕ^o	Frequency KC
9.30	+ 8.50	.02
9.50	+ 5.75	.03
9.60	+ 4.30	.05
9.60	+ 3.50	.07
9.60	+ 2.80	.10
9.75	+ 1.50	.20
10.00	0	.30
10.00	0	.50
10.00	- 1.50	.70
10.00	- 2.80	1.00
10.00	- 5.00	2.00
10.00	- 5.75	3.00
10.20	- 6.50	5.00
10.25	- 6.50	7.00
10.80	- 8.50	10.00
11.20	- 10.00	12.00
12.15	- 12.00	14.00
12.75	- 13.00	16.00
13.85	- 16.00	18.00
15.50	- 17.50	20.00
18.60	- 25.20	22.00
22.40	- 45.00	24.00
25.00	- 55.60	25.00
26.50	- 63.00	25.80
24.75	- 90.00	27.00
13.50	-135.50	29.00
9.55	-139.50	30.00
3.75	-124.40	32.00
2.40	- 75.00	33.50
2.65	- 65.00	34.00
4.80	- 30.00	36.00
7.40	- 25.00	38.00
11.20	- 28.30	40.00
16.10	- 44.50	42.50
20.20	- 58.00	45.00
24.00	- 90.00	47.00
20.50	-139.50	50.00
8.25	-147.00	55.00

TABLE III (Cont.)

Amplification	Phase Angle	Frequency
4.20	-155.00	60.00
4.10	-160.00	65.00
3.50	-165.00	70.00

TABLE IV

Overall Amplification and Phase Characteristics. Amplifier Unneutralized and Input Transformer loaded with 100,000 ohms. E_I = 2 volts (constant).

Values are Plotted on Figure 7 and Figure 8.

Amplification E_o/E_I	Phase Angle ϕ^o	Frequency KC
8.10	+ 8.50	.02
7.80	+ 5.75	.03
7.80	+ 4.30	.05
7.80	+ 3.50	.07
7.80	+ 2.80	.10
7.80	+ 1.50	.20
7.80	0	.30
7.80	0	.50
7.90	- 2.25	.70
7.90	- 4.30	1.00
7.90	- 5.75	2.00
7.90	- 8.50	3.00
8.00	- 11.50	5.00
8.10	- 14.50	7.00
8.50	- 17.50	10.00
8.70	- 20.50	12.00
8.90	- 23.00	14.00
9.10	- 30.00	16.00
9.40	- 35.00	18.00
9.70	- 40.50	20.00
10.10	- 53.00	21.80
9.50	- 67.00	25.00
8.20	- 90.00	27.00
6.00	-110.00	29.00
5.00	-115.75	30.00
2.00	- 90.00	33.00
3.80	- 40.00	36.00
5.60	- 45.00	38.00
6.80	- 53.00	40.00
7.20	- 65.00	42.00
6.80	- 85.00	45.00
5.10	-119.00	50.00
3.20	-125.00	55.00
2.00	-131.50	60.00
1.50	-143.00	70.00
1.00	-147.00	75.00
0.80	-150.00	80.00

TABLE V

Overall Amplification and Phase Characteristics. Amplifier Neutralized and Input Transformer loaded with 100,000 ohms. E_I = 2 volts (constant).

Values are Plotted on Figure 9 and Figure 10.

Amplification E_o/E_I	Phase Angle ϕ^o	Frequency KC
7.00	+ 6.50	.02
7.00	+ 4.80	.03
7.05	+ 4.20	.05
7.10	+ 3.60	.07
7.10	+ 2.90	.10
7.15	+ 2.40	.20
7.20	+ 1.25	.30
7.25	0	.50
7.25	0	.70
7.25	0	1.00
7.25	- 1.25	2.00
7.25	- 2.40	3.00
7.35	- 4.50	5.00
7.40	- 7.75	7.00
7.50	- 12.20	10.00
7.75	- 15.70	12.00
7.85	- 17.50	14.00
7.95	- 22.25	16.00
8.20	- 27.70	18.00
8.55	- 35.25	20.00
8.75	- 41.80	22.00
8.95	- 60.10	25.00
8.05	- 74.10	27.50
7.30	- 90.00	28.50
7.00	-103.00	29.00
5.50	-109.50	30.00
3.00	-109.80	32.00
2.50	- 90.00	33.00
3.75	- 31.30	36.00
5.00	- 34.75	38.00
6.00	- 43.80	40.00
6.75	- 68.50	45.00
6.40	- 90.00	50.00
4.75	-105.00	55.00
3.40	-112.00	60.00
3.10	-130.00	70.00

TABLE VI

Overall Amplification Characteristics (Normalized). Input Transformer loaded with 100,000 ohms. (1) Amplifier Unneutralized (2) Amplifier Neutralized.

Values are Plotted on Figure 11 and Figure 12.

Relative Amplification (1)	Relative Amplification (2)	Frequency KC
1.025	0.965	.02
0.986	0.965	.03
0.986	0.972	.05
0.986	0.979	.07
0.986	0.979	.10
0.986	0.986	.20
0.986	0.993	.30
0.986	1.000	.50
1.000	1.000	.70
1.000	1.000	1.00
1.000	1.000	2.00
1.000	1.000	3.00
1.010	1.013	5.00
1.025	1.020	7.00
1.075	1.034	10.00
1.100	1.069	12.00
1.125	1.082	14.00
1.150	1.096	16.00
1.190	1.130	18.00
1.230	1.179	20.00
1.280	1.207	22.00
1.200	1.232	25.00
1.037	1.110	27.00
0.759	0.965	29.00
0.632	0.758	30.00
0.253	0.345	33.00
0.481	0.517	36.00
0.708	0.690	38.00
0.860	0.827	40.00
0.910	0.880	42.00
0.860	0.930	45.00
0.645	0.882	50.00
0.405	0.655	55.00
0.253	0.468	60.00
0.278	0.440	65.00
0.253	0.427	70.00

TABLE VII

Overall Amplification and Phase Characteristics. Amplifier Under Neutralized and Input Transformer loaded with 100,000 ohms. E_I = 2 volts (constant).

Values are Plotted on Figure 13 and Figure 14.

Amplification E_o/E_I	Phase Angle ϕ^o	Frequency KC
8.50	+ 6.70	.02
8.60	+ 4.80	.03
8.75	+ 2.90	.05
8.85	+ 2.10	.07
8.80	+ 2.10	.10
8.95	+ 1.50	.20
8.95	+ 0.75	.30
8.95	0	.50
9.00	0	.70
9.00	0	1.00
9.00	- 1.60	2.00
9.00	- 3.10	3.00
9.25	- 5.75	5.00
9.35	- 8.50	7.00
9.50	- 11.50	10.00
10.00	- 15.25	12.00
10.15	- 19.50	14.00
10.50	- 24.25	16.00
10.75	- 29.30	18.00
11.00	- 34.40	20.00
11.50	- 48.10	22.00
11.70	- 58.10	23.50
11.50	- 66.00	25.00
9.60	- 90.00	28.00
6.10	-112.00	30.00
3.00	-113.50	32.00
1.90	- 90.00	33.00
4.05	- 31.60	36.00
5.90	- 33.50	38.00
7.40	- 48.00	40.00
8.50	- 68.60	45.00
8.10	- 90.00	47.00
6.90	-110.00	50.00
4.70	-120.00	55.00
2.65	-126.00	60.00
2.40	-133.00	70.00

TABLE VIII

Overall Amplification and Phase Characteristics. Amplifier Over Neutralized and Input Transformer loaded with 100,000 ohms. E_I = 2 volts (constant).

Values are Plotted on Figure 15 and Figure 16.

Amplification E_o/E_I	Phase Angle ϕ^o	Frequency KC
8.30	+ 7.60	.02
8.30	+ 6.10	.03
8.40	+ 5.00	.05
8.45	+ 4.30	.07
8.60	+ 2.90	.10
8.60	+ 2.10	.20
8.60	+ 1.50	.30
8.70	0	.50
8.75	0	.70
8.75	0	1.00
8.75	- 0.80	2.00
8.85	- 2.90	3.00
8.85	- 5.75	5.00
8.85	- 7.20	7.00
8.90	- 11.50	10.00
9.00	- 13.00	12.00
9.00	- 17.50	14.00
9.00	- 19.00	16.00
9.20	- 22.10	18.00
9.25	- 25.20	20.00
9.45	- 31.70	22.00
9.65	- 41.80	25.00
9.70	- 54.00	27.00
8.60	- 69.20	29.00
6.60	- 90.00	30.00
3.50	-106.20	32.00
2.20	- 61.20	33.50
3.70	- 27.20	36.00
5.40	- 32.60	40.00
5.60	- 40.60	45.00
5.30	- 47.00	50.00
4.60	- 50.00	55.00
4.40	- 53.00	60.00
6.70	- 53.00	65.00
8.00	- 54.00	69.00
6.70	---	75.00

TABLE IX

Overall Amplification and Phase Characteristics. Amplifier Neutralized and Input Transformer loaded with 100,000 ohms (Grid-to-Plate Capacitance = 37 uuf). E_I = 2 volts (constant).

Values are Plotted on Figure 17 and Figure 18.

Amplification E_o/E_I	Phase Angle ϕ^o	Frequency KC
7.70	+ 6.40	.02
7.75	+ 4.80	.03
7.90	+ 3.20	.05
8.00	+ 2.30	.07
8.05	+ 1.60	.10
8.05	0	.20
8.05	0	.30
8.15	- 1.60	.50
8.25	- 2.30	.70
8.25	- 4.00	1.00
8.25	- 6.00	2.00
8.30	- 8.20	3.00
8.30	- 10.20	5.00
8.40	- 13.60	7.00
9.00	- 18.20	10.00
9.05	- 20.60	12.00
9.20	- 24.30	14.00
9.55	- 29.00	16.00
9.85	- 33.75	18.00
10.40	- 49.00	20.00
10.65	- 54.75	22.00
10.65	- 80.00	25.00
10.00	- 90.00	27.00
7.20	-108.00	29.00
5.75	-115.00	30.00
2.95	-112.30	32.00
2.00	- 90.00	33.00
3.00	- 44.50	35.00
5.40	- 44.50	37.50
7.20	- 58.20	40.00
8.25	- 90.00	45.00
7.75	-108.00	47.50
6.75	-128.00	50.00
4.40	-143.00	55.00
2.80	-147.00	60.00
2.50	-150.00	70.00

TABLE X

Overall Amplification and Phase Characteristics. Amplifier Under Neutralized and Input Transformer loaded with 100,000 ohms (Grid-to-Plate Capacitance = 37 uuf). E_I = 2 volts (constant).

Values are Plotted on Figure 19 and Figure 20.

Amplification E_o/E_I	Phase Angle ϕ^o	Frequency KC
7.40	+ 8.20	.02
7.55	+ 4.10	.03
7.75	+ 3.10	.05
7.80	+ 3.10	.07
7.80	+ 2.10	.10
7.95	0	.20
8.00	0	.30
8.00	- 1.10	.50
8.00	- 3.10	.70
8.00	- 4.10	1.00
8.10	- 7.20	2.00
8.10	- 8.20	3.00
8.35	- 12.80	5.00
8.35	- 16.30	7.00
8.50	- 21.10	10.00
9.25	- 26.20	12.00
9.50	- 30.00	14.00
9.85	- 36.40	16.00
10.30	- 45.60	18.00
11.00	- 53.10	20.00
11.15	- 61.10	22.00
10.90	- 74.80	24.00
10.50	- 90.00	25.00
8.65	-116.00	27.00
6.40	-124.50	29.00
5.00	-130.00	30.00
2.30	-123.50	32.00
1.65	- 90.00	33.00
2.85	- 53.10	35.00
5.20	- 48.60	37.00
7.50	- 71.25	40.00
8.00	- 90.00	42.00
7.10	-124.00	45.00
5.00	-150.00	50.00
3.00	-154.00	55.00
1.65	-157.00	60.00
1.50	-160.00	70.00

TABLE XI

Ratio of Secondary to Primary Voltage of Input Transformer. Amplifier Unneutralized. Input Transformer Unloaded.

E_p = 2 volts (constant).

Values are Plotted on Figure 21.

Voltage Ratio E_s/E_p	Frequency KC	Voltage Ratio E_s/E_p	Frequency KC
5.50	.02	15.75	27.00
5.60	.03	11.50	28.00
5.60	.05	7.25	29.00
5.60	.07	4.50	30.00
5.65	.10	2.00	32.00
5.65	.20	1.25	33.50
5.70	.30	1.40	34.00
5.65	.50	2.80	36.00
5.65	.70	4.40	38.00
5.70	1.00	6.70	40.00
5.70	2.00	9.75	42.50
5.70	3.00	14.50	45.00
5.95	5.00	15.00	46.00
6.10	7.00	14.50	47.50
6.60	10.00	9.75	50.00
7.00	11.00	5.10	55.00
7.50	12.00	3.50	60.00
7.35	12.50	2.70	65.00
5.70	13.00	1.80	70.00
4.70	13.50		
5.10	14.00		
5.75	15.00		
6.25	16.00		
7.20	18.00		
8.00	20.00		
10.50	22.00		
16.50	25.00		
17.00	26.00		

TABLE XII

Ratio of Secondary to Primary Voltage and Phase Characteristics of Input Transformer. Amplifier Unneutralized. Input Transformer loaded with 100,000 ohms.

E_p = 2 volts (constant).

Values are Plotted on Figure 22 and Figure 23.

Voltage Ratio E_s/E_p	Phase Angle ϕ^o	Frequency KC
4.95	0	.02
5.00	0	.03
5.00	0	.05
5.00	0	.07
5.00	0	.10
5.00	0	.20
5.00	- 0.75	.30
5.00	- 2.25	.50
5.00	- 2.80	.70
5.00	- 4.30	1.00
5.00	- 6.50	2.00
5.10	- 7.90	3.00
5.20	- 11.50	5.00
5.30	- 14.50	7.00
5.50	- 42.50	10.00
5.80	-102.00	12.00
5.20	- 98.00	12.50
3.90	- 90.00	13.00
3.60	- 63.00	13.50
4.20	- 44.50	14.00
4.80	- 35.00	15.00
5.10	- 27.00	16.00
5.50	- 23.50	18.00
5.85	- 27.00	20.00
6.10	- 37.00	22.00
6.25	- 49.00	24.00
6.10	- 53.00	25.00
5.60	- 70.00	27.00
4.50	- 85.00	28.50
3.15	- 90.00	30.00
1.50	- 77.00	32.00
1.05	- 53.00	33.00
1.20	- 25.00	34.00
2.25	- 11.50	36.00
3.40	- 15.00	38.00

TABLE XII (Cont.)

Voltage Ratio	Phase Angle	Frequency
4.20	- 27.00	40.00
4.65	- 45.00	42.00
4.90	- 58.00	45.00
4.75	- 72.00	47.50
4.3	- 80.00	50.00
3.2	- 93.00	55.00
2.5	- 98.00	60.00
2.0	-103.00	65.00
1.6	-103.00	70.00

TABLE XIII

Ratio of Secondary to Primary Voltage and Phase Characteristics of Input Transformer Alone.

E_p = 2 volts (constant).

Values are Plotted on Figure 24 and Figure 25.

Voltage Ratio	Phase Angle	Frequency
Es/Ep	ϕ°	KC
5.40	+ 2.85	.02
5.50	+ 1.40	.03
5.50	+ 0.75	.05
5.50	0	.07
5.50	0	.10
5.60	0	.20
5.60	0	.30
5.60	0	.50
5.60	0	.70
5.60	0	1.00
5.60	0	2.00
5.60	0	3.00
5.65	- 1.40	5.00
5.75	- 2.80	7.00
6.00	- 5.75	10.00
6.30	- 7.00	12.00
6.75	- 11.50	14.00
7.30	- 14.50	16.00
7.90	- 17.50	18.00
8.50	- 30.00	20.00
9.20	- 55.00	22.00
10.75	- 95.00	25.00
12.25	-120.00	27.00
12.00	-140.00	28.00
6.60	-147.00	30.00
2.50	-122.00	32.00
1.35	- 90.00	33.50
1.40	- 56.00	34.00
2.60	- 33.00	36.00
3.75	- 33.00	38.00
5.25	- 45.00	40.00
7.00	- 90.00	42.50
10.40	-140.00	47.50
16.75	-150.00	50.00
10.00	-160.00	55.00
5.50	-160.00	60.00
3.75	-142.00	65.00
2.40	-130.00	70.00

TABLE XIII (Cont.)

Voltage Ratio	Phase Angle	Frequency
1.60	-120.00	75.00
1.40	-100.00	77.50
1.70	- 90.00	80.00
3.10	-127.00	85.00
2.40	-136.00	90.00
1.50	-143.00	100.00

TABLE XIV

Amplifier Input Resistance and Reactance Characteristics. Amplifier Unneutralized. Input Transformer Unloaded.

Values are Plotted on Figure 32, Figure 33, and Figure 34.

Resistance	Inductive Reactance	Capacitive Reactance	Frequency
Ohms	Ohms	Ohms	KC
3,375	4,880		.04
3,945	5,410		.05
4,990	6,820		.08
5,650	7,580		.10
6,450	8,200		.12
7,630	9,090		.15
8,640	10,330		.18
10,280	10,600		.20
15,850	11,640		.30
21,850	10,200		.40
27,200	5,780		.50
30,000	Pole		.60
28,300		7,900	.70
25,500		12,780	.80
21,000		15,400	.90
17,180		16,320	1.00
14,380		16,250	1.10
10,880		16,030	1.20
9,100		15,190	1.30
7,440		14,350	1.40
6,340		13,550	1.50
3,108		10,190	2.00
1,180		6,560	3.00
640		4,810	4.00
450		3,760	5.00
344		3,080	6.00
279		2,595	7.00
244		2,215	8.00
215		1,932	9.00
195		1,700	10.00
175		1,330	12.00
156		1,058	14.00
155		848	16.00
150		662	18.00
147		531	20.00
143		396	21.00
144		322	22.00
146		248	23.00
148		178	24.00

TABLE XIV (Cont.)

Resistance	Inductive Reactance	Capacitive Reactance	Frequency
152		107	25.00
157		26	26.00
158	Zero		26.50
160	35		27.00
165	112		28.00
200	291		30.00
279	540		32.00
365	711		33.00
502	890		34.00
806	1,158		35.00
1,315	1,250		36.00
2,395	Pole		37.50
2,084		284	38.00
1,400		694	39.00
980		788	39.50
793		786	40.00
498		657	41.00
386		500	42.00
300		335	43.00
255		221	44.00
223		117	45.00
208		58	46.00
195	Zero		47.00
192	43		47.50
181	109		48.00
176	143		49.00
172	197		50.00
174	410		55.00
193	578		60.00
198	715		65.00
231	905		70.00

TABLE XV

Amplifier Input Resistance and Reactance Characteristics.
Amplifier Unneutralized. Input Transformer loaded with 100,000 ohms.

Values are Plotted on Figure 35 and Figure 36.

Resistance	Inductive Reactance	Capacitive Reactance	Frequency
Ohms	Ohms	Ohms	KC
915	9		.05
937	19		.10
945	24		.15
950	32		.20
954	36		.30
958	35		.40
958	32		.50
960	24		.60
963	15		.70
963	0		.80
964	Pole		.84
965		12	1.30
965		15	1.40
965		18	1.50
963		28	2.00
960		40	2.50
955		50	3.00
950		59	3.50
947		68	4.00
930		83	5.00
915		98	6.00
890		103	7.00
870		118	8.00
850		122	9.00
825		126	10.00
770		129	12.00
738		113	14.00
670		96	16.00
613		71	18.00
547		35	20.00
492	Zero		21.60
473	22		22.50
404	99		25.00
350	196		27.00
323	257		28.00
302	316		29.00
287	384		30.00
279	472		31.00
289	584		32.00

TABLE XV (Cont.)

Resistance	Inductive Resistance	Capacitive Reactance	Frequency
349	754		33.00
445	870		34.00
651	980		35.00
982	924		36.00
1155	689		37.00
1154	404		38.00
1059	259		39.00
934	191		40.00
847	168		41.00
750	170		42.00
689	182		43.00
631	208		44.00
582	239		45.00
503	308		47.50
444	398		50.00
405	488		52.50
382	563		55.00
366	710		60.00
358	834		65.00

TABLE XVI

Input Transformer Secondary Short-circuit Impedance Locus Characteristics.

Values are Plotted on Figure 37.

Resistance	Inductive Reactance		Capacitive Reactance	Frequency
Kilohms	Kilohms		Kilohms	KC
14.2	11.0			5.00
15.0	13.2			6.00
16.8	18.5			8.00
19.5	24.4			10.00
25.0	30.9			12.00
36.0	37.6			14.00
52.0	48.9			17.00
127.0	31.8			20.00
135.0	16.2			21.00
140.0		Pole		30.00
95.0			62.0	32.00
19.2		Zero		34.50
50.6	150.0			50.00
80.6	193.3			52.50
128.5	251.5			55.00
227.5	325.5			57.50
505.0	332.0			60.00
608.0	310.0			62.00
815.0		Pole		63.00
800.0			108.6	63.50
768.0			256.5	65.00
277.0			405.0	67.50
157.2			350.0	70.00
58.5			219.5	75.00
49.0			176.0	79.00
51.5			165.5	80.00
61.0			167.0	81.00
54.0			172.0	82.50
35.5			156.0	85.00
24.1			147.0	87.50
18.7			135.6	90.00
11.0			112.7	95.00

TABLE XVII

Input Transformer Primary Short-circuit Impedance Locus Characteristics.

Values are Plotted on Figure 38.

Resistance	Inductive Reactance	Capacitive Reactance	Frequency
Ohms	Ohms	Ohms	KC
104	173		10.00
105	206		12.00
106	237		14.00
106	256		15.00
106	286		17.00
107	325		19.00
107	328		20.00
109	377		21.00
109	397		22.00
110	438		24.00
110	464		25.00
113	506		27.00
118	556		29.00
124	585		30.00
155	648		32.00
172	663		32.50
198	681		33.00
233	686		33.50
298	651		34.00
307	605	Pole	34.50
278	546		35.00
220	533		35.50
188	545		36.00
168	560		36.50
155	574		37.00
144	601		37.50
138	618		38.0
133	630		38.5
130	642		39.0
127	665		39.50
126	676		40.00
123	708		41.00
122	738		42.50
121	769		44.00
120	803		45.00
119	820	Zero	46.00
120	851		47.50
121	865		49.00
123	922		50.00

TABLE XVII (Cont.)

Resistance	Inductive Reactance	Capacitive Reactance	Frequency
124	948		52.50
125	1006		55.00
128	1045		57.50
132	1134		60.00
134	1180		62.50
140	1243		65.00
144	1269		67.50
154	1354		70.00
166	1390		72.50
200	1475		75.00
250	1510		77.50
280	1475	Pole	80.00
274	1462		81.25
240	1461		82.50
215	1486		83.75
196	1515		85.00
185	1525		86.25
180	1530		87.50
170	1610		90.00
169	1640		92.50
168	1730	Zero	95.00
169	1740		97.50
170	1830		100.00
180	1920		105.00

TABLE XVIII

Input Transformer Primary Open-Circuit Impedance Locus Characteristics.

Values are Plotted on Figure 41.

Resistance	Inductive Reactance		Capacitive Reactance	Frequency
Ohms	Ohms		Ohms	KC
2,290	7,210			.10
4,790	12,040			.20
7,820	17,200			.30
12,200	21,700			.40
18,200	26,600			.50
27,100	30,500			.60
39,100	33,400			.70
55,900	29,600			.80
73,100	16,700			.90
84,000		Pole		1.00
69,200			40,300	1.20
28,100			47,000	1.50
9,740			32,600	2.00
5,090			14,800	3.00
2,360			10,800	4.00
1,340			8,420	5.00
900			6,850	6.00
650			5,740	7.00
510			4,900	8.00
360			3,760	10.00
280			3,350	12.00
227			2,070	15.00
210			1,810	17.00
194			1,335	20.00
191			966	22.00
195			693	24.00
200			542	25.00
206			415	26.00
216			270	27.00
226			139	28.00
240		Zero		29.00
264	168			30.00
290	318			31.00
328	498			32.00
380	714			33.00
453	958			34.00
560	1,240			35.00
720	1,580			36.00
950	1,980			37.00

TABLE XVIII (Cont.)

Resistance	Inductive Reactance		Capacitive Reactance	Frequency
1,580	2,700			38.00
2,645	3,400			39.00
4,890	3,620			40.00
6,410	3,030			41.00
8,700		Pole		42.00
8,100			1,990	42.50
3,560			4,160	44.00
2,264			3,920	45.00
925			2,620	47.50
488			1,790	50.00
365			1,385	52.50
283			1,030	55.00
240			786	57.50
210			562	60.00
191			396	62.50
180			267	65.00
173			125	67.50
169		Zero		70.00
173	109			72.50
188	210			75.00
292	348			80.00

TABLE XIX

Values of Circuit Components shown on the Complete Synthesized Equivalent Circuit Diagram for the Input Transformer. Figure 42.

$\ddot{u}$	= $\frac{N_2}{N_1}$ =	11.2
$-\ddot{u}K$	=	-2482 uuf
$\ddot{u}K$	=	2482 uuf
$\ddot{u}^2K_2$	=	1660 uuf
$\ddot{u}^2C_6$	=	2870 uuf
K_1	=	2734 uuf
C_5	=	779 uuf
L_1	=	8.25 h
L'	=	4.38 mh
L''	=	3.59 mh
L_{s_1}	=	3.0 mh
$\frac{L_o}{\ddot{u}^2}$	=	12.8 mh

TABLE XX

Variation of the Position of the Poles and Zero of the Input Transformer as a function of Externally Added Capacity across Secondary.

Values are Plotted on Figure 43.

Pole	Zero	Pole	Capacity
KC	KC	KC	u uf
27.0	35.0	67.5	0
25.5	35.0	49.0	25
24.5	34.5	43.0	50
21.0	34.5	39.0	106
20.0	34.5	38.0	136
19.0	34.0	38.0	165
18.0	34.0	37.5	196

APPENDIX II

DERIVATION

DERIVATION I

From equations (5) and (6), page 62, two equations involving K_2 and C_6 in terms of the zero and pole frequencies, w_1, w_2, and w_3, of the circuit of Figure 39, are derived.

$$w_2^2 \cdot w_3^2 = \frac{1}{L_{s_2} L_o C_6 K_2} \tag{1}$$

and

$$w_2^2 + w_3^2 = \frac{L_{s_2} (K_2 + C_6) + L_o K_2}{L_{s_2} L_o C_6 K_2} \tag{2}$$

$$\text{Since } w_1 = \frac{1}{\sqrt{L_o K_2}} \tag{3}$$

Equation (1) becomes,

$$w_2^2 \cdot w_3^2 = \frac{w_1^2}{L_{s_2} C_6} \tag{4}$$

and Equation (2) becomes

$$w_2^2 + w_3^2 = \frac{w_1^2 L_{s_2} (K_2 + C_6) + 1}{L_{s_2} C_6} \tag{5}$$

Then equation (4) rewritten is:

$$L_{s_2} C_6 = \frac{w_1^2}{w_2^2 \cdot w_3^2} \tag{6}$$

and equation (5) rewritten is:

$$L_{s_2} C_6 = \frac{w_1^2 L_{s_2} (K_2 + C_6) + 1}{w_2^2 + w_3^2} \tag{7}$$

By equating equations (6) and (7) and rearranging:

$$L_{s_2}\,(K_2 + C_6) = \frac{w_1^2\,(w_2^2 + w_3^2) - w_2^2\,w_3^2}{w_1^2 w_2^2 w_3^2} \tag{8}$$

$$L_{s_2}\,(K_2 + C_6) = \left[\frac{1}{w_2^2} + \frac{1}{w_3^2}\right] - \left[\frac{1}{w_1^2}\right] \tag{9}$$

Again starting with equations (1) and (2) and rearranging both equations the following relationships are evolved.

$$L_{s_2} = \frac{w_1^2}{C_6\,w_2^2\,w_3^2} \tag{10}$$

and

$$L_{s_2} = \frac{1}{C_6(w_2^2 + w_3^2 - w_1^2) - (w_1^2 K_2)} \tag{11}$$

By equating equations (10) and (11) and rearranging,

$$C_6\,w_2^2\,w_3^2 = C_6\,w_1^2(w_2^2 + w_3^2 - w_1^2) - (w_1^4\,K_2) \tag{12}$$

$$C_6\left[w_1^2\,(w_2^2 + w_3^2 - w_1^2) - (w_2^2\,w_3^2)\right] = K_2\,w_1^4 \tag{13}$$

$$\frac{K_2}{C_6} = \frac{\left[w_1^2\,w_2^2 + w_1^2\,w_3^2 - w_1^4\right] - \left[w_2^2\,w_3^2\right]}{w_1^4} \tag{14}$$

$$\frac{K_2}{C_6} = \left[\left(\frac{w_2}{w_1}\right)^2 + \left(\frac{w_3}{w_1}\right)^2 - \left(\frac{w_2}{w_1}\right)^2\left(\frac{w_3}{w_1}\right)^2 - 1\right] \tag{15}$$

APPENDIX III

TRANSLATION

THE INFLUENCE OF CAPACITANCE BETWEEN THE WINDINGS OF A TRANSFORMER ON ITS CHARACTERISTICS

by

Von H. Knapp

Siemens and Halske Co.

Berlin, Germany

Translated from the German publication, Elektrische Nachrichten Technik, Volume 20, Issue 8, August 1943, by A. F. Rothschild, Georgia Institute of Technology.

1948

TABLE OF CONTENTS

I. INTRODUCTION

Numerous publications have dealt with the transformer as an important constituent in communication technique. As far as they concern the enclosed transformer with close coupling, it is generally assumed that only magnetic coupling exists between primary and secondary and that the capacitative coupling is to be neglected. We then get a star or a triangle circuit (Figures 5 and 6) for the equivalent circuit diagram; in order to gain a better perspective, all magnitudes are generally related to one side of the transformer by a suitable "transformation ratio" and for the transformation of potential an ideal transformer is connected in front of or behind the equivalent circuit (Figure 7). In this equivalent circuit diagram all capacitative influences are generally taken into consideration by a single capacitance parallel to the shunt inductance; its magnitude is determined by the parallel resonance. But now it is known that the stray resonance frequency determined from the leakage inductance and this capacitance often does not correspond with the one actually measured. It seems likely that the reason for this deviation lies in the too rough appoximation of the capacitances. In addition to the distributed capacitances of the windings, one must consider the capacitances between the windings, and the driving potentials on these interwinding capacitances are the differences in potential between the various windings. Generally, a certain pair of terminals of a quadripole are considered as the input terminal, the other as the output terminal. If we assume that no further connection exists between the input and output terminal pairs, then a connection without resistance between an input and an output terminal is

possible. In this manner we arrive at the star or triangular equivalent circuit diagram. The effect of capacitances between the transformer windings cannot be reproduced in the equivalent circuit diagram without further ado. But these capacitances result in a series of highly undesirable phenomena. We only have to be reminded of a concept of the "earth symmetry" of a transformer where they play the main role. The representation of the earth symmetry in the normal equivalent circuit diagram is impossible for the same reasons as above. Ways are known to improve the symmetry of a transformer. The best method is an electrostatic screen. But since a penetration-factor-free screening is not simple from the viewpoint of construction, besides the fact that, thereby, characteristics of the transformer may change (for example, an increase in the leakage, etc.), we often are satisfied with screen foils between the windings. Here a residual coupling capacitance remains, and it is important if we are able to judge the influence of this capacitance on the problem at hand. Up till now, a usable method of calculation for this has been lacking. If we now try to construct a more complete equivalent circuit diagram, we may expect that this is possible only with considerably increased effort. It will be shown that an equivalent circuit diagram in unusual form will be required for consideration of the symmetry relationships. But if only the transformation characteristics (for instance, stray resonances) are to be accurately represented, then the erstwhile star or triangular equivalent circuit diagram can be expanded in a manner which would also take into consideration the effect of capacitances between the windings. Since the equivalent circuit diagram derived in the next chapters shows the same characteristic features for

the simplified transformer forms (for example, shunt inductance infinitely large) as for the general case, it is advantageous to begin with it right here. So, very generally we are looking for the equivalent circuit diagram of a quadripole which correctly represents the potential relationships between all terminals (as compared with the equivalent circuit diagram of the two-pair terminals).

II. THE COMPLETE EQUIVALENT CIRCUIT DIAGRAM OF A QUADRIPOLE

The most important stipulation for this equivalent circuit diagram may be expressed as follows: The apparent impedances between terminals at random of the equivalent circuit diagram must coincide with the actual impedances of the quadripole between these terminals. The equivalent circuit diagram which fulfills these requirements is at the same time the most general representation for a quadripole: The complete rectangle with six apparent resistances, r_1' to r_6' independent of each other (Figure 1a) [1].

Six equations are required to express these six magnitudes by apparent impedances, capable of measurement at the quadripole. Three equations are obtained by the usual open-circuit and short-circuit impedances of the quadripole, measured from terminals 1-2 and 3-4. A whole series of possibilities exists for the rest. The following magnitudes have proven themselves to be especially useful for the problem at hand since the measurements involved may be easily accomplished:

1) the admittance S with short circuit of terminals 1,2 and 3,4 (Figure 1b)

$$S = \frac{1}{r_3'} + \frac{1}{r_4'} + \frac{1}{r_5'} + \frac{1}{r_6'} \qquad (1)$$

2) with short circuit of terminals 3,4 the difference D_1 of the admittances between 1-(3,4) and 2-(3,4) (Figure 1c)

$$D_1 = \left[\frac{1}{r_3'} + \frac{1}{r_5'}\right] - \left[\frac{1}{r_4'} + \frac{1}{r_6'}\right] \tag{2}$$

3) with short circuit of the terminals 1,2 the difference D_2 of the admittances between 3-(1,2) and 4-1,2) (Figure 1d):

$$D_2 = \left[\frac{1}{r_3'} + \frac{1}{r_6'}\right] - \left[\frac{1}{r_4'} + \frac{1}{r_5'}\right] \tag{3}$$

As will be shown later, these admittances are mainly capacitances with the transformer and may easily be measured with a capacitance bridge. As further equations we may choose, for instance:

4) Primary short-circuit impedance r_1 measured on 1-2 with short circuit of 3,4:

$$\frac{1}{r_1} = \frac{1}{r_1'} + \frac{\left(\frac{1}{r_3'} + \frac{1}{r_5'}\right)\left(\frac{1}{r_4'} + \frac{1}{r_6'}\right)}{\frac{1}{r_3'} + \frac{1}{r_4'} + \frac{1}{r_5'} + \frac{1}{r_6'}} \tag{4}$$

5) Secondary short-circuit impedance r_2, measured on 3-4 with short circuit of 1,2:

$$\frac{1}{r_2} = \frac{1}{r_2'} + \frac{\left(\frac{1}{r_3'} + \frac{1}{r_6'}\right)\left(\frac{1}{r_4'} + \frac{1}{r_5'}\right)}{\frac{1}{r_3'} + \frac{1}{r_4'} + \frac{1}{r_5'} + \frac{1}{r_6'}} \tag{5}$$

6) Primary open-circuit impedance R_1, measured on 1-2 with open terminals 3 and 4: After reforming of the star with center 3 and the arms 1-3, 2-3, 4-3 into a triangle we get:

$$\frac{1}{R_1} = \frac{1}{r_1'} + \frac{1}{r_3' r_6' \Sigma} + \frac{\left(\frac{1}{r_5'} + \frac{1}{r_2' r_3' \Sigma}\right)\left(\frac{1}{r_4'} + \frac{1}{r_2' r_6' \Sigma}\right)}{\frac{1}{r_4'} + \frac{1}{r_5'} + \frac{1}{r_2' \Sigma}\left(\frac{1}{r_3'} + \frac{1}{r_6'}\right)} \tag{6}$$

where

$$\Sigma = \frac{1}{r_2'} + \frac{1}{r_3'} + \frac{1}{r_6'}$$

From equation (4) we get with equations (1), (2), and (3)

$$\frac{1}{r_1'} = \frac{1}{r_1} - \frac{S^2 - D_1^2}{4\,S} \tag{7}$$

Similarly, we get: utilizing equation (5):

$$\frac{1}{r_2'} = \frac{1}{r_2} - \frac{S^2 - D_2^2}{4\,S} \tag{8}$$

From equation (6) we get, after some troublesome calculations which shall be passed over here, with the aid of equations (1) to (5):

$$\frac{1}{r_3'} = \pm\sqrt{\frac{1}{r_1 r_2}\left(1 - \frac{r_1}{R_1}\right) + \frac{(S + D_1)(S + D_2)}{4\,S}} \tag{9}$$

With the aid of equations (1) to (3) we finally get:

$$\frac{1}{r_4'} = \pm\sqrt{\frac{1}{r_1 r_2}\left(1 - \frac{r_1}{R_1}\right) + \frac{(S - D_1)(S - D_2)}{4\,S}} \tag{10}$$

$$\frac{1}{r_5'} = \pm\sqrt{\frac{1}{r_1 r_2}\left(1 - \frac{r_1}{R_1}\right) + \frac{(S + D_1)(S - D_2)}{4\,S}} \tag{11}$$

$$\frac{1}{r_6'} = \pm\sqrt{\frac{1}{r_1 r_2}\left(1 - \frac{r_1}{R_1}\right) + \frac{(S - D_1)(S + D_2)}{4\,S}} \tag{12}$$

Herewith the six apparent impedances of the equivalent circuit diagram are expressed by six measurable magnitudes. The result is worth noticing insofar as the admittances $1/r_1'$ to $1/r_6'$ are each the sum of two

admittances of which the one contains only the usual open-circuit and short circuit impedances, while the other contains only the three newly introduced admittances S, D_1, and D_2. We do not wish to enter further into the general characteristics of the equivalent circuit diagram, but rather, immediately, derive from it the equivalent circuit diagram of the transformer; we shall begin with the simplest case in which the two windings are coupled only magnetically:

We must mention beforehand that, taken in its strictest sense, five terminals (a complete pentagon) are required for the complete identification of the quadripole. The fifth terminal is the reference point for the potentials of the quadripole terminals ("surroundings," "Ground," or similarly), see Figure 2. As we can see, the apparent resistances r_7' to r_{10}' can at first be omitted in the mathematical examination of the characteristics of the quadripole 1-2-3-4, since at the end they can always be added from the four terminals as compared with five. But they cannot be separated from the true quadripole, that is, in the measurement of the six values S, D_1, D_2, r_1, r_2, and R_1 they could falsify the result of the measurement.

But now it is possible to separately measure the apparent impedances r_7' to r_{10}' by themselves with suitable bridges. If we now think of the star as being solved with the center at 5, the pentagon changes into a rectangle, and r_7' to r_{10}' distribute themselves in a known manner over the apparent impedances r_1' to r_6'. The six apparent impedances of this rectangle may be determined in the manner just described and finally r_1' to r_6' may be taken from them. Herewith the pentagon equivalent circuit diagram is proven satisfactorily.

With the transformer r_7' to r_{10}' are usually small capacitances and their effect is unimportant. Therefore, we want to disregard the effect of the surroundings in the problems dealt with here.

III. EQUIVALENT CIRCUIT DIAGRAM WITHOUT OPPOSITE CAPACITANCES

As can easily be seen from Figure 3a, in this case the apparent impedances between terminals 1 and 3 or 2 and 4 must be infinitely great; that is, S and also D_1 and D_2 become zero. If we set

$$\frac{1}{r} = \pm\sqrt{\frac{1}{r_1 r_2}\left(1-\frac{r_1}{R_1}\right)}$$

as an abbreviation, we get Figure 3b with values;

$$r_1' = r_1,\ r_2' = r_2,\ r_3' = r_4 = r \text{ and } r_5' = r_6' = -r$$

r_1' and r_2' are the primary and the secondary short-circuit impedance. We wish to discuss the importance of r more fully. For this purpose we represent the quadripole equations in matrix form. We can think of the equivalent circuit diagram 3b as having originated by the parallel connection of a symmetrical X-circuit from resistances r and -r with the end resistances r_1 and r_2 (Figure 4).

We get

$$\|Y\| = \begin{Vmatrix} \frac{1}{r_1} & -\frac{1}{r} \\ \frac{1}{r} & -\frac{1}{r_2} \end{Vmatrix}$$

as the admittance matrix.

From this we see that 1/r is the transfer admittance of the transformer which represents the relationship of output short circuit current to input potential. Herewith the magnitudes appearing in the

equivalent circuit diagram of the transformer are referred back to simple, known values.

Some time ago J. Wallot [2] already derived this equivalent circuit diagram for a transformer in another connection. We can work any transformation we like on it which would actually be undertaken on the transformer, the correct result will definitely come out of it since it properly represents all potential relationships. It is disadvantageous for the reason that it does not have the same simplicity of ease of comprehension as the usual equivalent circuit diagram. We now wish to derive this latter from the former. Here we have to stipulate only that two end points of the two windings, for instance 2 and 4, may be connected with each other without resistance. If we accomplish this, we get from Figure 3b the equivalent circuit diagram in a triangular circuit, Figure 5.

From this we may easily calculate the transformation ratio of the potentials under no-load operation.

$$\left(\frac{U_2}{U_1}\right)^1 = \frac{-\frac{r_2 r}{r_2 - r}}{-\frac{r_2 r}{r_2 - r} + r} = \frac{r_2}{r} = \pm\sqrt{\frac{r_2}{r_1}}\sqrt{1 - \frac{r_1}{R_1}}$$

Generally, $\frac{r_1}{R_1} \ll 1$, with this the relationship becomes approximately equal to the ratio of the number of windings: $\ddot{u} = \frac{n_2}{n_1}$

The equivalent circuit diagram in the star circuit is better known; we transform the triangle in Figure 5 into a star and get Figure 6a.

If we consider a loss - free transformer, we get

$$R_1 = j\omega L_1, \qquad R_2 = j\omega L_2$$

$$\text{and} \quad \frac{r_2}{r} = \pm\sqrt{\frac{L_2}{L_1}}\sqrt{1-\sigma}$$

when, as usual, the leakage coefficient is designated as $\sigma = \frac{r_1}{R_1}$.

Therewith the transverse resistance becomes

$$\frac{r_2}{r} R_1 = \pm j\omega L_1\sqrt{\frac{L_2}{L_1}}\sqrt{1-\sigma} = \pm j\omega\sqrt{L_1 L_2}\sqrt{1-\sigma} = j\omega M$$

The equivalent circuit diagram is generally used in this form in high frequency technique (Figure 6b).

In communication technique it is usual to relate all values of the equivalent circuit diagram to one side, for instance the primary side, and to undertake the transformation of the potential by a fore-or after-connected ideal transformer [3]. The derivation is simplest with the help of the matrix calculation. From the $\|Y\|$ matrix we get the chain matrix for

$$\|A\| = \begin{Vmatrix} \frac{r}{r_2} & r \\ \frac{r}{r_1 r_2} - \frac{1}{r} & \frac{r}{r_1} \end{Vmatrix}$$

The chain matrix of an ideal transformer with transformation ratio v reads

$$\|A'\| = \begin{Vmatrix} \frac{1}{v} & 0 \\ 0 & v \end{Vmatrix}$$

For the chain matrix of the residual equivalent circuit diagram the relationship $\|A''\| \cdot \|A'\| = \|A\|$ or $\|A''\| = \|A\| \cdot \|A'\|^{-1}$

$$\left\| A'' \right\| = \begin{Vmatrix} \frac{r}{r_2} & r \\ \frac{r}{r_1 r_2} - \frac{1}{r} & \frac{r}{r_1} \end{Vmatrix} \cdot \begin{Vmatrix} v & 0 \\ 0 & \frac{1}{v} \end{Vmatrix} = \begin{Vmatrix} v\frac{r}{r_2} & \frac{1}{v} r \\ v\left(\frac{r}{r_1 r_2} - \frac{1}{r}\right) & \frac{1}{v}\frac{r}{r_1} \end{Vmatrix}$$

then exists.

In itself, v can still be selected at random. In order to obtain a (longitudinally) symmetrical equivalent circuit diagram, v must be selected so that the members of the main diagonals become equal, so:

$$v\frac{r}{r_2} = \frac{1}{v}\frac{r}{r_1} \; ; \quad v^2 = \frac{r^2}{r_1} \; ; \quad v = \pm\sqrt{\frac{r_2}{r_1}}$$

$$\left\| A'' \right\| = \begin{Vmatrix} \pm \frac{r}{\sqrt{r_1 r_2}} & \pm\sqrt{\frac{r_1}{r_2}}\, r \\ \pm\sqrt{\frac{r_2}{r_1}}\left(\frac{r}{r_1 r_2} - \frac{1}{r}\right) & \pm \frac{r}{\sqrt{r_1 r_2}} \end{Vmatrix}$$

From the elements of this matrix we easily get the apparent impedances of the appropriate equivalent circuit diagram according to Figure 7A [4].

An unsymmetrical equivalent circuit diagram in which the entire short-circuit resistance lies in front of the shunt impedance results when v is chosen so that $A''_{22} = 1$, so:

$$\frac{1}{v}\frac{r}{r_1} = 1 \quad \text{or} \quad v = \frac{r}{r_1} = \sqrt{\frac{r_2}{r_1}}\,\frac{1}{\sqrt{1 - \frac{r_1}{R_1}}}$$

The chain matrix belonging to it reads:

$$\left\| A'' \right\| = \left\| \begin{array}{cc} \frac{r^2}{r_1 r_2} & r_1 \\ \frac{r}{r_1}\left(\frac{r}{r_1 r_2} - \frac{1}{r}\right) & 1 \end{array} \right\|$$

with equivalent circuit diagram 7b.

All derived equivalent circuit diagrams are now to be compared with each other by means of simple numerical examples. The transformer will have no losses, but leakage inductance and a turns ratio of 1:20.

We furthermore have the primary inductance

$$L_1 = \frac{r_1}{j\omega} = 0.5 \text{ H}$$

the primary leakage inductance $L_{s_1} = \frac{r_1}{j\omega} = 0.005$ H

and therewith the secondary leakage inductance $L_{s_2} = \frac{r_2}{j\omega} = 2.0$ H

then the leakage coefficient is $\sigma = \frac{r_1}{R_1} = 0.01 = 1\%$

Furthermore:

$$\frac{r}{j\omega} = \frac{1}{j\omega}\sqrt{\frac{r_1 r_2}{1 - \frac{r_1}{R_1}}} = 0.1005 \text{ H}$$

and $M = \frac{r_2}{r} \cdot \frac{R_1}{j\omega} = 9.95$ H

Figures 8a and 8b show the equivalent circuit diagrams with ideal transformers, Figure 8c the simple star circuit, Figure 8d the triangular circuit, and finally Figure 8e the complete rectangle.

All equivalent circuit diagrams are of equal value as far as the normal transformation characteristics are concerned. But only with the complete rectangle can we measure the relationships when the driving potential does not lie between terminals 1-2 or 3-4, but, for instance,

between 1-4 or between 1 and another point of the total circuit (for instance, "ground").

IV. EQUIVALENT CIRCUIT DIAGRAM OF THE TRANSFORMER WITH CAPACITIES BETWEEN THE WINDINGS

We now turn to the general case, that besides the magnetic coupling a capacitative coupling is also at hand. The magnitudes S, D_1 and D_2 of the general four-pole equivalent circuit diagram then do not equal to zero. The magnitudes in equations (7) to (12), formed from these values, are then likewise [positive or negative] resistances for which we introduce the following abbreviations:

$$j\omega C_1 = \frac{(S+D_1)(S+D_2)}{4S}, \qquad j\omega C_2 = \frac{(S-D_1)(S-D_2)}{4S}$$

$$j\omega C_3 = \frac{(S+D_1)(S-D_2)}{4S}, \qquad j\omega C_4 = \frac{(S-D_1)(S+D_2)}{4S}$$

$$j\omega C_5 = -\frac{S^2 - D_1^2}{4S}, \qquad j\omega C_6 = -\frac{S^2 - D_2^2}{4S}$$

With the already introduced abbreviation

$$r = \pm\sqrt{\frac{r_1 r_2}{1 - \frac{r_1}{R_1}}}$$

We then get the following equations for the apparent impedance of the equivalent circuit diagram:

$$\frac{1}{r_1'} = \frac{1}{r_1} + j\omega C_5, \qquad \frac{1}{r_2'} = \frac{1}{r_2} + j\omega C_6$$

$$\frac{1}{r_3'} = \frac{1}{r} + j\omega C_1, \qquad \frac{1}{r_4'} = \frac{1}{r} + j\omega C_2$$

$$\frac{1}{r_5'} = -\frac{1}{r} + j\omega C_3 , \qquad \frac{1}{r_6'} = -\frac{1}{r} + j\omega C_4$$

Figure 9 shows the circuit. So now, every apparent resistance is composed of two parts; one we already know from the preceding chapter. In addition, a capacity is added to each. We can think of the equivalent circuit diagram as a superposition of a transformer with only magnetic coupling and a lattice circuit of capacities which represent the capacitative coupling. We shall use this in the last chapter. Above all, we shall now consider capacities C_1 to C_4 which give the additional energy exchange between the primary and the secondary side. An example will show this more clearly.

V. EXAMPLE: THE EARTH SYMMETRY OF THE TRANSFORMER

We are given a transformer with two windings 1-2 and 3-4; the winding 3-4 is loaded with impedance $\mathfrak{Z}$ (Figure 10). Point 4 is grounded. We wish to find the earth symmetry of winding 1-2. For this we need the admittance of point 1 and 2 with relation to ground.

With the aid of equivalent circuit diagram Figure 9, we can solve for the star with the center point 3 and calculate the admittance values G' and G". We find

$$G' = \frac{j\omega\left[C_1+C_3-\frac{r_2}{r}\,\frac{C_1+C_4}{1+\frac{r_2}{\mathfrak{Z}}}\right] - \omega^2 \,\frac{r_2}{1+\frac{r_2}{\mathfrak{Z}}}\left[C_3(C_1+C_4+C_6)+C_1C_6\right]}{1 + j\omega r_2 \,\frac{C_1+C_4+C_6}{1+\frac{r_2}{\mathfrak{Z}}}}$$

$$G'' = \frac{j\omega\left[C_2+C_4+\frac{r_2}{r}\,\frac{C_1+C_4}{1+\frac{r_2}{z}}\right] - \omega^2\,\frac{r_2}{1+\frac{r_2}{z}}\left[C_2(C_1+C_4+C_6)+C_4C_6\right]}{1+j\omega r_2\,\frac{C_1+C_4+C_6}{1+\frac{r_2}{z}}}$$

If we express C_1 to C_6 by S, D_1, and D_2, we see that the second member in the numerator equals zero. So,

$$G' = j\omega\,\frac{C_1+C_3-\frac{r_2}{r}\,\frac{C_1+C_4}{1+\frac{r_2}{z}}}{1+j\omega r_2\,\frac{C_1+C_4+C_6}{1+\frac{r_2}{z}}}$$

$$G'' = j\omega\,\frac{C_2+C_4+\frac{r_2}{r}\,\frac{C_1+C_4}{1+\frac{r_2}{z}}}{1+j\omega r_2\,\frac{C_1+C_4+C_6}{1+\frac{r_2}{z}}}$$

In the main, G' and G" represent capacities. Only with higher frequencies does their value change; in addition, a phase appears. The relationship of the sum to the difference of the two admittance values is, as is known, a measurement for the outer symmetry s_a [5]. If we set

$$e^{s_a} = \frac{G'+G''}{G'-G''}$$

we get

$$e^{s_a} = \frac{C_1+C_2+C_3+C_4}{(C_1+C_3)-(C_2+C_4)-2\,\frac{r_2}{r}\,\frac{C_1+C_4}{1+\frac{r_2}{z}}}$$

$$\approx \frac{C_1 + C_2 + C_3 + C_4}{(C_1 + C_3) - (C_2 + C_4) \mp 2 \ddot{u} \frac{C_1 + C_4}{1 + \frac{r_2}{z}}}$$

when, as already mentioned, we set

$$\frac{r_2}{r} \approx \pm \frac{n_2}{n_1} = \pm \ddot{u}$$

in the normal transformer range.

If we next consider the special case that $\ddot{u}$ is very small, so that the last member in the denominator may be neglected, we have

$$e^{s_a} \approx \frac{(C_1 + C_3) + (C_2 + C_4)}{(C_1 + C_3) - (C_2 + C_4)}$$

which is therefore independent of frequency and load. More interesting is the second case $\ddot{u} \gg 1$ with which only the last member remains in the denominator.

$$e^{s_a} \approx \frac{C_1 + C_2 + C_3 + C_4}{2 \ddot{u} (C_1 + C_4)} \cdot \left(1 + \frac{r_2}{z}\right)$$

The symmetry decreases with increasing $\ddot{u}$ and, in addition, depends on load z.

For Input transformers we can set $z \gg r_2$ in the rule; we then get

$$e^{s_a} \approx \frac{C_1 + C_2 + C_3 + C_4}{(C_1 + C_3) - (C_2 + C_4) \mp 2 \ddot{u} (C_1 + C_4)}$$

In this case by balancing C_2, relative to C_3, we can make the denominator small, and therefore the symmetry large, as long as $r_1/R_1 \ll 1$, that is, as long as the stray resonance does not yet play a part. Mutual coupling improvement, however, is achieved only by keeping $C_1 + C_4$ small; that means, by electrostatic screening.

The relationships become still clearer when the admittance values

G' and G" themselves are considered. The denominator is set equal to one and $Z \gg r_2$. Then

$$G' \approx j\omega\left[C_1 + C_3 - \frac{r_2}{r}(C_1 + C_4)\right] \approx j\omega\left[C_1 + C_3 \mp \ddot{u}(C_1 + C_4)\right]$$
$$= j\omega C'$$
$$G'' \approx j\omega\left[C_2 + C_4 + \frac{r_2}{r}(C_1 + C_4)\right] \approx j\omega\left[C_2 + C_4 \pm \ddot{u}(C_1 + C_4)\right]$$
$$= j\omega C''$$

If we take, as an example, a normal Input transformer for a telephone amplifier in which the capacities C_1 to C_4 are each about equal to 10 pF, then with a transformation ratio $\ddot{u} = 20$ (with the top sign):

$C' \approx -380$ pF and $C'' \approx +420$ pF

So the dissymmetry is considerable.

If we place an electrostatic shield between the windings and connect it with point 4 of the transformer (see Figure 16), then C_1 and C_4 become very small, while C_2 and C_3 generally increase somewhat. If we figure with the following values

$C_1 \approx C_4 = 1$ pF $\qquad C_2 \approx C_3 = 20$ pF

then

$C' = -9$ pF and $C'' = +61$ pF

So the dissymmetry is actually less because the electrostatic shield has been introduced.

If we increase (without screen) C_3 by 380 pF, then $G' = 0$. Point 1 then has no more grounding action toward the earth. By proper balancing, therefore, a similar effect may be achieved as through electrostatic screening. Generally the condition for the disappearance of G', relatively G", is, according to polarity:

$$C_1 + C_3 - \frac{r_2}{r}(C_1 + C_4) = 0,$$

that is

$$C_3 = \frac{r_2}{r}(C_1 + C_4) - C_1$$

$$C_2 + C_4 + \frac{r_2}{r}(C_1 + C_4) = 0,$$

$$C_2 = -\frac{r_2}{r}(C_1 + C_4) - C_4$$

The balancing is independent of the frequency as long as $\frac{r_2}{r}$ can be set equal to $\ddot{u}$.

In order to prove the validity of the derived relationships, the value G'--G" was measured in magnitude and phase on a Input transformer as a function of frequency. The transformer had a transformation ratio of $\ddot{u} = 23$. Furthermore, S, D_1, and D_2 were determined, which showed themselves to be independent of the frequency in the tested frequency range from 0.3 to 10 KC. G' and G" were calculated with the likewise measured r_2, r_1, and R_1. The complex difference G'--G" was shown as capacity Δ C with the ohmic parallel resistance Δ G. Figure 11 (above) shows the capacity.

With low frequencies it is constantly equal to 800 pF. It rises with higher frequencies and reaches a value of around 1700 pF at the stray resonance frequency. Above this it goes beyond zero into the negative range. It is exactly the same course followed by the image transfer of the transformer. In a corresponding manner is the course of the ohmic conductance value (Figure 11, below). It reaches considerable values in the vicinity of the stray resonance frequency. The agreement between test result and calculations is satisfactory.

These phenomena have practical applications with, for instance, the telephone repeater, in which the amplification in the upper range of frequencies is emphasized (accentuated) by a series-type attenuation equalizer. This mainly occurs through an inductance in front of the Input transformer. The "stray resonance frequency" and with it the critical range of Figure 11 is thereby placed in the vicinity of the highest frequency transformed. Now we could think of the Input transformer including the apparent impedance of the attenuation compensator as a new transformer with correspondingly changed open-circuit and short-circuit impedance, and, as shown above, calculate the admittance values against the earth. The following way is simpler (Figure 12): Attenuation compensator W lies in front of the essential portion of the transformer equivalent circuit diagram. By solving the star with the middle point 2 we obtain the new earth admittance values Γ' and Γ''.

With permissible approximations, we have:

$$\Gamma' = G' + \frac{G''}{1 + \frac{R_1}{W} + G''R_1} \approx G' + \frac{G''}{1 + \frac{R_1}{W}}$$

$$\Gamma' = \frac{G''}{1 + \frac{W}{R_1} + G''W} \approx \frac{G''}{1 + \frac{W}{R_1}}$$

The change of the attenuation constant (image transfer) caused by the attenuation compensation is $\Delta g = \Delta b + j\Delta a$. It amounts to

$$e^{\Delta g} = 1 + \frac{W}{R_1}$$

With this value we get

$$\Gamma' \approx G' + G'' (1 - e^{-\Delta g}) = G' + G'' - G'' e^{-\Delta g}$$

$$\approx - G'' e^{-\Delta g} = - G'' e^{-\Delta b} \cdot e^{-j\Delta a}$$

since G' and G'' is generally so small that it can be neglected. Likewise,

$$\Gamma'' \approx G'' e^{-\Delta g} = G'' e^{-\Delta b} \cdot e^{-j\Delta a}$$

For example, if the increase in amplification is 1 Neper due to the attenuation compensator, then $\Delta b = -1$. In the unfavorable case $\Delta a = 0$, the admittance values against the earth are then increased by the factor $e^1 = 2.7$. For the Input transformer used in the example, $G''/j\omega \approx 400$ pF (without the ohmic conductance value). Herewith we have

$$\frac{\Gamma'}{j\omega} \approx - 1100 \text{ pF}$$

and

$$\frac{\Gamma''}{j\omega} \approx + 1100 \text{ pF}$$

the reactance of these unsymmetries, for instance on the cross-talk transmission in the four-wire telephone repeater, or on the apparent resistance of the two wire repeater, can be considerable. We shall not enter further into this matter.

VI. THE CAPACITIES IN THE NORMAL EQUIVALENT CIRCUIT DIAGRAM

The example shows the application of the derived transformer equivalent circuit diagram. But it deviates so far from the normal equivalent circuit diagram that we can hardly neglect such characteristics as attenuation constant, and open-circuit or short-circuit

impedance. Therefore, it is to be attempted, with disregard of the characteristics used until now with the aid of the usual equivalent circuit diagram, to represent opposite capacities as well as the self-capacitance of the windings. We first limit ourselves to the range of frequencies in which we can still disregard the effect of the capacitance distribution. Figure 3b serves as the starting point. The magnitudes r_1, r_2, and r are to represent the data of the transformer without any capacitances, therefore consisting only of ohmic and inductive impedances. Now we add the self-capacitances parallel to r_1 and r_2, and moreover, as before, the opposite capacitances (Figure 13a). We get the admittance matrix of the entire transformer as the sum from the transformer matrix and capacitance matrix to

$$\left\| Y \right\| = \left\| \begin{array}{ll} \frac{1}{r_1} + j\omega(K_1 + C_5) & -\left[\frac{1}{r} + j\omega K\right] \\ \frac{1}{r} + j\omega K & -\left[\frac{1}{r_2} + j\omega(K_2 + C_6)\right] \end{array} \right\|$$

with the abbreviations

$$K_1 = \frac{(C_1 + C_3)(C_2 + C_4)}{C_1 + C_2 + C_3 + C_4}, \qquad K_2 = \frac{(C_1 + C_4)(C_2 + C_3)}{C_1 + C_2 + C_3 + C_4}$$

$$K = \frac{C_1C_2 - C_3C_4}{C_1 + C_2 + C_3 + C_4}$$

From this we get the chain matrix

$$\left\| A \right\| = \left\| \begin{array}{cc} \frac{r}{r_2} \frac{1 + j\omega(K_2 + C_6)r_2}{1 + j\omega K r} & \frac{r}{1 + j\omega K r} \\ \frac{r}{r_1 r_2} \frac{1+j\omega(K_1+C_5)r_1}{1 + j\omega Kr}\left(1+j\omega(K_2+C_6)r_2\right) - \frac{1+j\omega Kr}{r} & \frac{r}{r_1} \cdot \frac{1+j\omega(K_1+C_5)r_1}{1 + j\omega Kr} \end{array} \right\|$$

We now try to find an equivalent circuit diagram corresponding to Figure 7b, we next build up an ideal transformer with the transformation ratio $1 : r/r_1$ using the same method as before. The residual matrix then reads:

$$\left\| A' \right\| = \left\| A \right\| \cdot \left\| \begin{array}{cc} \frac{r}{r_1} & 0 \\ 0 & \frac{r_1}{r} \end{array} \right\|$$

$$= \left\| \begin{array}{cc} \frac{r^2}{r_1 r_2} \frac{1+j\omega(K_2+C_6)r_2}{1 + j\omega Kr} & \frac{r_1}{1 + j\omega Kr} \\ \frac{r^2}{r_1^2 r_2} \cdot \frac{1+j\omega(K_1+C_5)\, r_1}{1 + j\omega Kr}\left(1+j\omega(K_2+C_6)r_2\right) - \frac{1+j\omega Kr}{r_1} & \frac{1+j\omega(K_1+C_5)r_1}{1 + j\omega Kr} \end{array} \right\|$$

It can be represented by an unsymmetrical π circuit arrangement. The values of the equivalent circuit arrangement can easily be formed by comparison with the elements of the $\left\| A' \right\|$ matrix [6]. So, the line resistance is equal to A'_{12}; that is, it can be represented as a parallel circuit arrangement of r_1 and the capacitance $\frac{r}{r_1} K$, the two cross-resistances result in a similar manner from A'_{11} and A'_{22}. Figure 13b shows the complete equivalent circuit diagram. r_1 is composed of the

ohmic resistances and a stray inductance, while $(R_1 - r_1)$ is equal to the shunt inductance when the core losses are neglected. The capacitance which generally is summarily designated as self-capacitance is split into two parts: one capacitance at the entrance to the equivalent circuit diagram, and a second one parallel to the shunt inductance. Furthermore, parallel to the short-circuit impedance r_1 we have a capacitance $\frac{r}{r_1} K$ which reappears in the two other parts with the opposite sign. While until now the opposing capacitances C_1 to C_4 always appeared in all equations in wholly determinable sums or differences which were directly usable for the actual measurement; K contains the capacitances singly:

$$K = \frac{C_1C_2 - C_3C_4}{C_1 + C_2 + C_3 + C_4}$$

If we attempt to determine the value of K utilizing the values of C_1 to C_4 used in Figure 9, we get

$$j\omega K = \frac{(S^2 - D_1^2)(S^2 - D_2^2) - (S^2 - D_1^2)(S^2 - D_2^2)}{16\, S^3}$$

This result is surely wrong, because, for instance, connecting a capacitance to C_1 should make K finite. The reason for this discrepancy lies in the fact that in the derivation of the last equivalent circuit diagram we expressly assumed that r_1 and R_1 did not have capacitances, because these are exactly what we wished to construct in the equivalent circuit diagram.

However, on a finished transformer we can not undertake this separation during the measurement; that is, the influence of the capacitances is already manifest in values r_1, r_2, and r of the equivalent

circuit diagram, Figure 9; we then calculate the value zero for K. From equivalent circuit diagram 13b we can easily see that we can also determine K by apparent impedance measurements with certain particular frequencies.

With low frequencies r_1 is to be neglected. The two shunt capacitances then lie directly parallel. By measuring at two frequencies, the shunt inductance $(R_1 - r_1)$ and the "self-capacitance" C_o can be determined in the usual manner, with $r/r_1 \approx \ddot{u}$, we have; $C_o = K_1 + C_5 + \ddot{u}^2 (K_2 + C_6) - 2 \ddot{u} K$.

We get r_1 from a short-circuit measurement at such low frequencies that the capacitances do not yet play a part. It can be seen that the primary short-circuit impedance also goes through a resonance. From its resonance frequency we get the capacitance

$$C_{s_1} = K_1 + C_5$$

K_1 is determined as before by direct measurement of the capacitances between the windings to

$$K_1 = \frac{S^2 - D_1^2}{4 S}$$

Then the self capacitance of the primary winding results:

$$C_5 = C_{s_1} - \frac{S^2 - D_1^2}{4 S}$$

The same measurements from the secondary side give,

$$C_{s_2} = K_2 + C_6$$

and with,

$$K_2 = \frac{S^2 - D_2^2}{4 S}$$

the self-capacitance of the secondary side becomes,

$$C_6 = C_{s_2} - \frac{S^2 - D_2^2}{4\,S}$$

Finally we get K:

$$K = \frac{K_1 + C_5 + \ddot{u}^2\,(K_2 + C_6) - C_o}{2\,\ddot{u}} = \frac{C_{s_1} + \ddot{u}^2\,C_{s_2} - C_o}{2\,\ddot{u}}$$

With this, all individual elements of the equivalent circuit diagram are determined. Figure 14 once more shows the equivalent circuit diagram with the magnitudes just introduced.

Rapidly we can now follow the nature of the apparent impedance of the transformer. As already mentioned, the primary and secondary short-circuit impedance goes through a resonance. The resonance frequencies generally do not coincide. The open-circuit impedances are in series resonance at the same frequencies, and the series resonance of the primary open-circuit impedance, R_1, coincides with the parallel resonance of the secondary short-circuit impedance, r_2, and vica versa. Besides the parallel resonance of the open-circuit impedance through shunt inductance and "self-capacitance," another point of resonance can appear between r_1 and $\ddot{u}K$. Finally it is possible to get a parallel resonance for R_1 and R_2 at high frequencies in the vicinity of the short-circuit resonances. R_1, R_2 then approximately fall together with r_1 and r_2 together. Just to what extent these occurrences actually do appear naturally depends upon the construction of the transformer.

We now still consider the open-circuit voltage transformation; it results from the chain matrix

$$\left(\frac{U_2}{U_1}\right)^1 = \frac{1}{A_{11}} = \frac{r_2}{r}\,\frac{1 + j\omega K r}{1 + j\omega(K_2 + C_6)r_2} \approx \ddot{u}\,\frac{1 + j\omega\ddot{u}\,K\,r_1}{1 + j\omega\ddot{u}^2(K_2 + C_6)r_1}$$

With low frequencies this relationship is equal to $\ddot{u}$; with higher frequencies, resonances appear which reduce the secondary voltage when the numerator is resonant and increase it when the denominator is resonant. With very high frequencies we have

$$\left(\frac{U_2}{U_1}\right)^1 \rightarrow \frac{K}{K_2 + C_6}$$

Energy will then be transferred through the capacitance. It is only necessary to make the numerator and denominator of the fraction equal. For example, $\ddot{u}^2 (K_2 + C_6) = \ddot{u}K$. This means (see Figure 13b) that the capacitance parallel to the shunt inductance becomes zero. We then get

$$\left(\frac{U_2}{U_1}\right)^1 = \ddot{u}$$

at any frequency.

This balance can not be achieved in all cases. If we put $C_6 = 0$ into the equation of condition, it reads:

$$\ddot{u} \cdot \frac{(C_1 + C_4)(C_2 + C_3)}{C_1 + C_2 + C_3 + C_4} = \frac{C_1C_2 - C_3C_4}{C_1 + C_2 + C_3 + C_4}$$

or

$$\ddot{u} = \frac{C_1C_2}{(C_1 + C_4)(C_2 + C_3)} - \frac{C_3C_4}{(C_1 + C_4)(C_2 + C_3)}$$

From this, we immediately see that the following must hold true:

$$\ddot{u} \leq 1$$

Figure 15 shows an example of the effect of this balancing. We see how the balancing causes the voltage ratio to remain practically

constant up to 100 KC, while without the balancing, the ratio sinks quickly to very small values after the sharp resonance peak at 47 KC.

However, this holds true only for Input transformers. For transformers under load, the potential division remains between the load impedance and the parallel circuit r_1 and $\ddot{u}k$. But in this case it is often advisable to provide one of the two windings with a static screen as is shown in Figure 16.

C_1 and C_4 then become zero and therewith $K = K_2 = 0$.

The relationship of the potentials of a transformer, without a screen, loaded with an impedance $\underline{z}$ is

$$\frac{U_2}{U_1} \approx \ddot{u} \quad \frac{1 + j\omega \ddot{u} K r_1}{1 + \ddot{u}^2 \left[j\omega (K_2 + C_6) + \frac{1}{\underline{z}} \right] r_1}$$

So with a screen we get:

$$\frac{U_2}{U_1} \approx \ddot{u} \quad \frac{1}{1 + \ddot{u}^2 \left[j\omega C_6 + \frac{1}{\underline{z}} \right] r_1}$$

With the two formulas it can be decided from case to case whether the transmission range can be extended despite the unavoidable increase in self-capacitance C_6 and leakage inductance r_1, caused by the shield.

Finally, the influence of the capacitance distribution remains to be explained. Until now it was assumed that C_1 to C_6 represent pure capacitances. Generally, this would hold true for the lower frequencies. With high frequencies we must consider that the capacitances are distributed between the windings and that C_1 to C_6 first result from this through the transformation at the four corner points. However, the outlay of energy for calculation with the usual aids is so great that we generally must be satisfied with approximations. Let us think of the

windings of the transformer as being composed of partial windings. Each of these partial windings can be replaced by a short-circuit impedance r_n in equivalent circuit diagram 3b. We find it as the apparent resistance of the windings in question with a short-circuit of all the rest. Every magnetic linkage of a partial winding p with another q is represented by four-paired-oppositely-equal coupling resistances (transfer impedances) $r_{p,q}$. If we now connect the partial windings to its right circuit, a number of resistances will be short-circuited, others can be summarized, and there finally remains, with n partial windings, a complete (n + 2) polygon with $\frac{(n + 2)(n + 1)}{2}$ resistances as the equivalent circuit diagram. The capacitances can then be applied between the corner points corresponding to their actual distribution; we can next step-by-step solve for the unnecessary corner points through delta-star transformation, until finally only a complete rectangle with input and output terminals remains. With special symmetrical arrangements of the capacitances this transformation can be effected in a simple manner, but in the majority of cases the effort of calculation will be too great. But generally it can be said that with the transformation (conversion) ohmic resistances and stray inductances appear in series with the capacitances; we must think of K, K_1, K_2, C_5, and C_6 as being composed of different capacitances of which every one contains certain stray inductances and ohmic resistances in series. With this the number of the resonance locations in the apparent impedances and in the attenuation constant increase. Nevertheless, the equivalent circuit diagram, without regard to the capacitance distribution, should for most purposes represent a sufficient approximation.

VII. EXAMPLE: EQUIVALENT CIRCUIT DIAGRAM DETERMINATION

It is now to be shown on a tested example how the equivalent circuit diagram of the transformer can be determined from the position of the resonance locations in the apparent impedances. At the first approximation, a certain series inductance can be assigned to every capacitance K, K_1, K_2, C_5 and C_6. We then get for the equivalent circuit diagram, for instance, for the primary short-circuit impedance, the following Figure 17 wherein the ohmic resistances have been neglected. We get

$$R_1^K = j\omega L_{s_1} \cdot \frac{(1 - \omega^2 L'K_1)(1 - \omega^2 L''C_5)}{1 - \omega^2\left[L'K_1 + L''C_5 + L_{s_1}(K_1 + C_5)\right] + \omega^4 K_1 C_5\left[L'L'' + L_{s_1}(L' + L'')\right]}$$

This function has two zero positions with the real angular frequency:

$$\omega_1 = \frac{1}{\sqrt{L'K_1}} \quad \text{and} \quad \omega_2 = \frac{1}{\sqrt{L''C_5}}$$

Further two poles with the real angular frequency Ω_1 and Ω_2. For these two solutions of the nominal equation of the 4th degree, the following well-known relationship exists:

$$\Omega_1^2 \cdot \Omega_2^2 = \frac{1}{K_1 C_5} \cdot \frac{1}{L'L'' + L_{s_1}(L' + L'')}$$

$$\Omega_1^2 + \Omega_2^2 = \frac{L'K_1 + L''C_5 + L_{s_1}(K_1 + C_5)}{K_1 C_5\left[L'L'' + L_{s_1}(L' + L'')\right]}$$

From these two equations the following relationships may be derived:

$$L_{s_1}\,(K_1 + C_5) = \left[\frac{1}{\Omega_1^2} + \frac{1}{\Omega_2^2}\right] - \left[\frac{1}{\omega_1^2} + \frac{1}{\omega_2^2}\right]$$

and

$$\frac{K_1}{C_5} = \frac{\left[1 - \left(\frac{\Omega_1}{\omega_1}\right)^2\right]\left[\left(\frac{\Omega_2}{\omega_1}\right)^2 - 1\right]}{\left[1 - \left(\frac{\Omega_1}{\omega_2}\right)^2\right]\left[1 - \left(\frac{\Omega_2}{\omega_2}\right)^2\right]}$$

With known zero and pole frequencies, K_1 and C_5 are obtained through a knowledge of L_{s_1}.

In a similar manner, K_2 and C_6 for the secondary short circuit impedance can be derived from the locus curve.

This method is to be more clearly brought out by an example. Figure 18 shows the construction of the transformer. The primary winding of 1800 turns lies over the cylindrical winding of 9000 turns.

It is obvious that the greatest capacitance is situated between the end of the first and the beginning of the second winding; in the Figure it is C_3. Measured were:

$$S = (C_1 + C_2) + (C_3 + C_4) = 150 \text{ pF}$$

$$D_1 = (C_1 + C_3) - (C_2 + C_4) = 108 \text{ pF}$$

$$D_2 = (C_1 + C_4) - (C_2 + C_3) = -135 \text{ pF}$$

From this follows:

$$K_1 = 18 \text{ pF}$$

$$K_2 = 7 \text{ pF}$$

For K we can at least give an upper and a lower limit by the

following consideration; by addition and subtraction, the following equations can be derived from S , D_1, and D_2:

$$C_1 + C_3 = 129 \text{ pF} \qquad C_2 + C_3 = 142.5 \text{ pF}$$

$$C_2 + C_4 = 21 \text{ pF} \qquad C_1 - C_2 = -13.5 \text{ pF}$$

$$C_1 + C_4 = 7.5 \text{ pF} \qquad C_3 - C_4 = 121.5 \text{ pF}$$

From this we gain the following limits for C_1 ..... C_4, since C_1 ..... $C_4 \geqq 0$:

$$0 \leqq C_1 \leqq 7.5 \text{ pF} \qquad 121.5 \leqq C_3 \leqq 129 \text{ pF}$$

$$13.5 \leqq C_2 \leqq 21 \text{ pF} \qquad 0 \leqq C_4 \leqq 7.5 \text{ pF}$$

$$\text{For } K = \frac{C_1C_2 - C_3C_4}{C_1 + C_2 + C_3 + C_4}$$

We herewith have:

$$-6.5 \leqq K \leqq +1.0 \text{ pF}$$

Now the open-circuit and short-circuit impedances of the transformer were measured (Figures 19 to 22). If we next consider the primary short-circuit impedance, we see that in the region up to 90 KC two poles, namely at 52.5 and 62 KC, appear and likewise two zero positions at 56 and 80 KC. So for the primary short-circuit impedance we can apply the equivalent circuit diagram of Figure 17. The point by point evaluation gives the following values (see also Figure 19):

$$K_1 = 18 \text{ pF} \qquad C_5 = 161 \text{ pF}$$

$$L' = 450 \text{ mh} \quad \text{and} \quad L'' = 24 \text{ mh}$$

So for K_1 we get the same value as for the direct measurement. The separation of the transformer capacitances, as it was derived in the equivalent circuit diagram, is therefore actually present as is borne out by further measurements on all different kinds of transformers.

We shall not attempt here to show the importance of the values L' and L" since they are without value in the range of frequencies in which the transformer works. Noticeable is value L" which lies in series with the self-capacitance C_5. Even with other transformers it resulted almost equal to the leakage inductance L_{s_1}.

For the secondary short-circuit impedance (see Figure 20) up to 100 KC we get only a simple resonant circuit with the resonance frequency at 26 KC. With the secondary leakage inductance L_{s_2} = 530 mh we get $K_2 + C_6$ = 70 pF.

So a further separation in this case is impossible. The reason for the different behavior of the primary and secondary side probably lies in the fact that the primary winding has a thicker wire and therefore a winding somewhat in layers, while the secondary winding is wound irregularly.

The regularly recurring layer capacitance causes the layered winding to be favorable for the appearance of a characteristic resonance, while an irregular winding suppresses it.

Finally, K can yet be calculated. From measurements at lower frequencies this self-capacitance was determined to be C_o = 2000 pF.

With this we get

$$2\,\ddot{u} \cdot K = K_1 + C_5 + \ddot{u}^2 \cdot (K_2 + C_6) - C_o = -70 \text{ pF}$$

$$\ddot{u} \cdot K = -35 \text{ pF}$$

With $\ddot{u} = +5$, we therefore have K = -7 pF.

Here again the agreement with limits of K given above is satisfactory when we consider that the value of C_o is generally not very accurate and that $\ddot{u}$ K is the small difference of two large numbers.

The complete equivalent circuit diagram for the transformer has been drawn in Figure 18; here the inductances L' and L" are to be neglected for the normal range of transformation.

In the primary open-circuit impedance (Figure 21) we again see, from the "stray resonance frequency" at 25 KC, the parallel resonance frequency ($\approx$ 26 KC) of the secondary short-circuit impedance. With even higher frequencies it behaves similar to the primary short-circuit impedance.

The nature of the secondary-open circuit impedance (Figure 22) may not be comprehended as easily because of inductances L' and L". With high frequencies it behaves similarly to that of the primary, only shifted by (K_2 + C_6) into the capacitative range.

SUMMARY

The usual equivalent circuit diagram for a transformer takes in the effect of the capacities in the transformer in an unsatisfactory manner by means of a single capacitance parallel to the shunt inductance. To calculate the earth symmetry and the exact comprehension of transformation characteristics, especially at high frequencies, the capacitances between the windings must be considered. It is shown that for the problem at hand it is sufficient to use a complete rectangle as the equivalent circuit diagram; its application on the transformer is shown. After examples which relate to the symmetry characteristics of the transformer, an equivalent circuit diagram for the transformer is derived in the usual manner which takes into consideration the capacitances between the windings and is sufficient for the calculation of the transformation characteristics.

BIBLIOGRAPHY

[1.] K. Kuepfmueller, Introduction to Theoretical Electrotechnology, page 215, 1932.

[2.] J. Wallot, "Proof of the Determinants Relationship of the Four Pole Theory with the Aid of Transformation Theorems," WVSK, Vol. 5, page 212, 1927.

[3.] H. Barkhaussen, "To the Theory of Transformers," ETZ, Vol. 48, page 1463.

[4.] R. Feldtkeller, Introduction to the Four Pole Theory of Electrical Communication Technology, page 123, 1937.

[5.] A. Wirk, "Concerning Comprehension of Symmetry in Electrical Systems, especially in Measuring Instruments," TFT 22, page 111, 1933.

[6.] See [4] page 130.

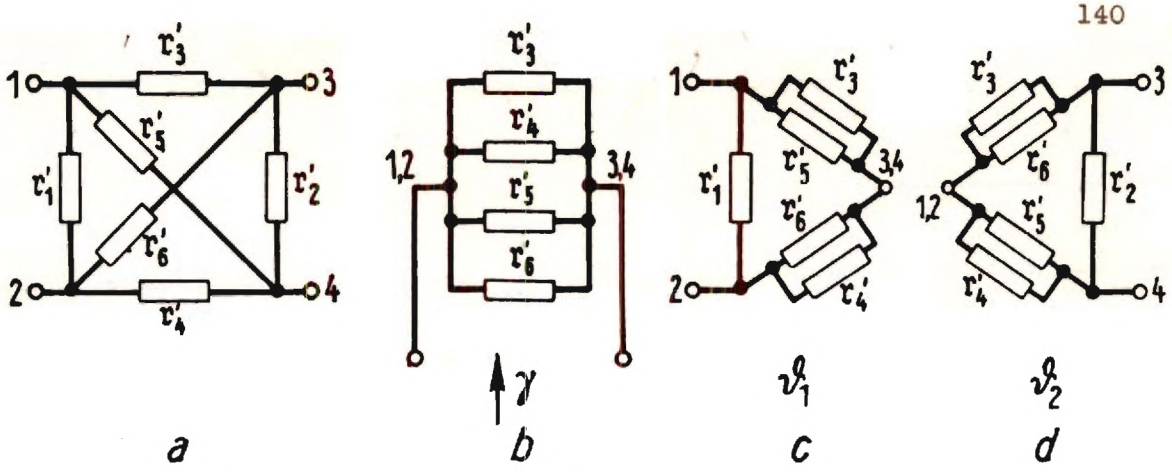

Fig. I - Equivalent Circuit diagram of a quadripole in the most general form through a complete rectangle.

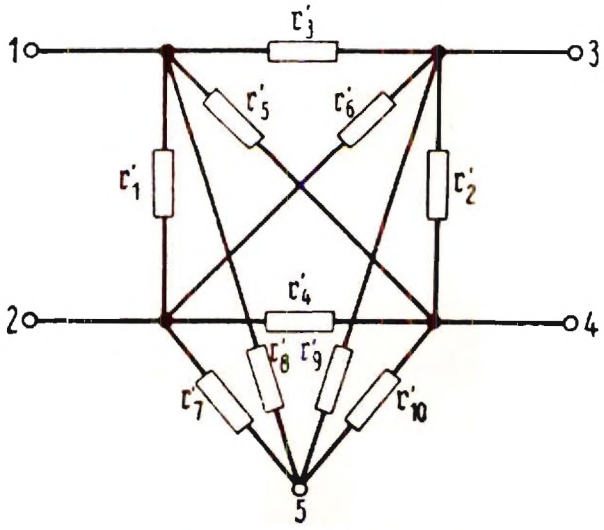

Fig. 2. - Equivalent circuit diagram of a quadripole with reference point for the potentials of the four terminals.

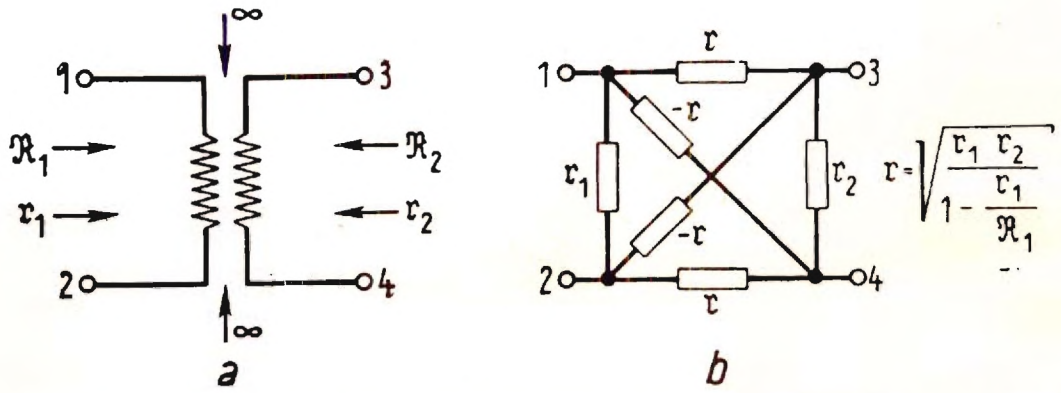

Fig. 3. - Complete rectangle as equivalent circuit diagram of a transformer without capacitances between the windings.

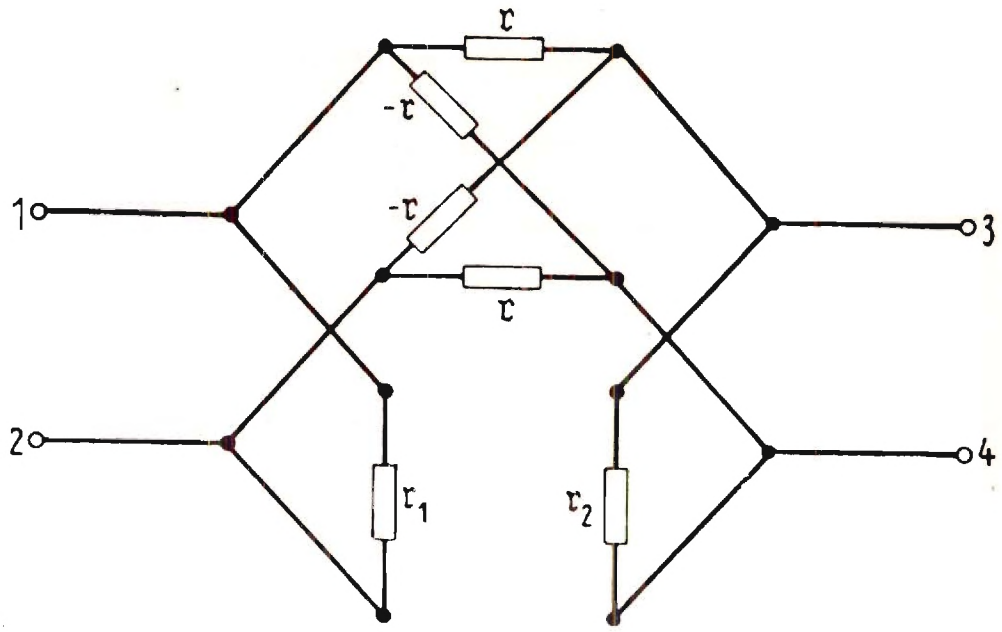

Fig. 4. - For the derivation of the $\|Y\|$ matrix.

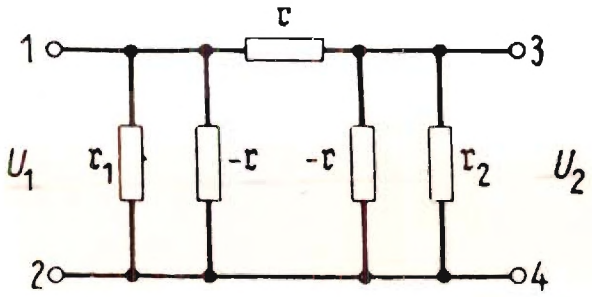

Fig. 5. - Transformer equivalent circuit diagram in triangle circuit, obtained from Fig. 3b by short circuit of 2 and 4.

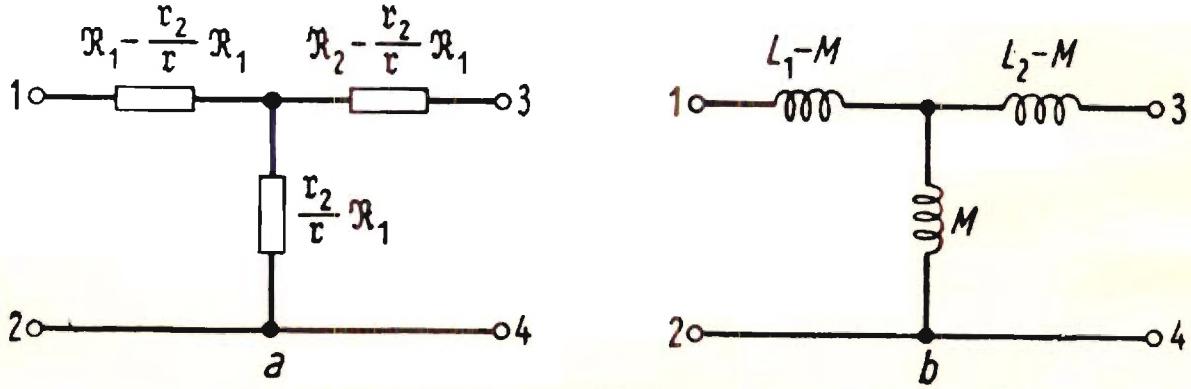

Fig. 6. - Transformer equivalent circuit diagram in star circuit by transformation of Fig. 5.

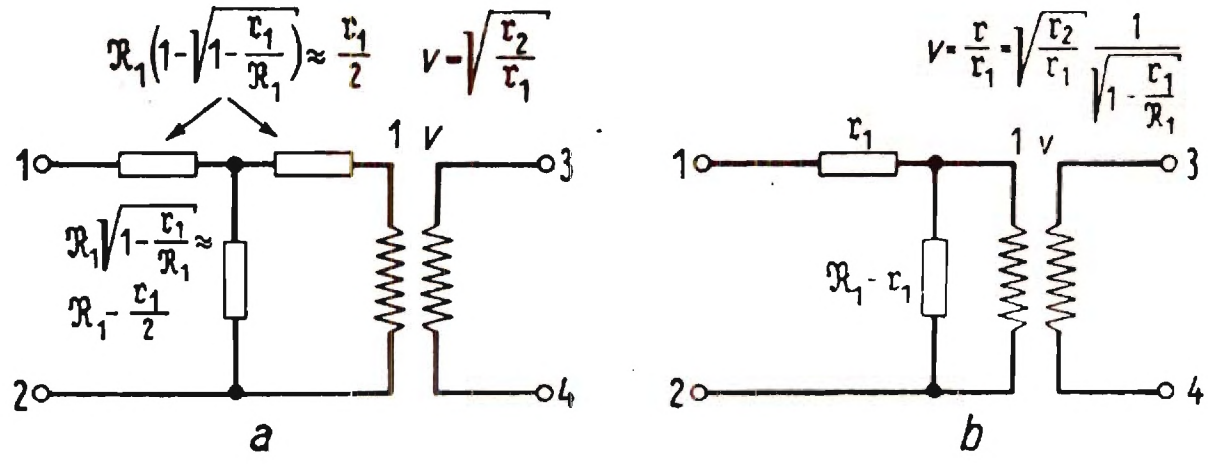

Fig. 7. - Equivalent circuit diagram with ideal transformer.

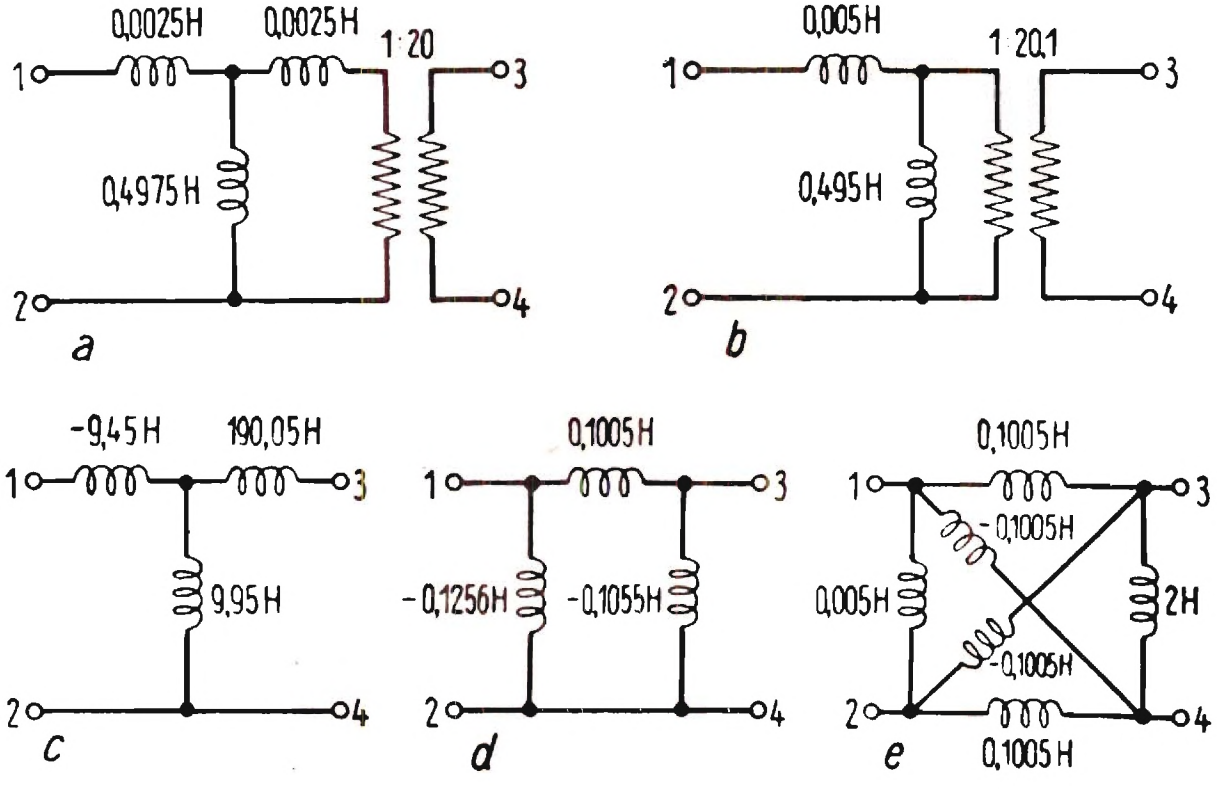

Fig. 8. - Different equivalent circuit diagrams for a transformer.

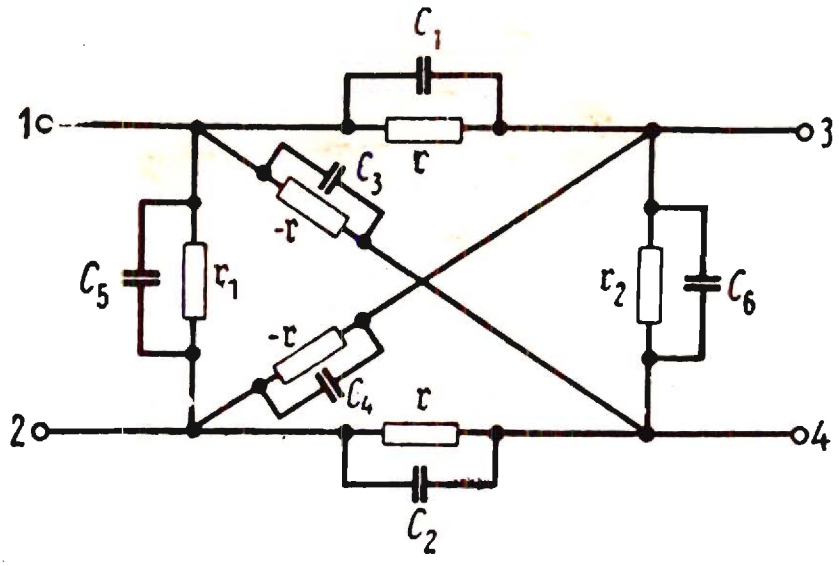

Fig. 9. - Equivalent circuit diagram of a transformer with capacitances between the windings.

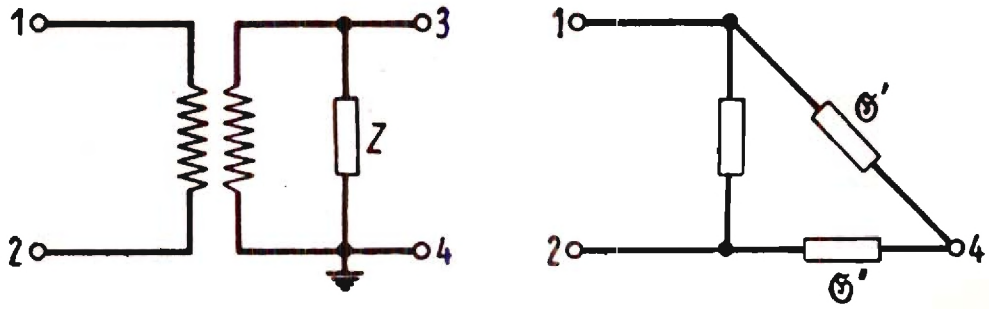

Fig. 10. - For the earth symmetry of the transformer.

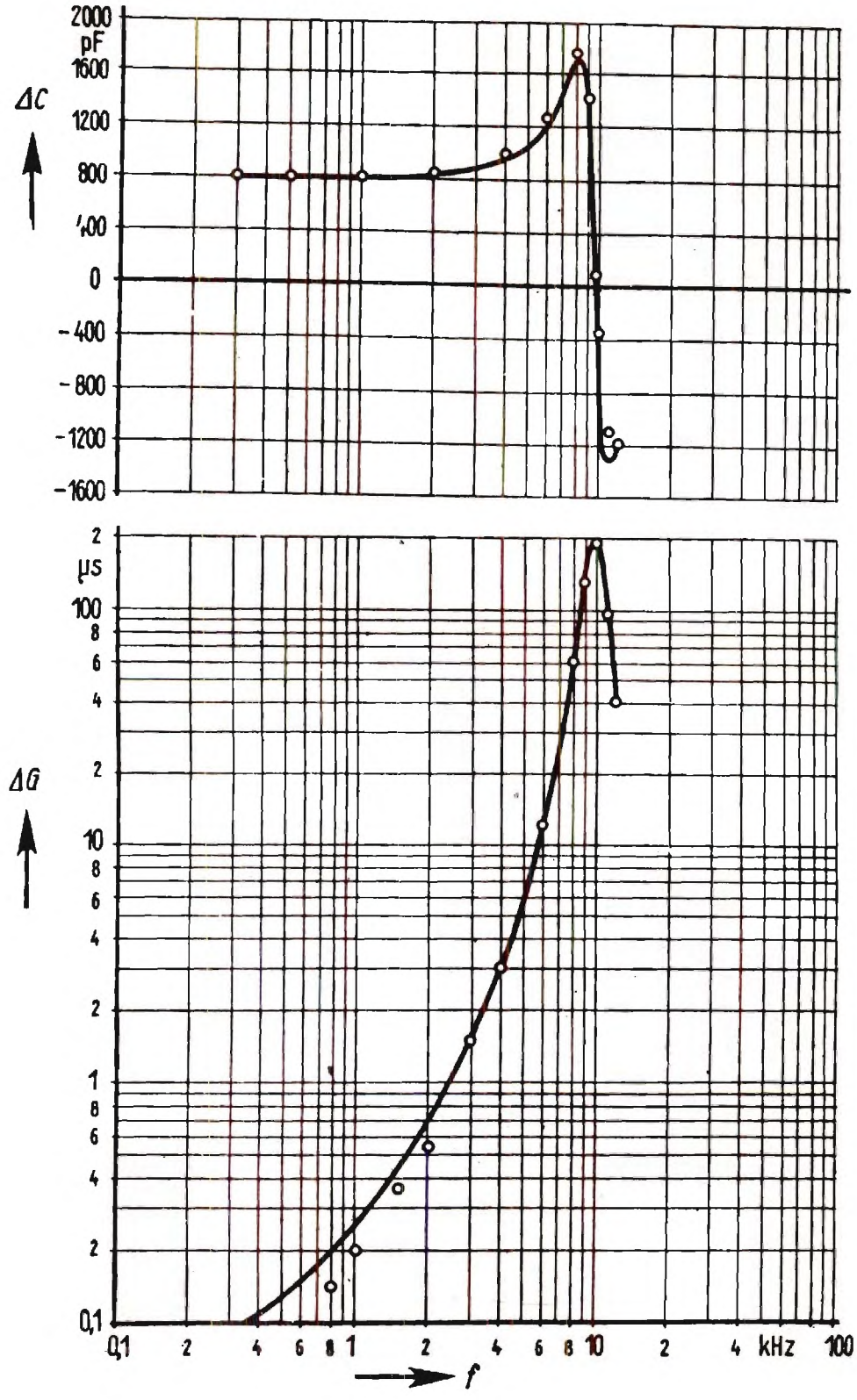

Fig. 11 - Above $-\Delta C = J\,m\,(G' - G'')$ as a function of the frequency.

_____ measurement values o calculated values

Fig. 11 - Below $-\Delta G = Re\,(G' - G'')$ as a function of the frequency.

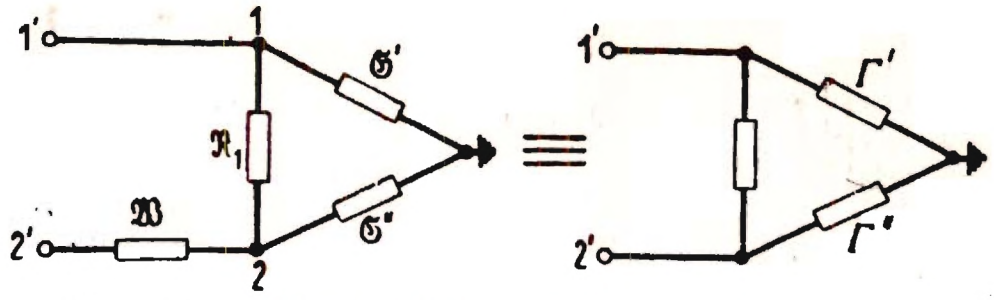

Fig. 12 - Effect of the series-type attenuation compensator on the earth symmetry.

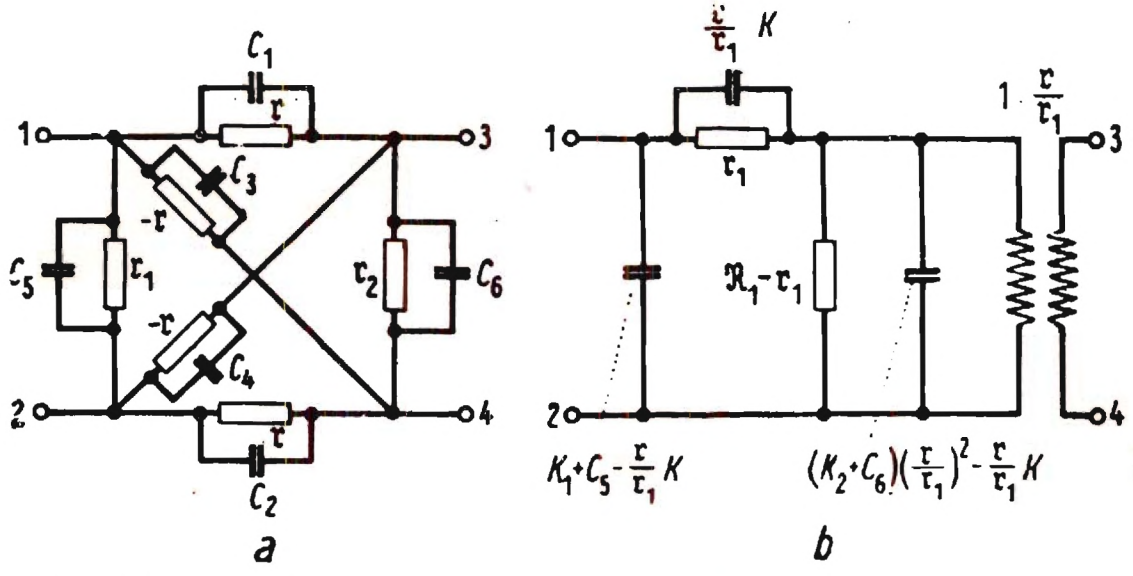

Fig. 13 - Representation of the capacitances in the normal transformer equivalent circuit diagram.

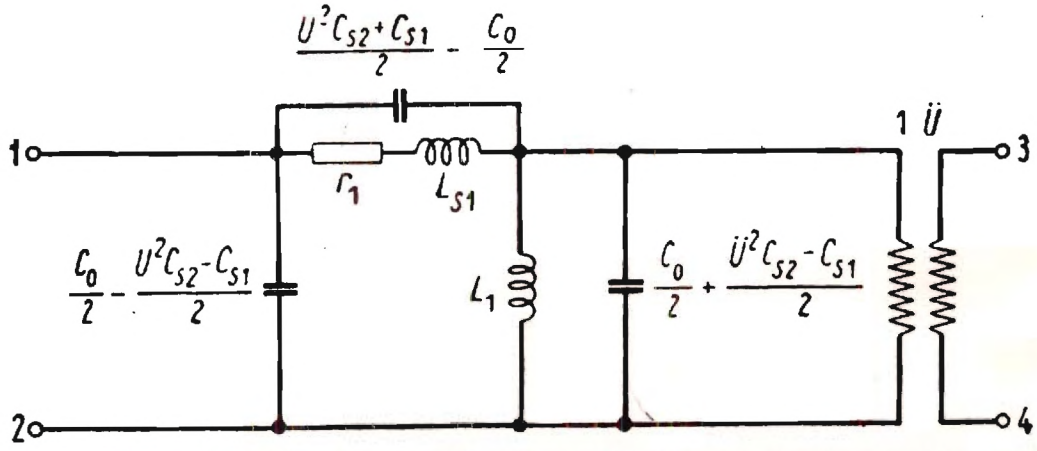

Fig. 14 - For the determination of the equivalent circuit diagram by apparent impedance measurements.

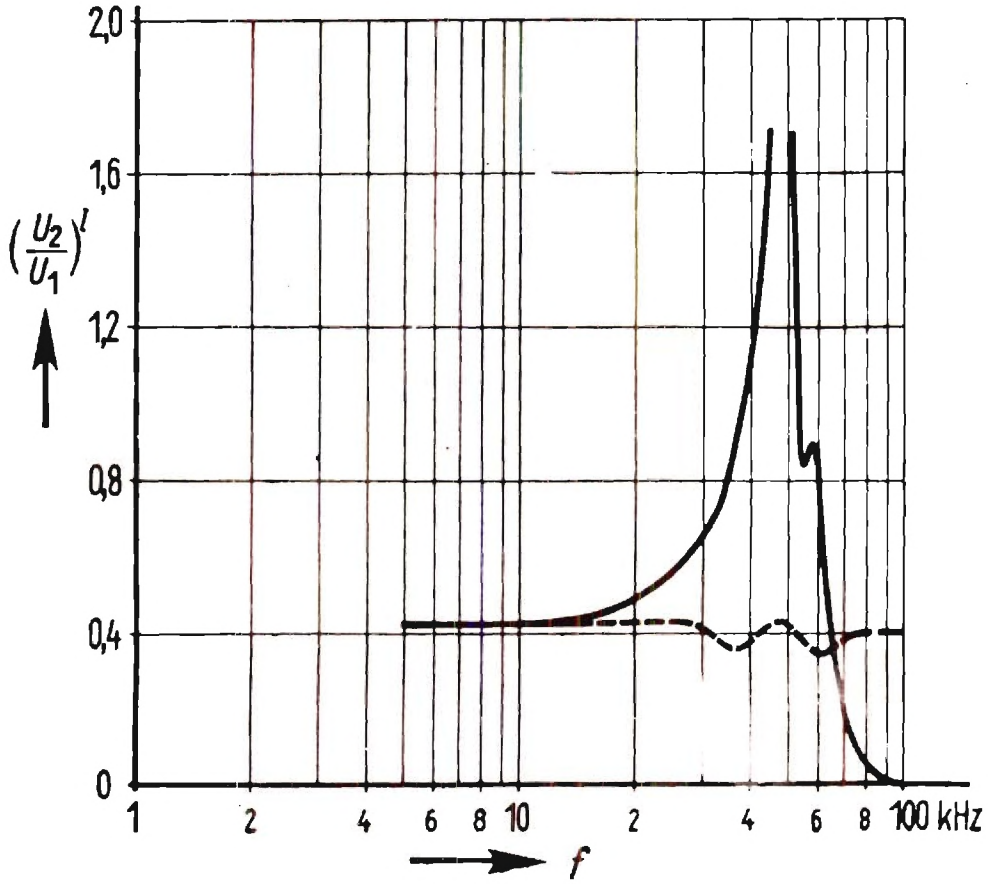

Fig. 15 - Suppression of the stray resonance by balancing of the capacitances.

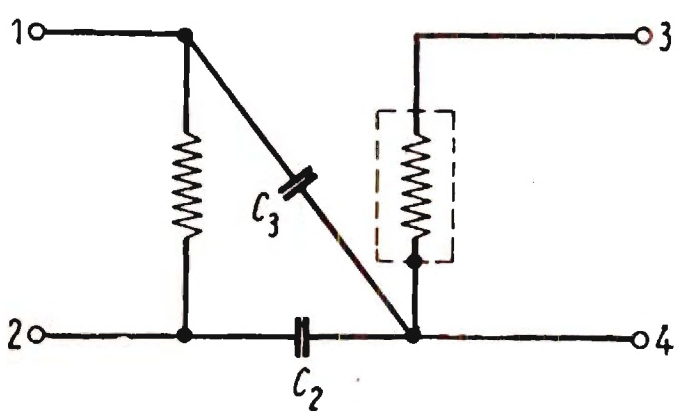

Fig. 16 - Screened transformer.

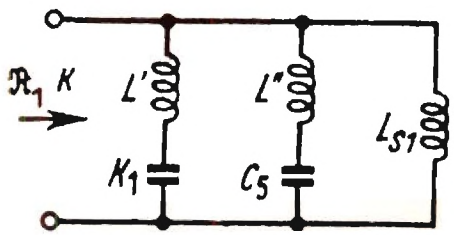

Fig. 17 - Short circuit impedance with distributed capacitances (without losses).

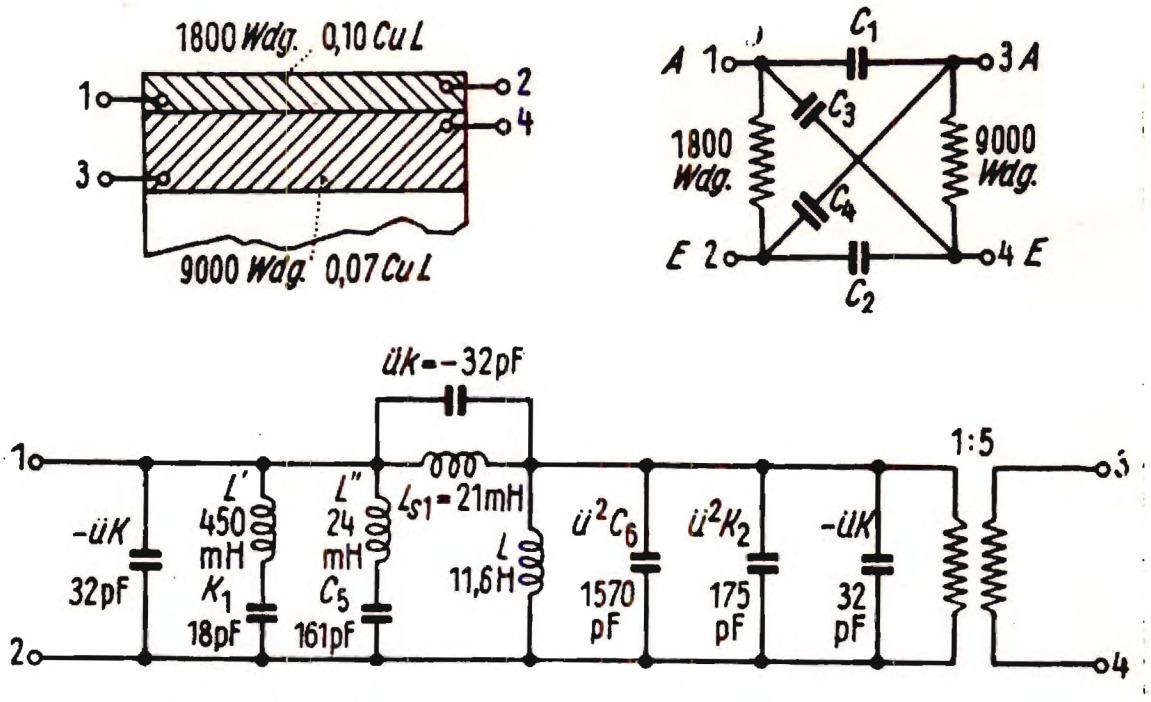

Fig. 18 - Construction of the transformer and the equivalent circuit diagram.

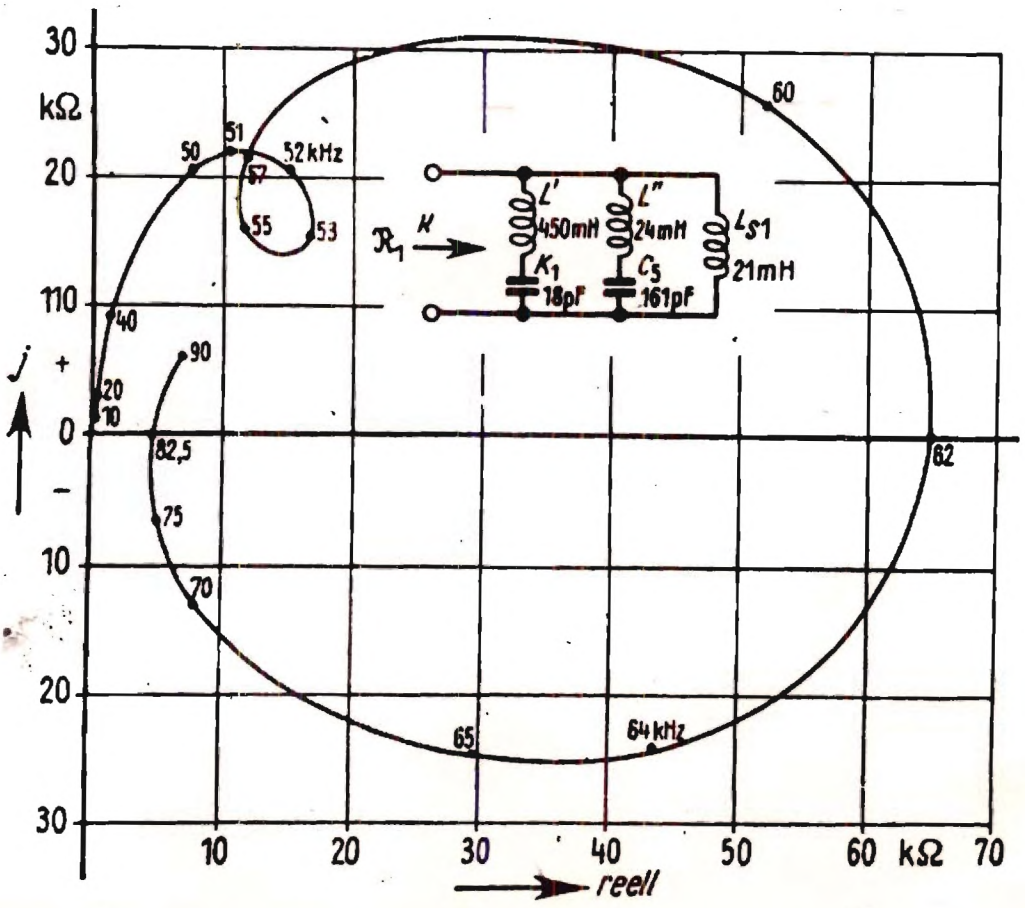

Fig. 19 - Primary short-circuit impedance - R_1^K.

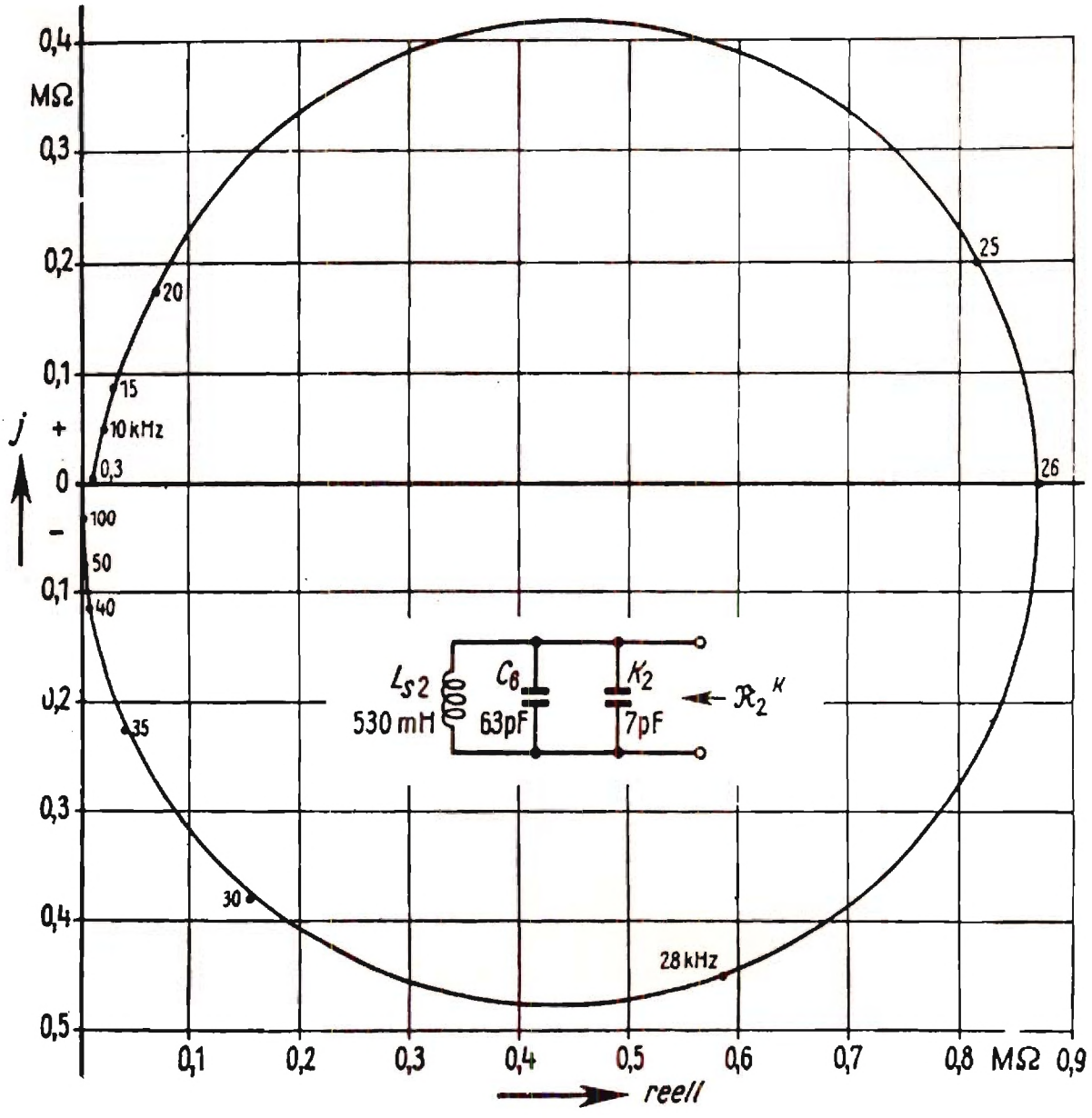

Fig. 20 - Secondary short-circuit impedance - R_2^K

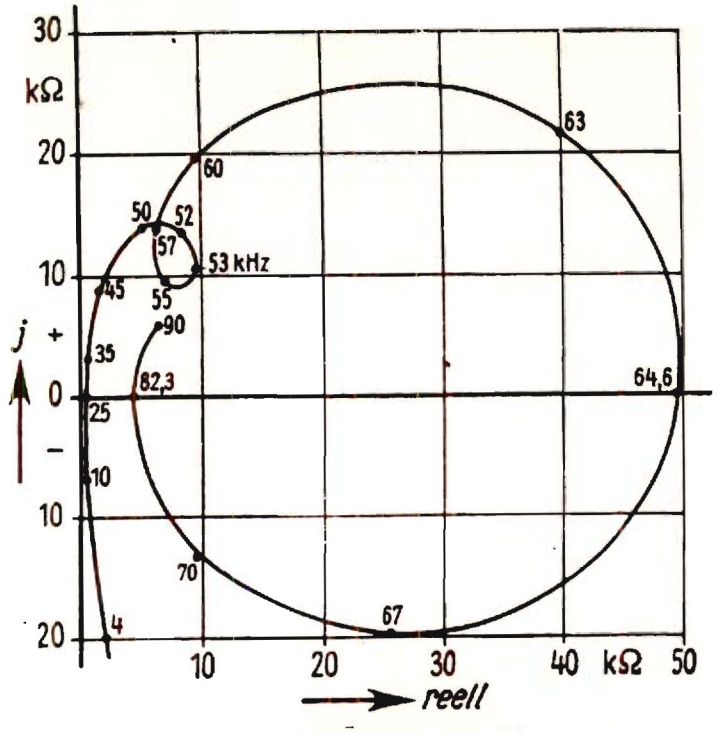

Fig. 21 - Primary open-circuit impedance - R_1^l.

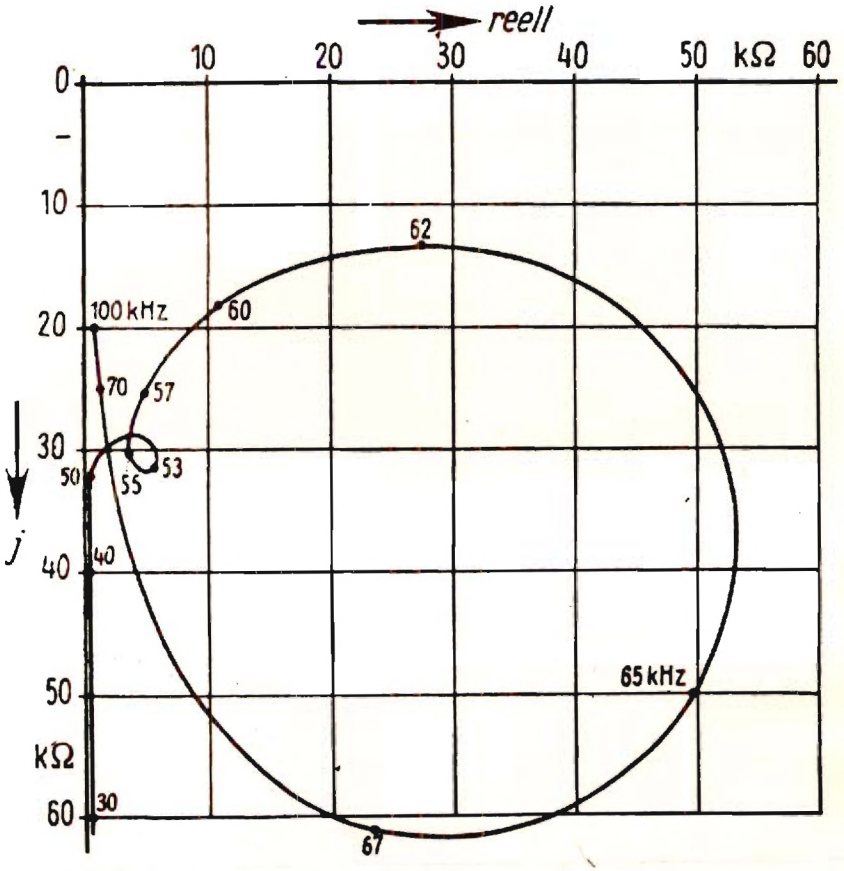

Fig. 22 - Secondary open-circuit impedance R_2^l.